5105-88
Solar Thermal Power Systems Project
Parabolic Dish Systems Development

DOE/JPL-1060-21
Distribution Category UC-62

A Comparative Assessment of Solar Thermal Electric Power Plants in the 1-10 MWe Range

L. S. Rosenberg
W. R. Revere

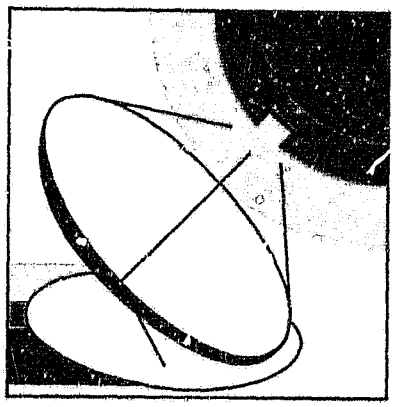

June 1981

Prepared for
U.S. Department of Energy
Through an agreement with
National Aeronautics and Space Administration
by
Jet Propulsion Laboratory
California Institute of Technology
Pasadena, California

(JPL PUBLICATION 81-53)

5105-88
Solar Thermal Power Systems Project
Parabolic Dish Systems Development

DOE/JPL-1060-21
Distribution Category UC-62

A Comparative Assessment of Solar Thermal Electric Power Plants in the 1-10 MWe Range

L. S. Rosenberg
W. R. Revere

June 1981

Prepared for
U.S. Department of Energy
Through an agreement with
National Aeronautics and Space Administration
by
Jet Propulsion Laboratory
California Institute of Technology
Pasadena, California

(JPL PUBLICATION 81-53)

Prepared by the Jet Propulsion Laboratory, California Institute of Technology, for the U.S. Department of Energy through an agreement with the National Aeronautics and Space Administration.

The JPL Solar Thermal Power Systems Project is sponsored by the U.S. Department of Energy and forms a part of the Solar Thermal Program to develop low-cost solar thermal and electric power plants.

ABSTRACT

A major activity within the Solar Thermal Power Systems (TPS) Project of the Jet Propulsion Laboratory is the implementation of a series of engineering experiments to test selected technologies in application environments.

A comprehensive analysis was necessary and undertaken to examine the power system options in order to ensure that the most feasible systems are selected and tested. This study focused on a number of candidate small (1 to 10 MWe) thermal power systems for the small community electric power market.

The objectives of this study were to rank the candidate power system technologies in terms of the cost of electric energy each system produces. In all cases, it was assumed that development programs would result in mature power plant systems that could be commercially manufactured.

This report presents the results of the study, a brief description of the systems examined, and the methodologies used.

FOREWORD

The study documented in this report was performed by the Jet Propulsion Laboratory (JPL) to aid in the management of the parabolic dish application and experiment activities that are part of the Solar Thermal Power Systems (TPS) Project. The TPS Project supports the Solar Thermal Energy Systems Program of the U.S. Department of Energy (DOE). The goal of this program is to develop solar thermal power technologies for a variety of uses.

A major activity within the TPS Project is the implementation of a series of engineering experiments which are designed to test selected technologies in application environments. In order to ensure that the most feasible technologies are tested, a comprehensive analysis of the options was necessary and undertaken. Thus, this study focused on a number of candidate small (1 to 10 MWe) thermal power systems that are applicable to the small community electric power market.

The objective of the study was to rank the candidate power system technologies in terms of the cost of the electric energy they produce. In all cases, it was assumed that development programs would result in mature power systems that could be commercially manufactured. It should be noted that the results presented are to be considered on a relative basis and not as an absolute assessment.

After the JPL ranking study was initiated, DOE contracted with the Solar Energy Research Institute (SERI) and Battelle Pacific Northwest Laboratories (PNL) to perform independent ranking studies of similar options. The SERI and PNL studies were performed separately to provide DOE with a broader technical base for program planning (References 1 and 2).

This report presents the results of the JPL ranking study, a brief description of the systems examined, and the methodologies used. A significant solar energy data base was also established by JPL in performing the course of this study.

ACKNOWLEDGMENT

The cooperation and support of persons from both industry and other government research laboratories in providing performance and design data on collectors from which independent performance and cost analyses could be made was invaluable to this study. For this support, we would especially like to thank D. Curphey, W. Treyth, and D. DiCanio of FMC Corporation, Santa Clara, California; R. Cole of Argonne National Laboratory, Argonne, Illinois; J. Reichert of Texas Tech University, Lubbock, Texas; J. Russell, Jr. and J. Housman of General Atomic Company, San Diego, California; R. Hunke and S. Thunborg of Sandia National Laboratories, Albuquerque, New Mexico; and P. Eicker of Sandia National Laboratories, Livermore, California.

Many persons at JPL assisted in the publication of this report. However, special mention of several persons must be made for their untiring efforts that resulted in this comprehensive study. These include Z. Antoniak, R. Bourke, L. Flinn, H. Fortgang, A. Marriott, N. Moore, K. Selcuk, and V. Truscello. We are also grateful to R. Case for his initial contribution, persistence, and support of this study.

CONTENTS

Figures

Tables

EXECUTIVE SUMMARY

The objective of this study was to rank various generic solar thermal electric power generation systems in terms of the cost of the electric energy they produce at sizes of 1, 5, and 10 MWe. The electrical power costs were expressed in terms of the levelized busbar energy cost (BBEC), which is the ratio of annualized life-cycle cost to annual electrical energy production. Energy production levels were described in terms of the plant capacity factor, which was defined as the ratio of annual actual plant energy generation to the hypothetical annual energy production based on continuous full-load operation.

In evaluating energy costs of the various plants, designs were optimized for minimum BBEC at every capacity factor. Thus, all candidate systems were compared on the basis of their minimum cost performance. Results were based on insolation conditions at Barstow, California, and were determined by using a Jet Propulsion Laboratory (JPL)-developed solar energy simulation code.

The evaluation was performed by analyzing nine generic plants, which consisted of seven collectors and three engine types. These plants were identified as follows:

Collector/Engine Concept	Abbreviation
Low Concentration Non-Tracking/Central Rankine Engine	LCNT
Line-Focusing Distributed Receiver, Tracking Concentrator/ Central Rankine Engine	LFDR-TC
Line-Focusing Distributed Receiver, Tracking Receiver/ Central Rankine Engine	LFDR-TR
Line-Focusing Central Receiver/Central Rankine Engine	LFCR
Fixed-Mirror Distributed Focus/Central Rankine Engine	FMDF
Point-Focusing Central Receiver/Central Rankine Engine	PFCR
Point-Focusing Distributed Receiver/Central Rankine Engine	PFDR/R
Point-Focusing Distributed Receiver/Distributed Brayton Engine	PFDR/B
Point-Focusing Distributed Receiver/Distributed Stirling Engine	PFDR/S

The various concepts considered are in different stages of development and none have achieved commercial readiness at the system level although some components of all systems are in common use. In order to make an equitable comparison of all candidate systems, it was necessary to assume that each concept would reach the same degree of maturity at some time. Therefore, a

developmental period resulting in commercial introduction sometime between 1985 and 1990 was assumed for all systems. Projections of the performance and cost of these systems at maturity were made. To generate valid system comparisons, each subsystem was estimated on a relative basis to the others, using the best developed (therefore, the best understood) system as a baseline. For instance, concentrator cost and performance parameters for each of the nine generic designs were estimated to be consistent with the PFCR heliostat parameters.

The study determined that costs of energy from the candidate power plants generally are categorized into three distinct groups for the power ranges considered. The lowest costs are achievable with two-axis tracking, point-focusing collectors (i.e., PFDR and PFCR). Intermediate costs are achievable with one-axis tracking, line-focusing collectors (i.e., LFDR-TC and LFCR). The highest costs are likely with non-tracking systems (i.e., LCNT).

At the 1-MWe size, the lowest cost plant was a distributed engine system (PFDR/B). At 5 MWe, the performance of the lowest cost, distributed engine system (PFDR/B) was matched at high capacity factors by one of the two-axis tracking, central engine systems (PFDR/R). At 10 MWe, the central engine PFDR/R was a lower cost system than the PFDR/B at high capacity factors (0.5 to 0.7). It should be noted that the point-focusing concepts (PFDR/B, PFDR/R, PFDR/S, and PFCR) are all very close, and the cost differentials that separate them are equivalent to the uncertainties in the analysis. However, the separation between the one- and two-axis tracking systems is large when compared to the uncertainties; hence, one can confidently conclude that the lowest electricity costs are associated with the point-focusing technology.

Figure 1 shows the electricity cost as a function of the capacity factor for the 5-MWe systems studied; the dashed left ends of the curves represent no storage, while the solid portion includes storage (the slope discontinuity arises from the fact that the plots shown are the combination of two curves: to the left of the discontinuity, one can operate with storage, but the no-storage case is less expensive; hence, only the latter is shown). Figure 2 shows a breakdown of the electricity costs at the optimal no-storage capacity factor for the 5-MWe systems considered.

Because the results above only apply to technology development and costs expected in this decade, they do not reflect the far-term potential for solar thermal generated power. To illustrate further improvements that can be expected in the early 1990s, two advanced engine designs currently under development for automobile applications were added to the lowest cost (PFDR) system. The results are shown in Figure 3, where 5-MWe plant electricity costs are displayed for the advanced Brayton and Stirling engines, as well as the baseline cases; these advanced engines result in an improvement in BBEC. Note that these advanced engines are in the early development phase, and their critical descriptive parameters have been taken from goals of the development projects; hence, their true cost and performance are uncertain.

In addition to engine changes, sensitivities to other elements (e.g. various production levels, improved maintenance) were calculated. This resulted in the observation that the BBEC was more sensitive to economic factors than those of a technological nature.

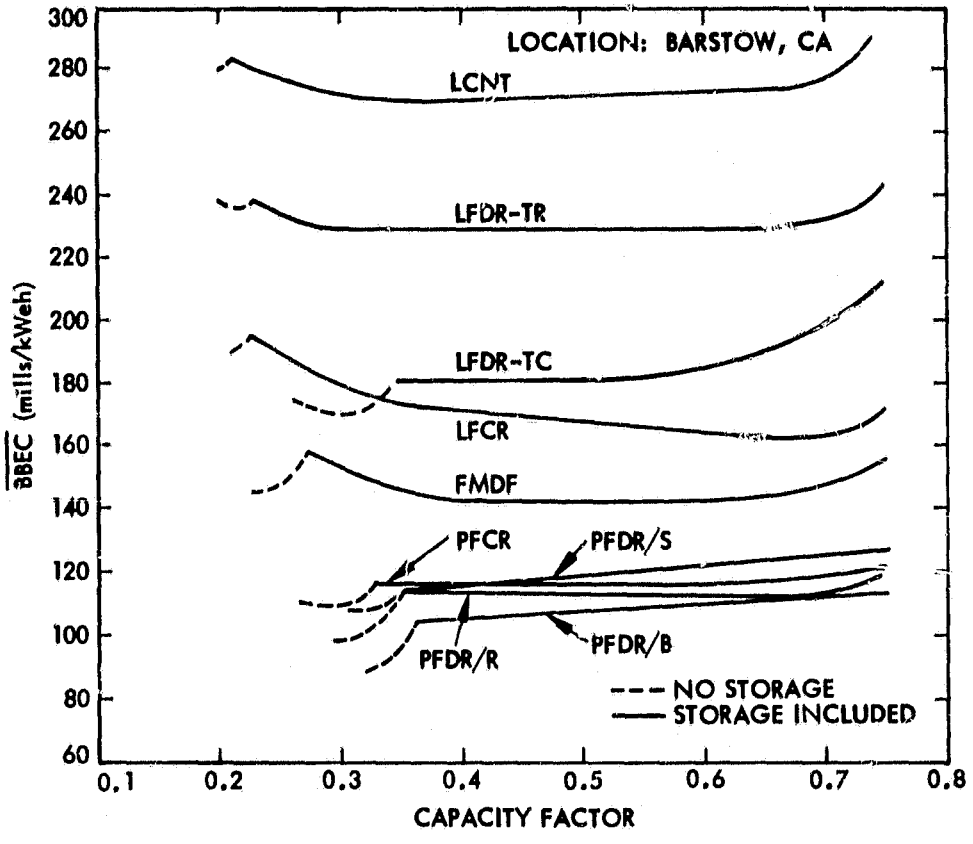

Figure 1. Energy Cost as a Function of Capacity Factor for 5-MWe Power Plants (1978 Dollars)

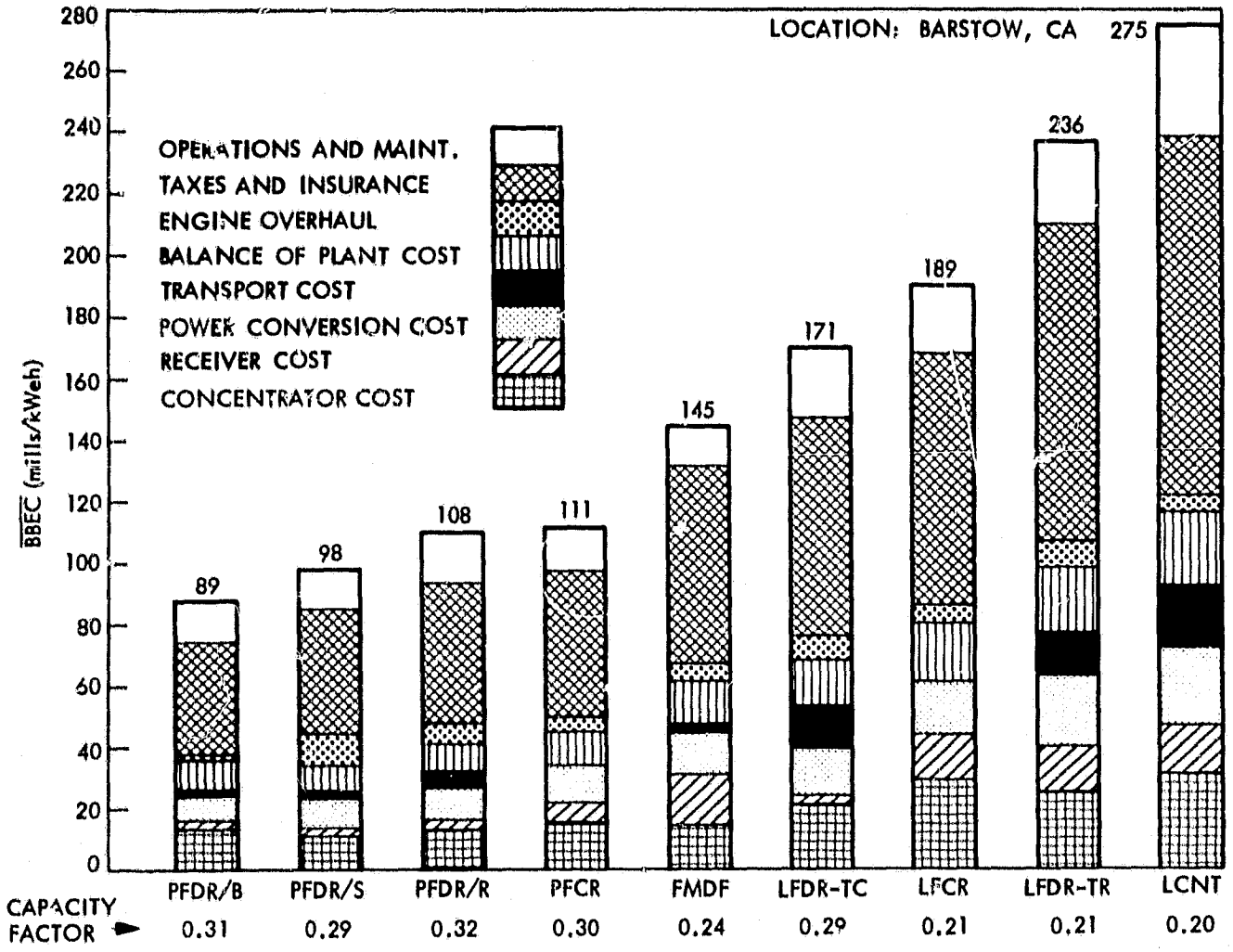

Figure 2. Cost Distribution for Optimal No-Storage 5-MWe Power Plants (1978 Dollars)

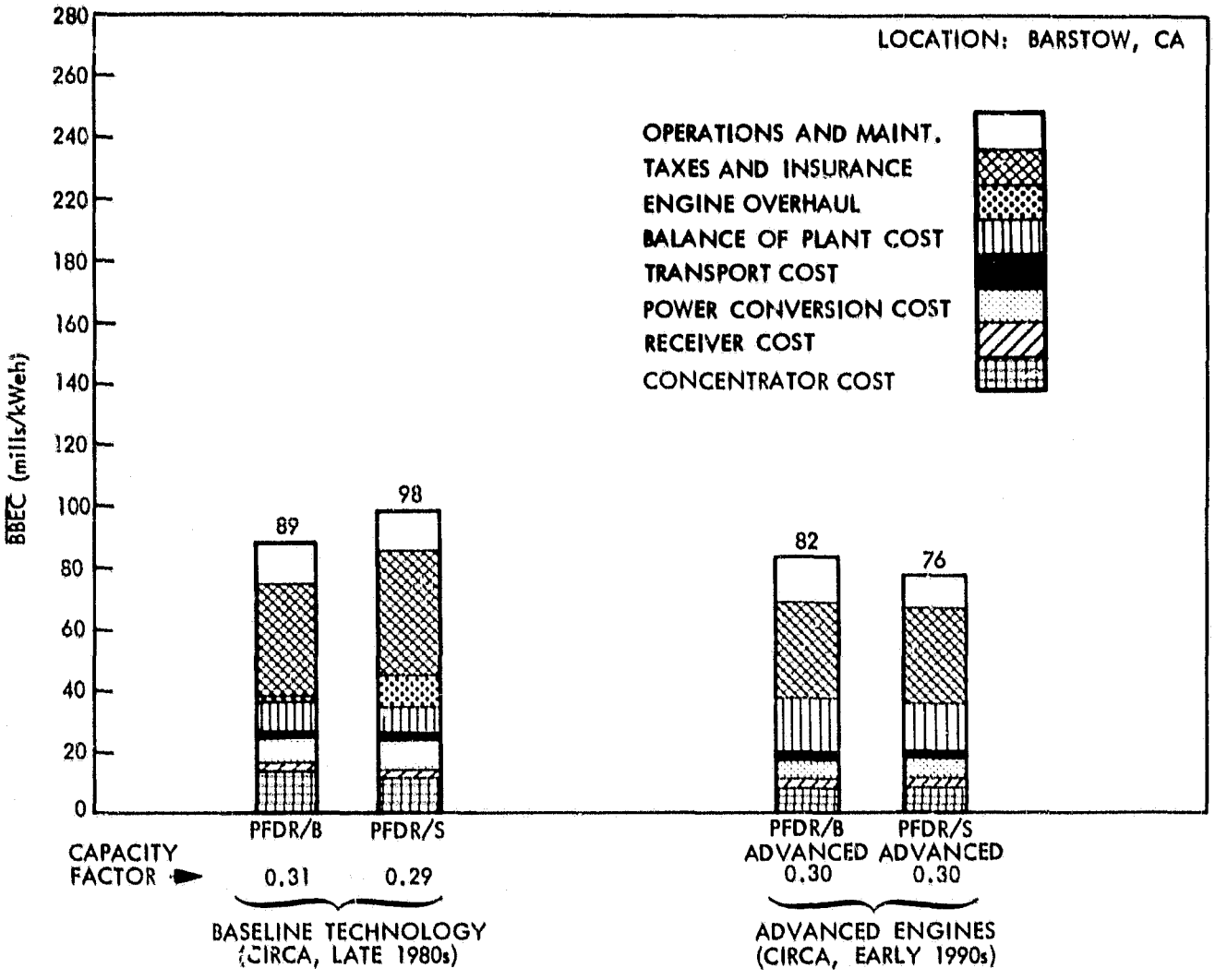

Figure 3. Comparison of PFDR Systems with Baseline and Advanced Engines for Optimal No-Storage 5-MWe Power Plants (1978 Dollars)

SECTION I

INTRODUCTION

A. BACKGROUND

The Jet Propulsion Laboratory (JPL) is conducting the Solar Thermal Power Systems (TPS) Project for the U.S. Department of Energy (DOE). The TPS Project includes a parabolic dish applications development activity. The major thrust of this activity centers around a series of engineering experiments whose purpose is to test small solar thermal power systems and to establish system feasibility. The solar thermal power plant ranking study summarized in this report was performed to aid JPL in managing the experiment activity as well as to support decisions for the selection of the most appropriate technological approach. This report provides a summary of the systems evaluated, the methodologies utilized, and the cost and performance results obtained.

B. OBJECTIVE AND APPROACH

The objective of this study was to rank the candidate power systems in terms of the cost of the electric energy they produce. These electrical power costs are expressed in terms of the levelized busbar energy cost (BBEC), which is the ratio of annualized life-cycle cost to annual electrical energy production. The life-cycle cost for a candidate power system consists of the costs of acquisition, ownership, operation, and maintenance over the system's lifetime. Electrical energy production is determined by the annual solar insolation at the plant site and the system performance parameters. By varying the plant's concentrator area and storage times, it is possible to examine system performance and costs over a wide range of energy production levels. These production levels are described in terms of the plant capacity factor, which is defined as the ratio of annual plant energy generation to the hypothetical annual energy production based on continuous full-load operation. BBEC is determined as a function of capacity factor for each candidate system. The values of BBEC are selected so that energy cost is minimized for increasing values of capacity factor. Thus, all candidate systems are compared in terms of their minimum cost performance so that the most cost-effective systems can be identified. The identified systems will have a greater potential for producing electric energy at a lower cost than the other systems analyzed. The cost and performance results for the individual power plants were determined by utilizing the solar energy simulation model known as SES II. This model is described in Reference 3.

C. GROUND RULES

In order to achieve consistency in the cost and performance evaluation, several ground rules were established. These ground rules included a definition of the economic evaluation technique, a specification of plant maximum

electrical generation capacity, and designation of certain annual capacity factors. A list of ground rules follows:

(1) All plants have a 30-year lifetime.

(2) Plant sizes of 1, 5, and 10 MWe are evaluated.

(3) All plants are located in Barstow, California. The annual insolation at the plant site is based on the 1976 data measured by West Associates and analyzed by the Aerospace Corporation (Reference 4). This insolation exists for the total lifetime of the plant.

(4) All the electric energy produced by the plant is utilized without regard to variation in load demand.

(5) $\overline{\text{BBEC}}$ is calculated using the JPL/EPRI (Electric Power Research Institute) economic evaluation methodology developed by JPL (Reference 5).

(6) $\overline{\text{BBEC}}$ is determined for the optimal no-storage capacity factors as well as capacity factors of 0.4 and 0.7.

(7) Initial capital cost for the various power systems is based on annual production levels of 25,000 units for components and subsystems unique to solar applications. Costs of other components and subsystems are based on current industrial values.

In addition to the ground rules above, a set of economic parameters as required by the JPL/EPRI evaluation methodology was also established. These economic values, based upon a typical investor-owned utility and general economic factors as of 1978, are as follows:

(1)	Cost of capital (discount rate)	0.086
(2)	Annual miscellaneous tax rate as a fraction of capital investment	0.020
(3)	Annual insurance premiums as a fraction of capital investment	0.0025
(4)	Effective income tax rate	0.400
(5)	General escalation rate	0.060
(6)	Escalation rate for capital costs	0.060
(7)	Escalation rate for operating costs	0.070
(8)	Escalation rate for maintenance costs	0.070
(9)	Base year	1978

(10) Year of Commercial Operation 1985-1990

(11) Plant construction period:

Size (MWe)	Total Construction Time (yr)	Distribution
1	1	100% - 1989
5	2	67% - 1988; 33% - 1989
10	3	50% - 1987; 25% - 1988; 25% - 1989

The various solar thermal concepts exhibit a disparity of developmental status. In order to make an equitable comparison of all candidate systems, it was necessary to assume that each concept would reach the same degree of maturity. Therefore, a developmental period resulting in commercial introduction sometime between 1985 and 1990 was assumed for all systems. Thus, any year within the 1985 to 1990 range can be chosen as the first year of commercial operation for the candidate systems. The maximum change in BBEC for any candidate system as a result of choosing any year within this period is less than 1%.

SECTION II

SOLAR THERMAL ELECTRIC POWER SYSTEMS

A. SYSTEM CONCEPTS

A solar thermal electric power system consists of collector, power conversion, energy transport, and energy storage subsystems (see Figure 2-1). The solar collectors considered in this study consist of a concentrator and receiver. The concentrator, using mirrors or lenses, collects sunlight and focuses it at the receiver. The receiver, a specially-designed heat exchanger, absorbs the solar flux and converts it to thermal energy. The power conversion subsystem, which consists of a heat engine and electrical generator, then converts the thermal energy into electricity. Storage subsystems are used for storing excess energy for later use.

The two major collector designs currently being examined are the central receiver and distributed receiver. Central receiver systems comprise a large

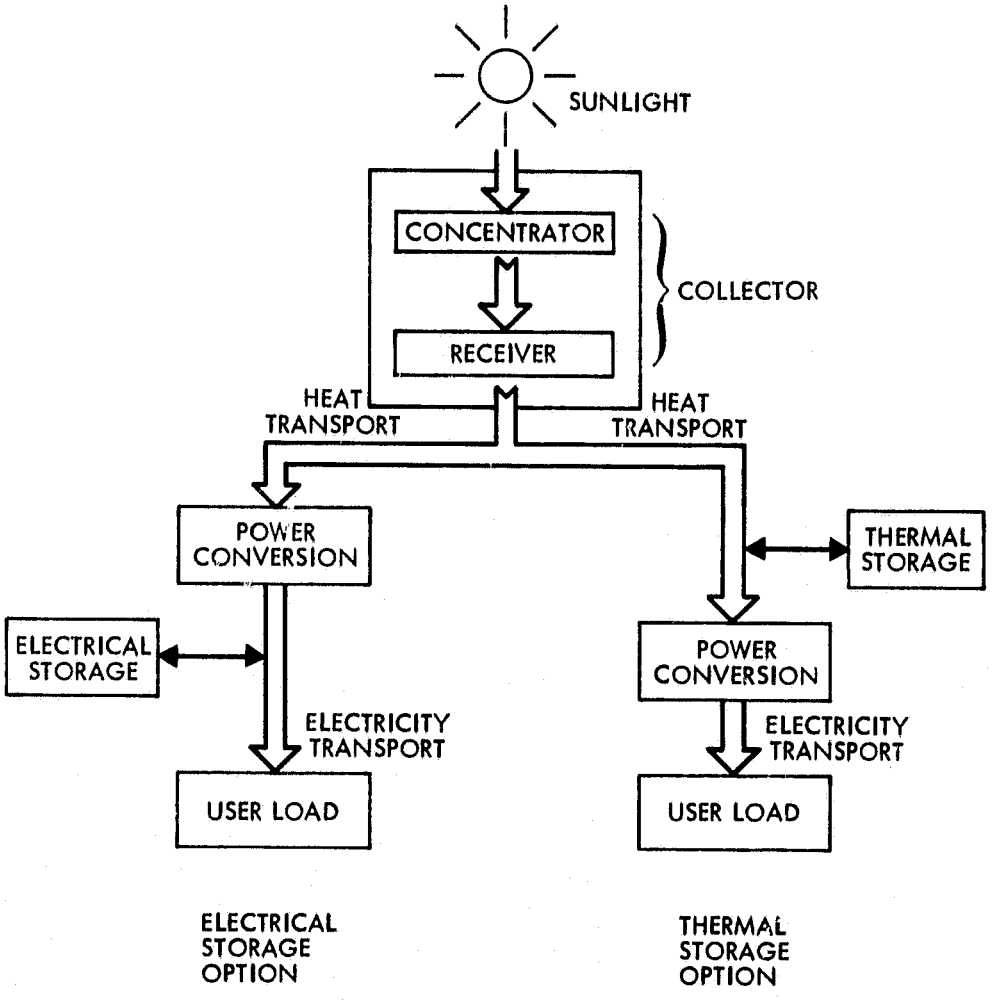

Figure 2-1. Solar Thermal Electric Power System

field of sun-tracking mirrors (heliostats), which focus sunlight on a centralized receiver. Distributed receiver systems consist of a field of many smaller concentrator/receiver modules. There is a trade-off between these two collector system designs to be considered between the savings resulting from the mass production of many small concentrator/receiver modules and the economy of scale provided by large central receivers. A further dimension in which collector designs may be distinguished is the type of sun-tracking mechanism employed. Collectors may be fixed (non-tracking), one-axis tracking, or two-axis tracking. The tracking capability may be included in either the concentrator or the receiver. Fixed collectors are usually flat-plate or low-concentration devices, which produce low collector operating temperatures (50 to 250°C) and low system efficiencies (2 to 10%). One-axis systems employ higher concentration ratios and linear receivers for higher temperatures (150 to 425°C) and higher system efficiencies (10 to 18%). Two-axis collectors with point-focusing capabilities can provide high temperatures (425 to 1100°C) as well as high system efficiencies (15 to 30% or better). A second trade-off exists between the higher cost, complexity, and higher performance of the two-axis systems, and the lower cost, relative simplicity, and lesser performance of the one-axis or non-tracking systems.

The power conversion subsystem may be either centrally located or distributed in the collector field. In central conversion, thermal energy from the receiver is converted into electricity at a nearby large, central heat engine/generator, while distributed power conversion is accomplished with many smaller heat engine/generators dispersed within the collector field. Distributed power conversion is only feasible with distributed receiver systems. In this study it was assumed that the point-focusing distributed receiver systems, which use distributed conversion, have the engine/generator mounted onto a module with the receiver near the concentrator focal point. There is a trade-off between the cost reduction potential of mass producing many small units versus the economy of scale realized by one large unit.

Solar thermal power systems may also differ from one another with respect to the type of thermodynamic conversion cycle employed. The conversion cycles most often considered are Rankine, Brayton, and Stirling engines. Although the Rankine-cycle engines studied are limited to lower temperatures (250 to 500°C) and have lower efficiencies (15 to 40%) than the Brayton or Stirling engines, the Rankine systems are commercially available and future cost/performance estimates are fairly certain. The Rankine-cycle engines considered in this study were applied to central power conversion systems with a capacity of 1 to 10 MWe with either distributed or central receiver systems. Efficiencies for Brayton-cycle engines (25 to 45%) are potentially better than those for Rankine systems because of higher temperature capabilities (750° or more) and differences in the thermodynamic cycle. The Brayton-cycle engines, however, require higher temperature receivers as well as additional development. Although large central Brayton-cycle engines could be used in distributed receiver systems, current development is focused on small dish-mounted engines. Stirling-cycle engines seem to offer higher performance potential than the Brayton engine when operating at the same temperature but would require more frequent major overhauls. It seems that the Brayton and Stirling engines are best suited to point-focusing distributed systems in which their small size and high temperature needs are well matched.

Energy storage for a solar power plant can be accomplished by storing the thermal energy received by the collector field or by utilizing electrical storage. The latter is most applicable to distributed energy conversion systems that utilize Brayton or Stirling engines. All other solar thermal power plant concepts were assumed to store thermal energy prior to conversion into electrical energy. Based on operational reliability and technological maturity, dual media thermal storage subsystems (composed of salt and rock for high and medium temperature systems, and oil and rock for low temperature systems) were chosen for this study. The electrical storage system assumed was a redox system. This system, which uses an iron and chromium electrolytic solution, is under development at NASA Lewis Research Center (LeRC) for DOE.

Figure 2-2 presents a morphological structure of the generic plant concepts evaluated in the study. Even though configurations other than the nine types shown can be synthesized, they were not considered because they are either sufficiently represented by those concepts evaluated, or they have a clearly identifiable cost disadvantage. The system abbreviations, as shown in Figure 2-2 and used elsewhere in this report, are defined as follows:

Collector/Engine Concept	Abbreviation
Low Concentration Non-Tracking/Central Rankine Engine	LCNT
Line-Focusing Distributed Receiver, Tracking Concentrator/Central Rankine Engine	LFDR-TC
Line-Focusing Distributed Receiver, Tracking Receiver/Central Rankine Engine	LFDR-TR
Line-Focusing Central Receiver/Central Rankine Engine	LFCR
Fixed-Mirror Distributed Focus/Central Rankine Engine	FMDF
Point-Focusing Central Receiver/Central Rankine Engine	PFCR
Point-Focusing Distributed Receiver/Central Rankine Engine	PFDR/R
Point-Focusing Distributed Receiver/Brayton Engine	PFDR/B
Point-Focusing Distributed Receiver/Stirling Engine	PFDR/S

B. SPECIFIC SYSTEM DESIGNS

1. Low Concentration Non-Tracking (LCNT)

This generic design covers both the symmetrical and asymmetrical vee trough as well as several configurations of compound parabolic concentrators (CPC). The system chosen for this study was based upon a University of Chicago CPC design, which has an evacuated tubular receiver (References 6, 7). This design provides the highest performance of any LCNT system.

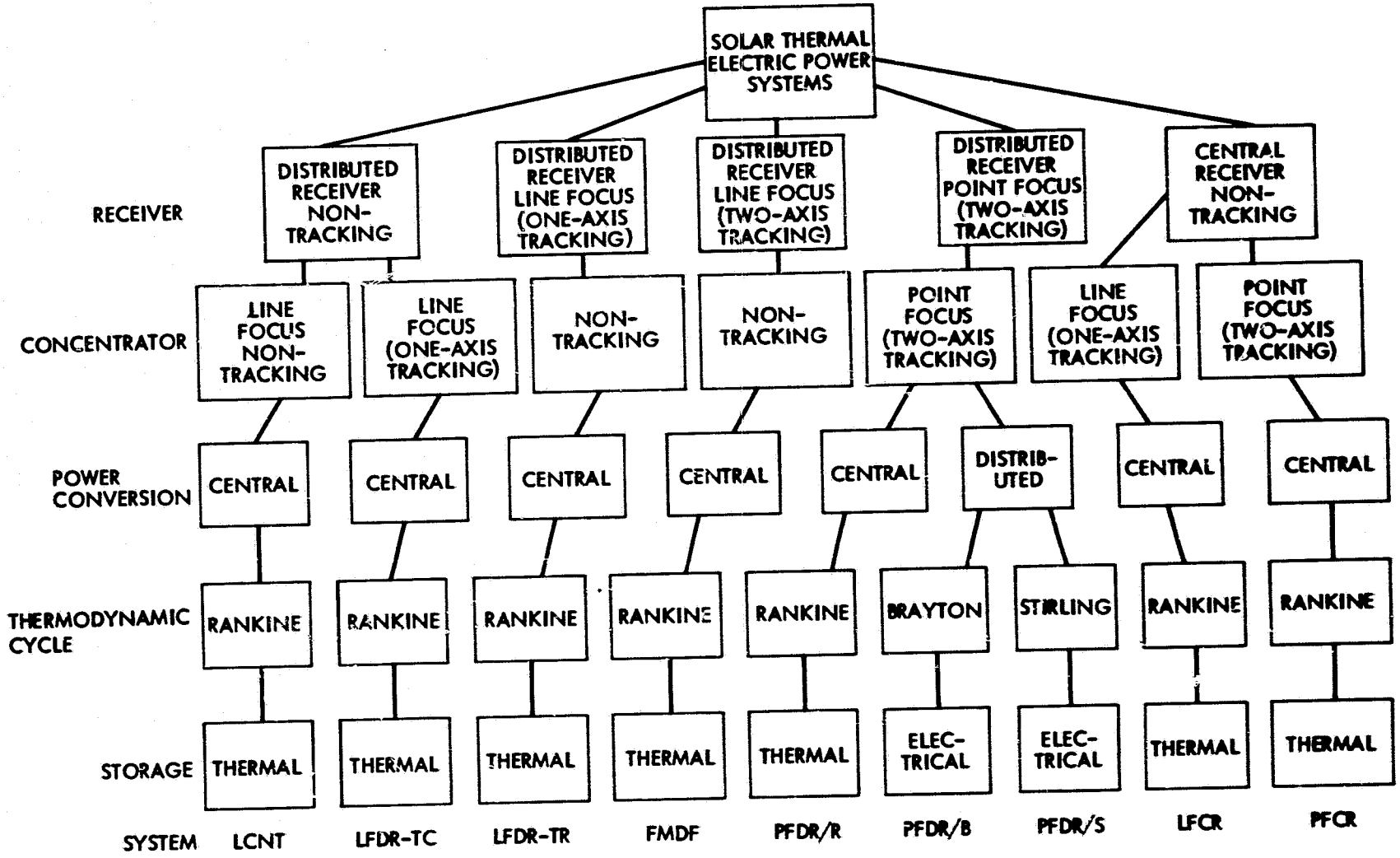

Figure 2-2. Morphology of Solar Thermal Power Plant Technology Options

Figure 2-3 shows a CPC and Figure 2-4 shows a typical LCNT solar power plant layout. The collector modules are oriented in an east-west direction and their tilt angles are adjusted monthly. These modules are placed in rows 6.1 m apart, which corresponds to a ground cover ratio of 0.45. Each receiver consists of a copper U-tube bonded to a fin and enclosed in an evacuated receiver. All modules are connected in parallel. The heat transport fluid (Caloria HT43 or equivalent such as Therminol 66) is heated and supplied through an insulated piping grid to the central energy conversion unit. A heat exchanger utilizes the heat supplied by the transport fluid to vaporize toluene, an organic working fluid for a Rankine-cycle engine. The engine operates an electrical generator, and any excess heat is routed to thermal (Caloria HT43 and rock) storage. A cooling tower rejects excess condenser heat.

2. Line-Focusing Distributed Receiver, Tracking Concentrator (LFDR-TC)

This generic plant is commonly referred to as a parabolic trough (see Figure 2-5). Figure 2-6 shows a typical LFDR-TC power plant. Although major design and test efforts have been conducted by several organizations, this study focused on a Sandia National Laboratories design (References 8, 9). This design consists of collector modules that are 61 m in length and have 2-m apertures. The modules are placed 5.7 m apart, which result in a ground cover ratio of 0.35. Although a polar orientation would collect slightly more energy, a north-south horizontal mounting was chosen in order to simplify the collector transport field. The receiver tube is enclosed in a glass jacket, which is evacuated in order to reduce thermal losses. Heat is transported

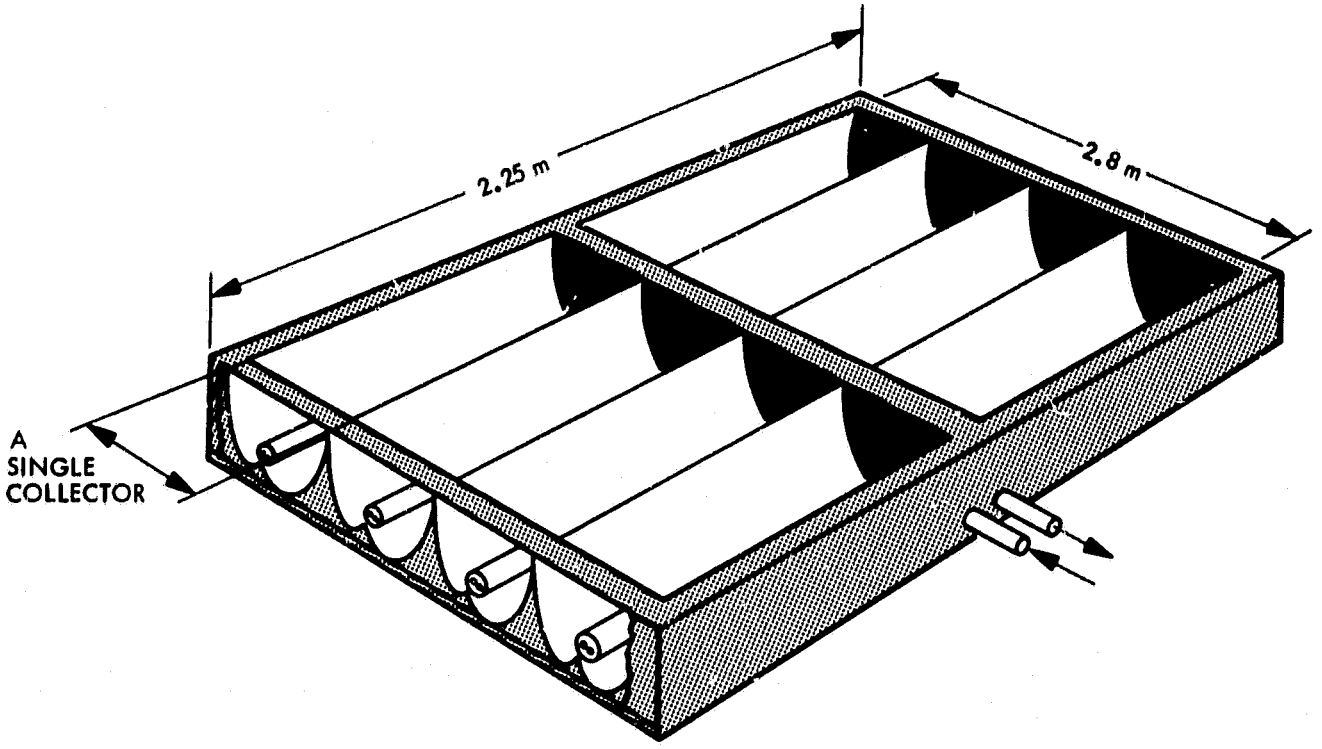

Figure 2-3. Low Concentration Non-Tracking (LCNT) Concept/Compound Parabolic Concentrator (CPC)

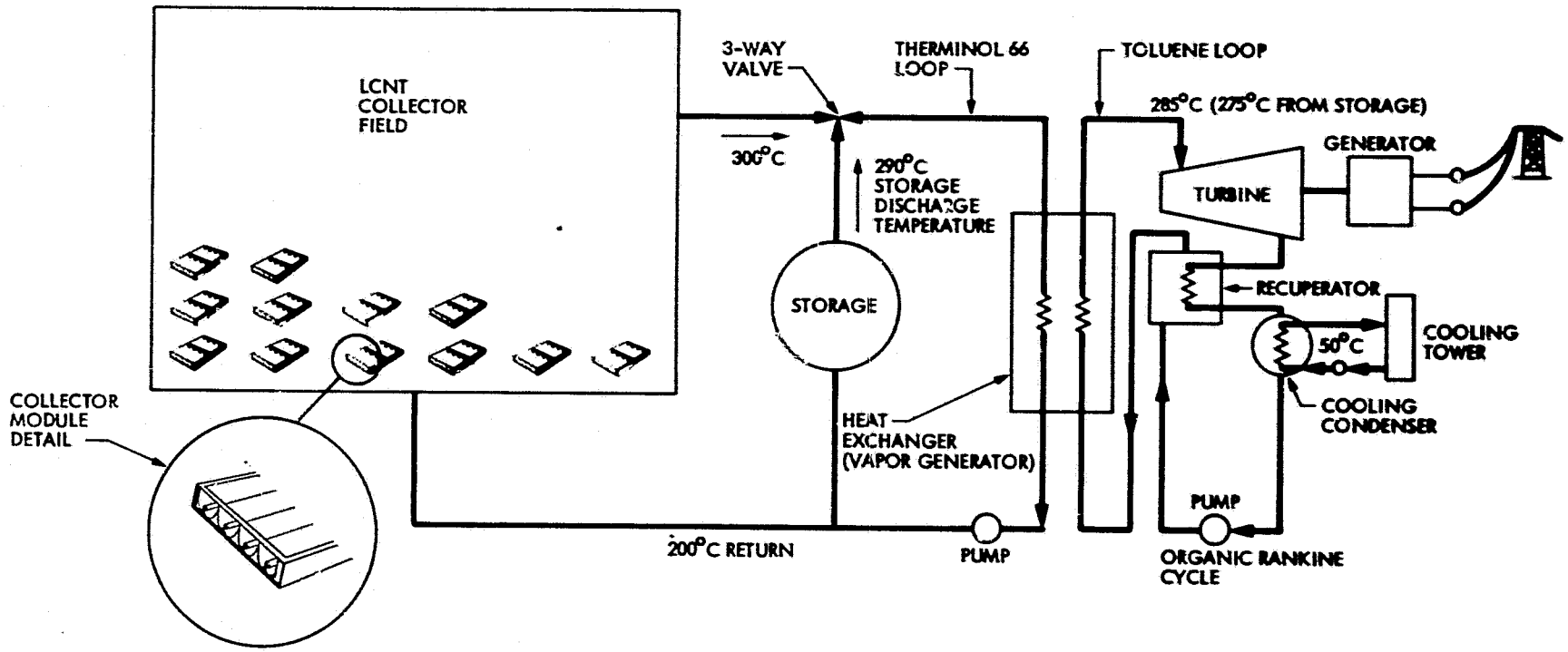

Figure 2-4. LCNT Power Plant Layout

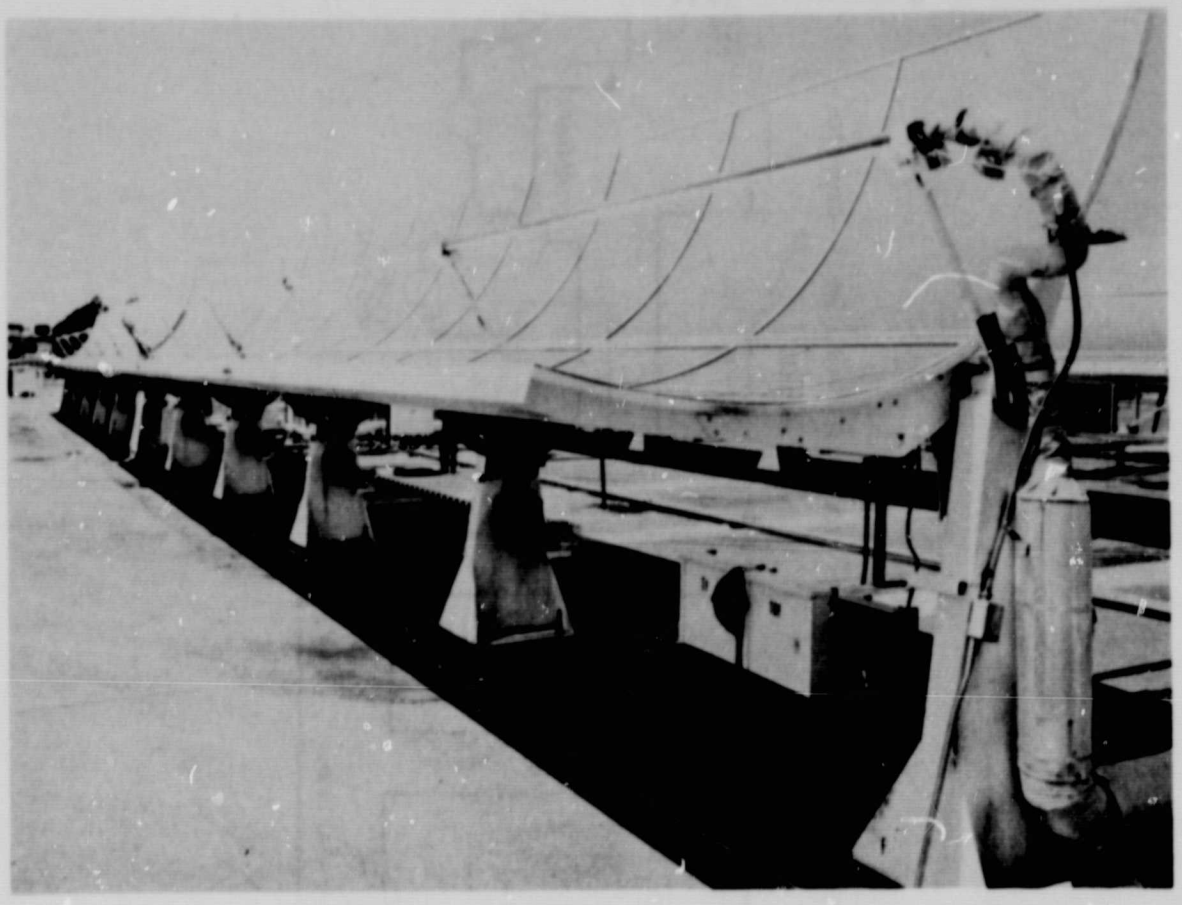

Figure 2-5. Line-Focusing Distributed Receiver Concept Using Parabolic Troughs (LFDR-TC)

from the collector to the central energy conversion unit by using a silicone fluid, such as Syltherm 800, which flows through an insulated piping grid. A heat exchanger utilizes the heat supplied by the transport fluid to vaporize toluene. As in the LCNT system, the organic-Rankine engine/generator produces electricity, and any excess heat is routed to thermal storage. The storage medium is Hitec[1] in combination with rock and sand. A wet-cooling tower rejects excess condenser heat.

3. Line-Focusing Distributed Receiver, Tracking Receiver (LFDR-TR)

This concept is sometimes referred to as the fixed faceted-mirror solar collector (FFMSC) because of the configuration of mirror segments over the concentrator surface. Figure 2-7 shows a segmented-mirror concentrator.

---

[1]Hitec is a trademark for a DuPont product which includes 53% KNO_3, 40% $NaNO_2$, and 7% $NaNO_3$.

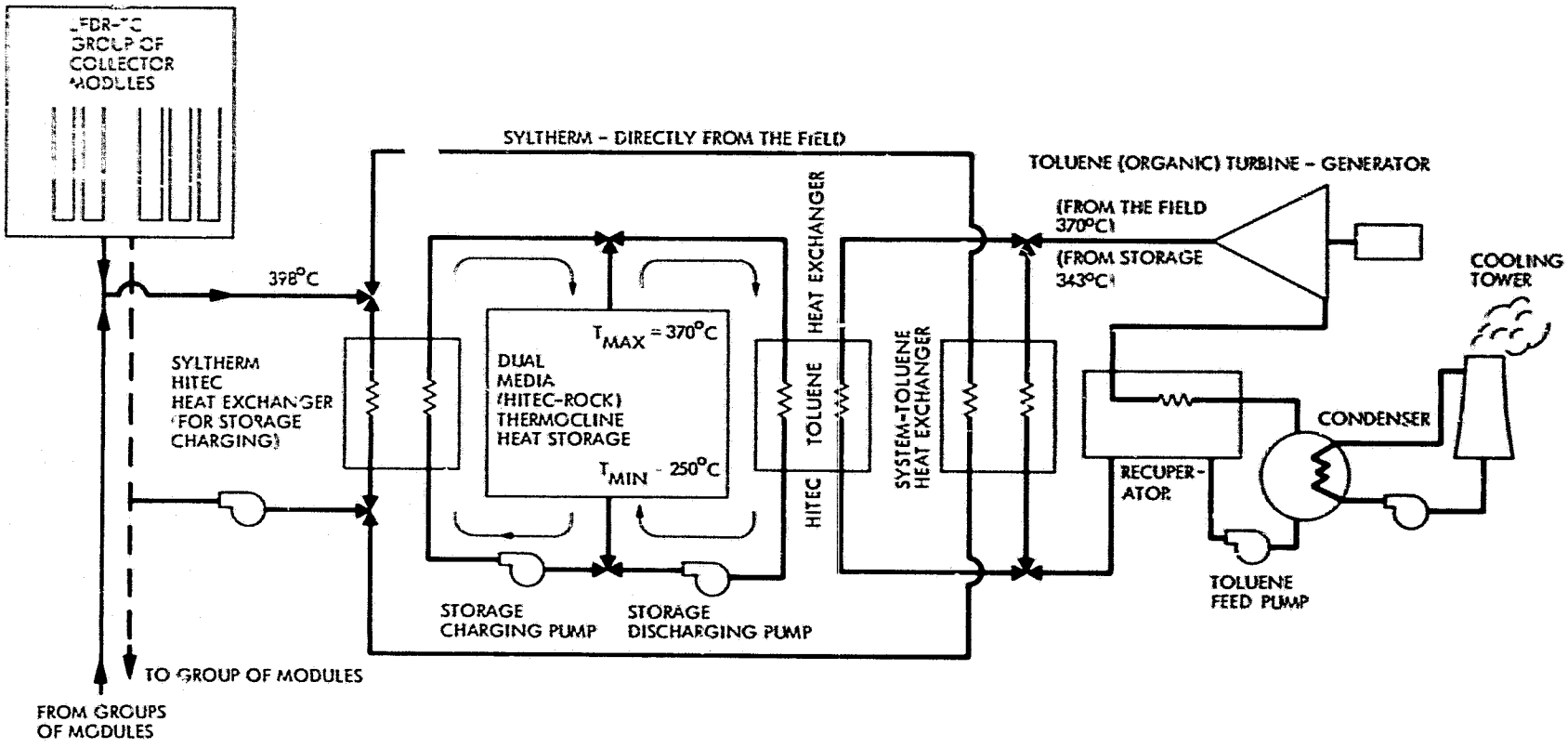

Figure 2-6. LFDR-TC Power Plant Layout

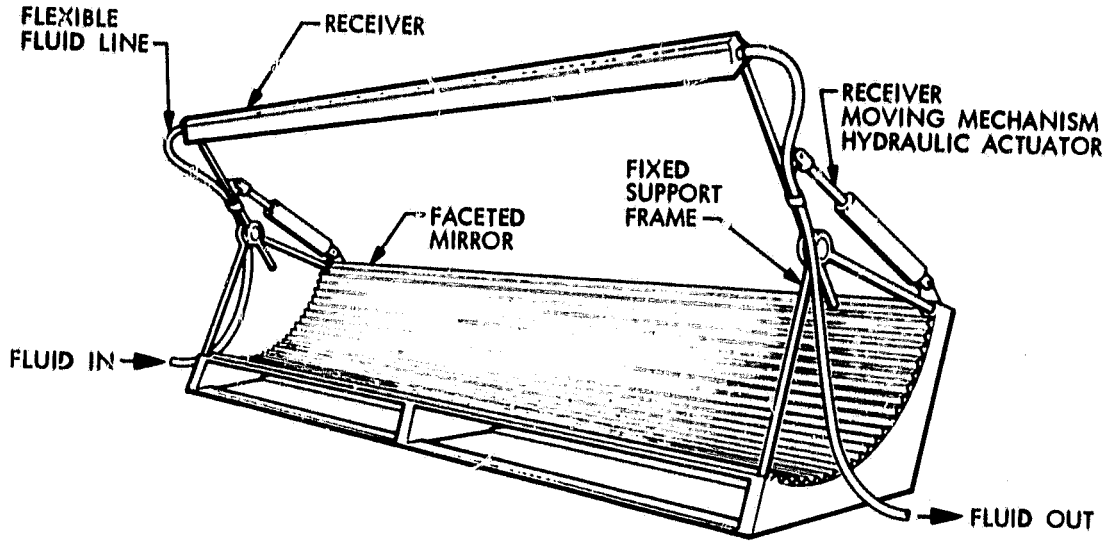

Figure 2-7. Line-Focusing Distributed Receiver Concept Using Fixed Mirrors and Movable Receiver (LFDR-TR)

A typical LFDR-TR solar power plant is identical to the LCNT plant illustrated on Figure 2-4 with the exception of the field layout. The system evaluated here has been investigated and developed by the General Atomic Company (References 10, 11, 12).

In this system, the receiver tracks the linear image produced by the FFMSC. The concentration flux intensity is increased by a factor of two by using a CPC as a secondary concentrator. The collector modules, which measure 3 m by 61 m, are oriented in an east-west direction and are situated 5.5 m apart. The heat transport fluid is Caloria HT43 or equivalent petroleum base oils. As in the LCNT and LFDR-TC designs, this fluid exchanges heat with toluene to generate power. The transport fluid also serves as the storage fluid in combination with sand and rock.

4. Point-Focusing Central Receiver (PFCR)

A typical PFCR (5 MWe) plant schematic layout is shown in Figure 2-8. All major subsystems and components are shown; the field of heliostats encircles the tower. A smaller plant (1 MWe), with a north-only field and a cavity receiver, appears in Figure 2-9. An unusual feature of the PFCR and LFCR systems is the use of optical, rather than thermal, energy transport. The PFCR plant evaluated is similar in design to the DOE 10-MWe pilot plant located at Barstow, California. (References 13, 14).

The PFCR concept has an array of two-axis tracking heliostats that direct the solar beam onto the surface of a receiver, where most of the solar flux is absorbed. This receiver is mounted on a tower. The working fluid enters the receiver tubes as pressurized water, exits as superheated steam, and is then piped to the bottom of the tower. Receiver steam can be routed either to the inlet of a conventional, central-Rankine turbine/generator set

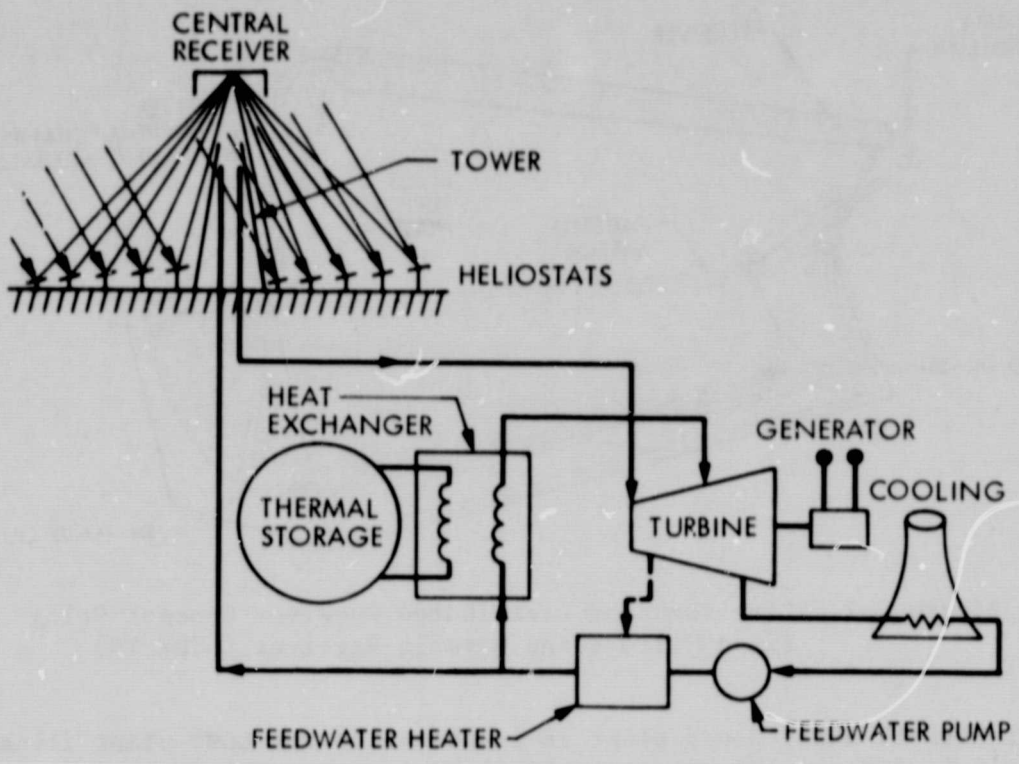

Figure 2-8. PFCR Power Plant Layout

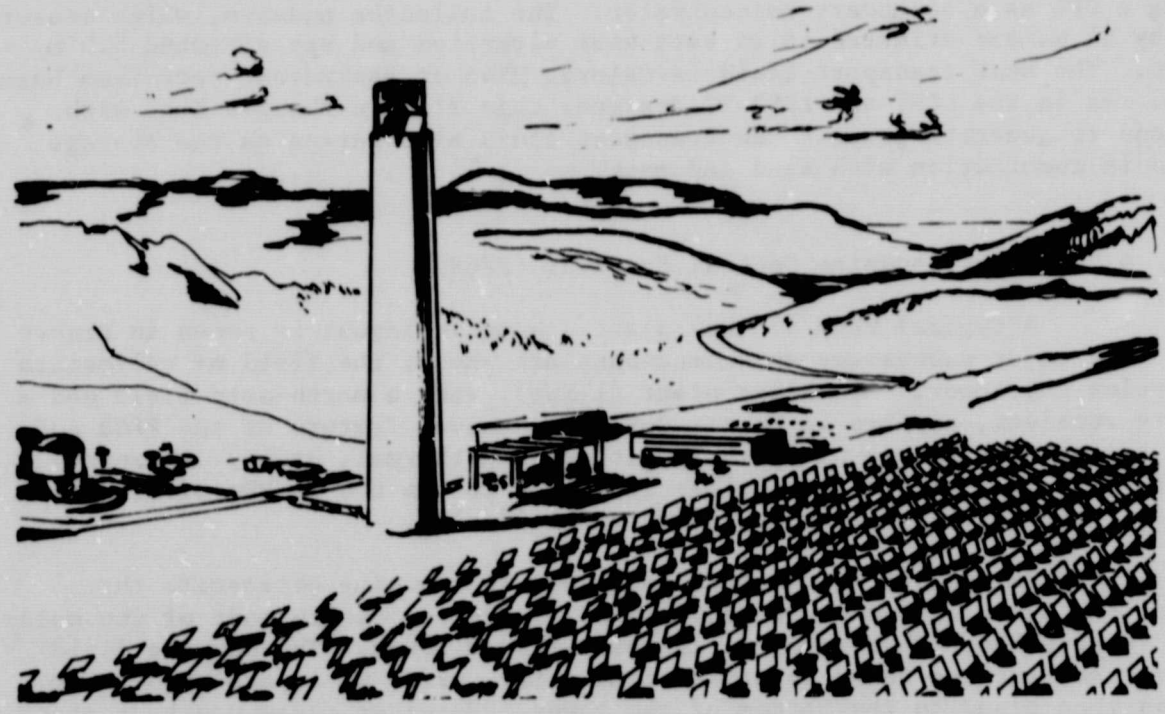

Figure 2-9. PFCR Plant with North Field

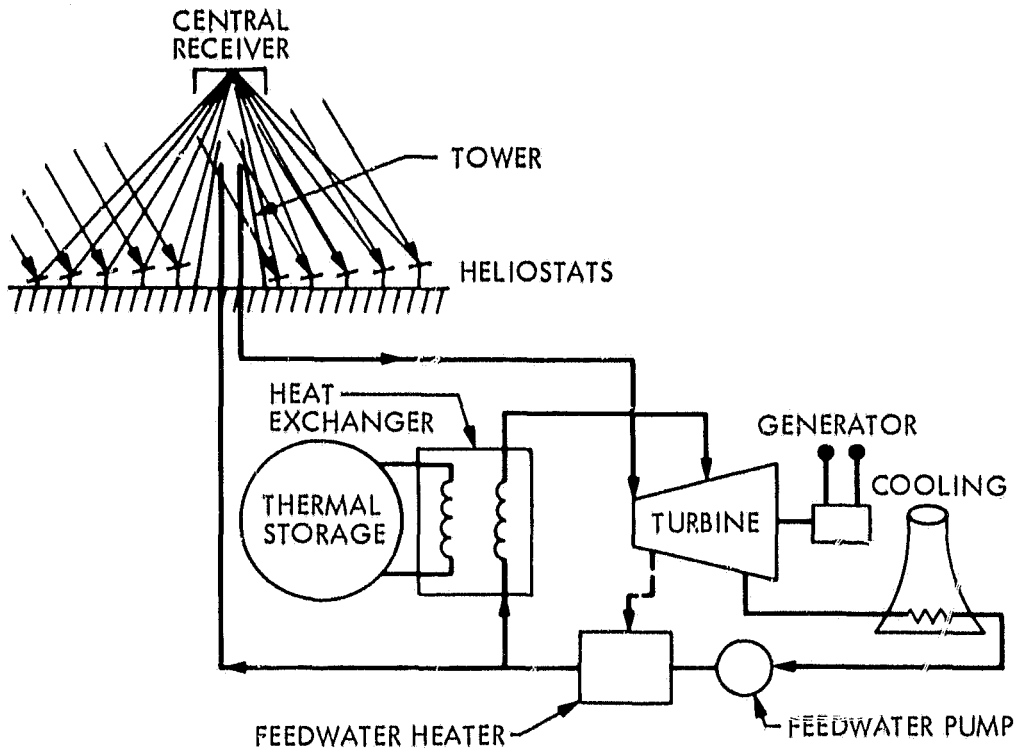

Figure 2-8. PFCR Power Plant Layout

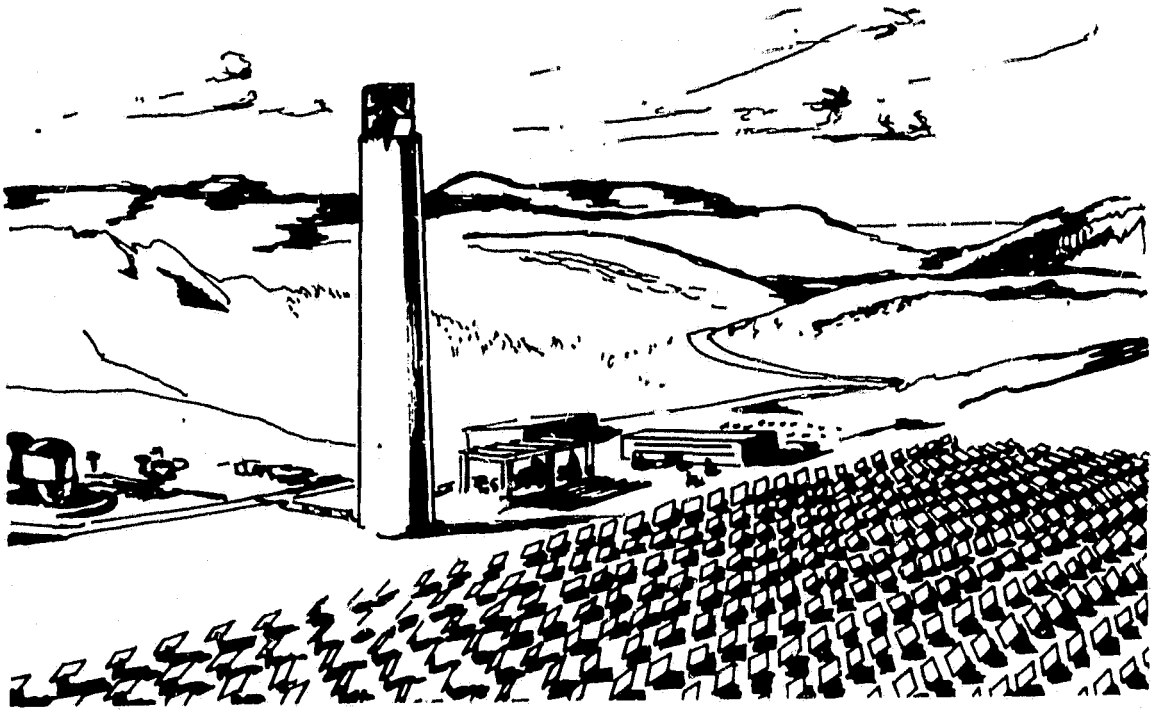

Figure 2-9. PFCR Plant with North Field

for immediate electrical power production or to the thermal storage subsystem. In the latter option, heat is transferred from steam to a Hitec, rock, and sand storage medium. The heliostat orientation is controlled through a central computer unit, in combination with peripheral equipment and software.

5. Line-Focusing Central Receiver (LFCR)

Basically, the LFCR system is a one-axis tracking version of the PFCR system. This concept has an array of long single-axis tracking heliostats that reflect the incident direct solar flux onto a cavity-type linear receiver (see Figure 2-10). In addition to an elevation tracking mechanism, the heliostats use a mechanism to flex the reflective surface that changes the focal length. This is necessary because the illumination is generally off-axis during early morning and late afternoon hours, introducing off-axis astigmatism. With an adjustable radius of curvature, a line focus can be maintained for off-axis illumination. When the tracking axis is oriented east-west for latitudes greater than 30 to 35°, the most efficient location of the heliostat field is on the north side of the receiver. The LFCR collector design in this study is based upon the work of the FMC Corporation (References 15, 16, 17, 18).

As in the PFCR system, optical energy transport plays a major role within the LFCR plant. Because of the one-axis tracking of the LFCR, a part of the flux reflected from the heliostats will miss the receiver at times other than solar noon. The length of receiver not illuminated is a function of the angle between the receiver and the sun. In order to reduce end losses (the amount of solar flux missing the receiver during non-noon hours), triangular-shaped heliostat field sections (called butterflies) are added at both ends of the heliostat field (see Figure 2-10). The butterfly area is designed to allow the full length of the receiver to be illuminated for the four hours centered around solar noon.

Figure 2-10 shows a typical (5 MWe) plant layout; the heliostat field is of the north-only type and has 21 rows. A schematic diagram of this plant would be similar to the PFCR system (Figure 2-8).

6. Fixed-Mirror Distributed Focusing (FMDF)

The FMDF system consists of a number of collectors, each having a large (61-m diameter) spherical-segment reflector that concentrates the incident solar flux onto a linear receiver. The system evaluated in this study is based upon the work of Texas Tech University and E-Systems, Inc. (References 19, 20, 21). The concentrator is fixed and is made up of many small, curved-mirror panels. Part of the concentrator is situated below ground level, and its aperture plane is tilted slightly toward the south. A long, linear two-axis tracking receiver is located within the concentrator bowl (see Figure 2-11). The receiver is designed so that only a small fraction of the solar flux reflected by the concentrator misses the receiver. The fixed nature of the concentrator produces large diurnal variations in the power available to the receiver. Furthermore, the flux variation along the receiver (a function of the spherical geometry of the reflector) is time

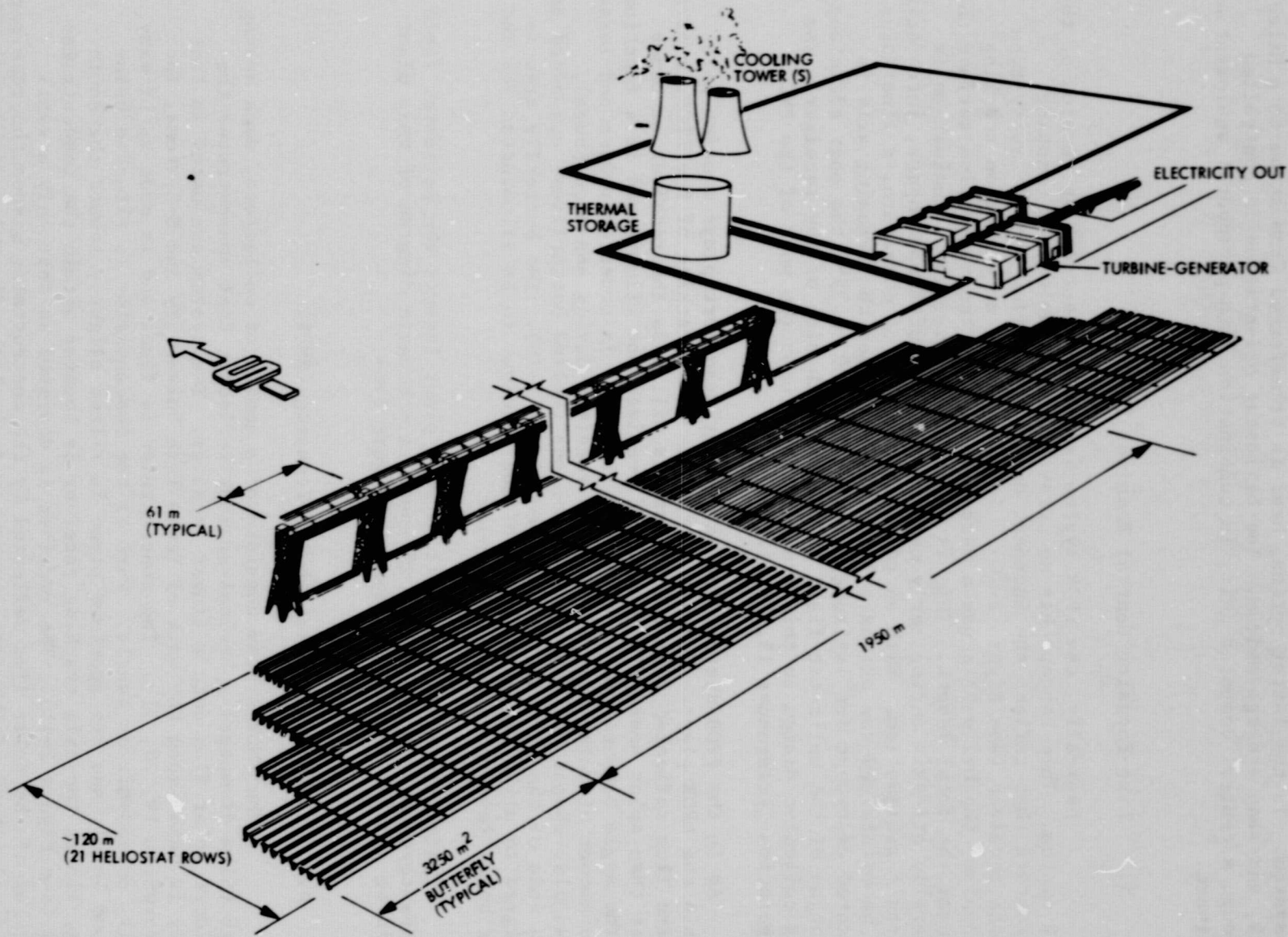

Figure 2-10. LFCR Power Plant Layout

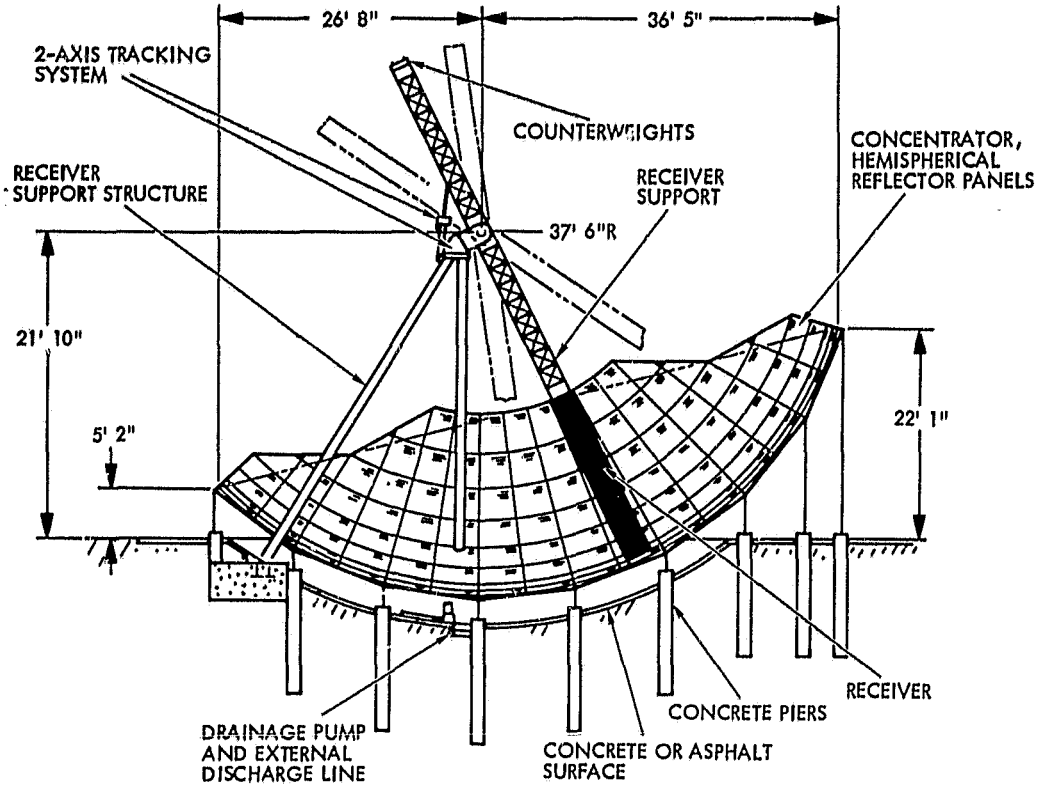

Figure 2-11. Fixed-Mirror Distributed Focusing (FMDF) Concept

dependent. The working fluid enters the bottom of the receiver as pressurized water and leaves the receiver as superheated steam at the top. As in the PFCR system, receiver steam can be routed either to the central turbine/generator or to thermal (Hitec and rock) storage. The receiver orientation is controlled by a central computer, together with peripheral equipment and software. A schematic diagram for such a plant would be similar to the one illustrated for the PFCR system (Figure 2-8).

7. Point-Focusing Distributed Receiver/Central Rankine Engine (PFDR/R)

The designs evaluated for the PFDR systems are not based on any one system, but on a composite of several designs. This concept has a collector field composed of two-axis tracking dishes. The reflective surface of the dish concentrates the direct component of solar radiation onto a small area on the focal plane where a cavity receiver is mounted. Figure 2-12 portrays one of the PFDR concepts developed by Acurex Corporation. The working fluid, which is circulated through the receiver, may be a heat transfer fluid or the working fluid of the heat engine. The heat engine can be one of several types. The engine specific to the PFDR/R design is a large central steam-Rankine turbine, similar to the one used in the PFCR system.

A ground cover ratio of 0.31 with a rectangular field layout was chosen because studies have indicated that such an arrangement results in only a minor amount of adjacent dish shadowing (about 5% annually). The dishes are

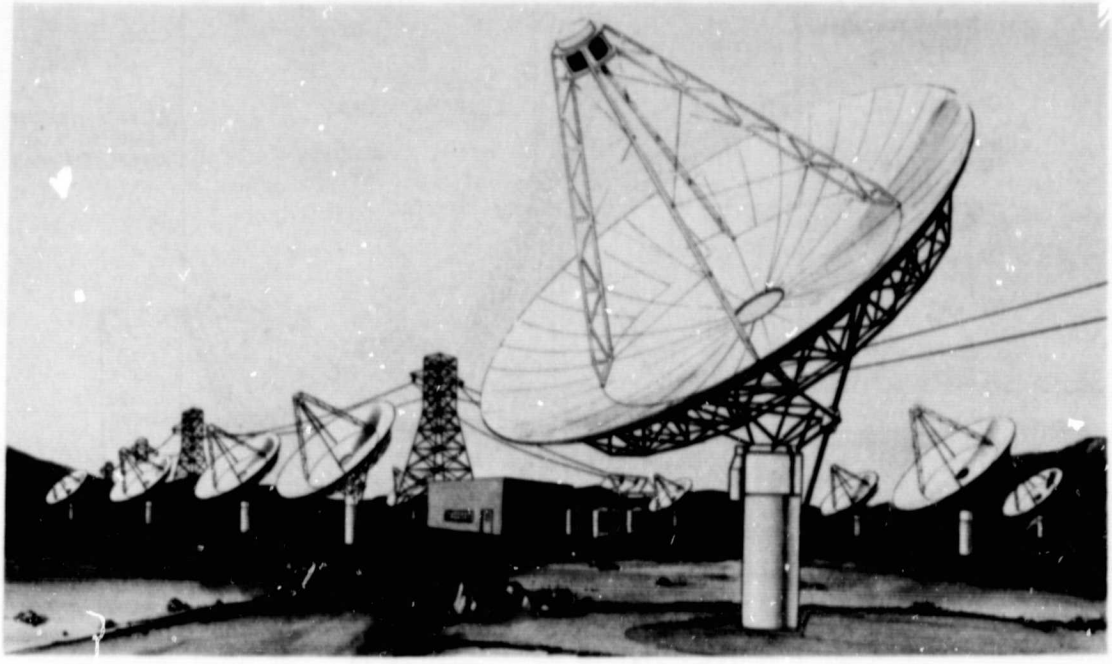

Figure 2-12. Concept of Point-Focusing Distributed Receiver (PFDR) Attached to a Two-Axis Tracking Concentrator

connected by a piping grid, which supplies superheated steam to the engine. A return line routes pressurized water to the inlet of each receiver. The storage system behaves the same as in the PFCR system. The thermal fluid transport system is of parallel design, where each receiver produces superheated steam. A typical PFDR/R, 5-MWe plant layout is shown in Figure 2-13. Collector tracking is controlled by a central computer, in combination with peripheral equipment and software.

8. Point-Focusing Distributed Receiver/Brayton Engine (PFDR/B)

The PFDR/B system is similar to the PFDR/R design. The PFDR/B system differs in the use of small, dish-mounted, Brayton-cycle engines (i.e., gas turbines) in place of the large central steam engine of the PFDR/R.

As in the case of the previous PFDR concept, the PFDR/B system has a collector field consisting of two-axis tracking dishes. A cavity receiver is mounted at the dish focus. A working fluid is circulated through the receiver and transfers heat to the engine, which is located behind the receiver. The conversion efficiency of the small Brayton cycle from heat to shaft energy is not very sensitive to size. This fact, combined with the Brayton's low weight, enables the engine to be connected to the receiver. Although it would be somewhat more efficient to use a large central Brayton engine, the necessity to transport high-temperature gas with its associated losses would eliminate any engine efficiency gain. For the selected PFDR collector system, the field layout is rectangular with a ground cover ratio of 0.31, which results in a 5% annual energy loss from shadowing. The dishes are connected only by electrical lines through which DC power is transferred to the inverter.

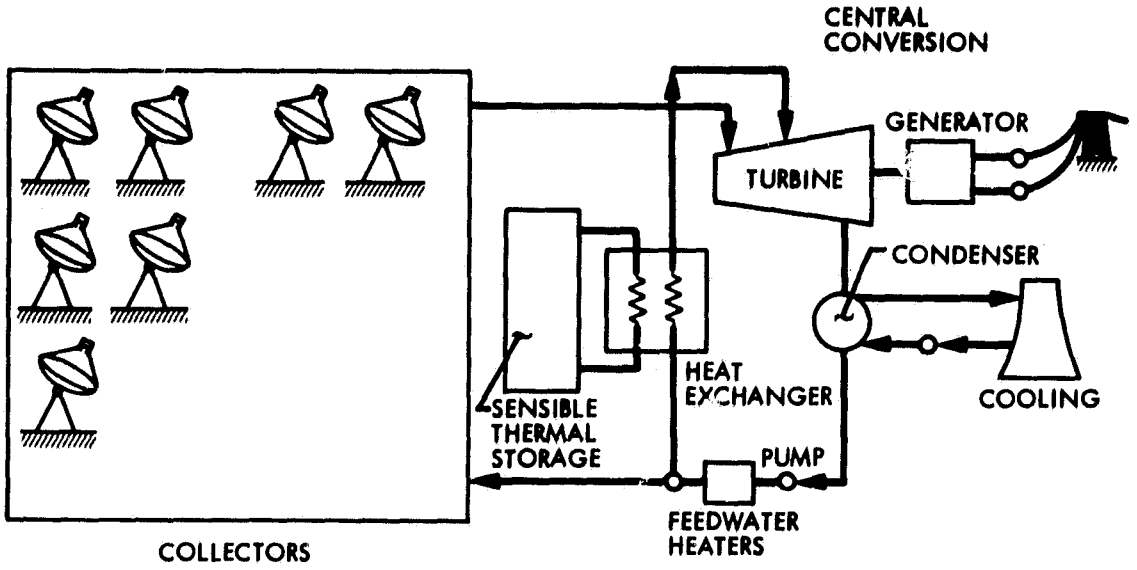

Figure 2-13. PFDR/R Power Plant Layout

Subsequently, AC power is then transferred to the substation. A typical PFDR/B schematic layout is shown on Figure 2-14. Figure 2-15 is a plant layout of a dish electric system. Energy storage is achieved with redox electrical storage. Thermal storage for periods of several hours or more is not suitable because of heat transfer difficulties and the problem of additional weight at the focal point. Buffer storage for short periods of several minutes might be desirable but was not considered in this study.

9. Point-Focusing Distributed Receiver/Stirling Engine (PFDR/S)

The PFDR/S system is identical to the PFDR/B system, with the exception of the energy conversion unit and receiver size. The PFDR/S engine assumed for this study is a kinematic Stirling design with the receiver serving as the engine head. Free-piston Stirling engines were not considered for this study because of their low state of development.

The collector field is similar to that of the PFDR/B and PFDR/R systems, but fewer dishes are required for the PFDR/S system since energy conversion is more efficient. The PFDR/S system also has a rectangular field layout with a ground cover ratio of 0.31, which results in a 5% annual energy loss from shadowing. The dishes are electrically interconnected. The plant uses electrical energy (redox) storage. Figures 2-14 and 2-15 also apply to the PFDR/S system.

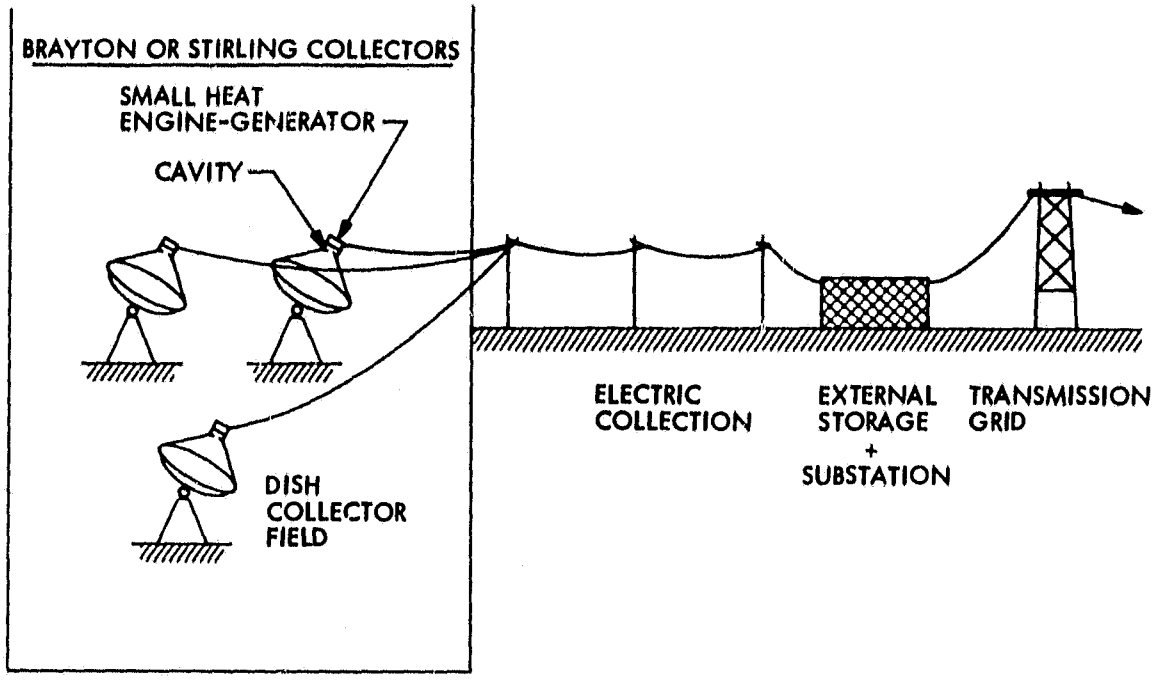

Figure 2-14. Schematic of PFDR/B and PFDR/S Systems

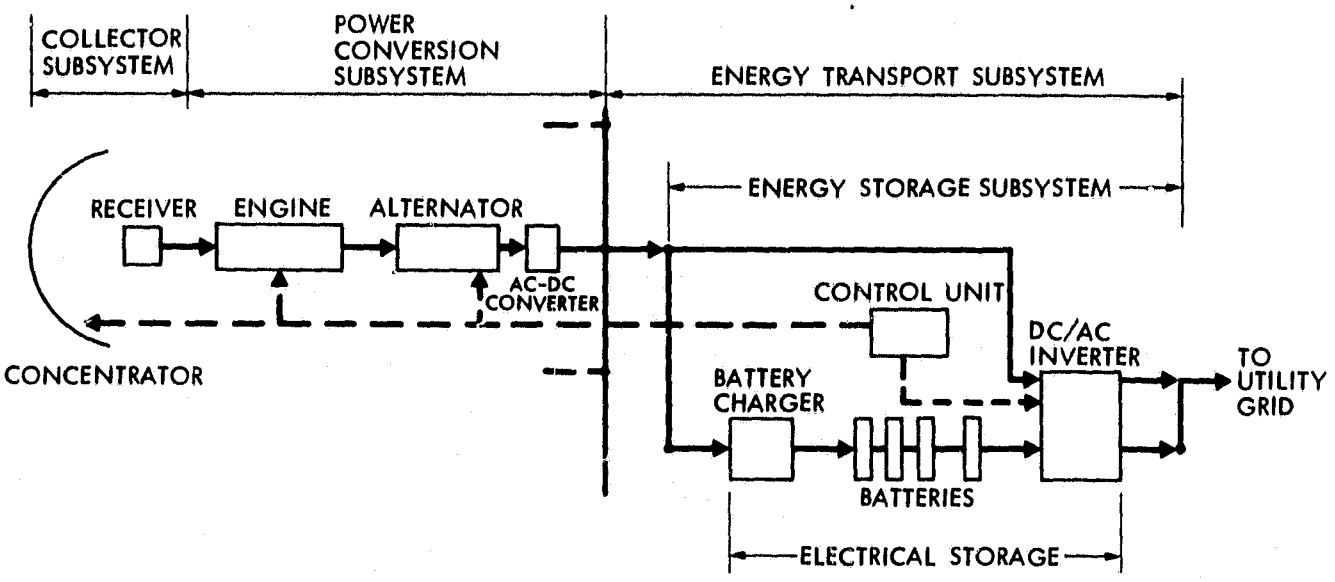

Figure 2-15. PFDR/B and PFDR/S Power Plant Layout

SECTION III

METHODOLOGY

A. INTRODUCTION

The generic plants evaluated in this study were ranked in terms of $\overline{BBEC}$ as determined by the SES II computer code. To calculate $\overline{BBEC}$, the code calculates annual electrical energy production from the system performance parameters. It also estimates annualized life-cycle costs. $\overline{BBEC}$ is the ratio of annualized life-cycle cost to annual energy production. To obtain these results, it was necessary to establish system and component costs and performance input parameters for all plants. Consistent data were developed through an extensive analysis and review of information supplied by equipment vendors, from open literature, and from previous work performed at JPL. With respect to the Brayton and Stirling engines, manufacturing cost estimates were developed for specific engine configurations on a piece-by-piece basis. The remainder of this section explains in detail the cost and performance methodology.

B. COST AND PERFORMANCE METHODOLOGY

To evaluate the generic plant systems, the cost and performance of the various component subsystems had to be characterized. Since the subsystems evaluated were in varying stages of development and production, it was necessary to use several different methodologies in determining the cost and performance data. The various subsystems were categorized into three developmental levels: present, mature, and advanced.

Subsystems in the present category exist today even though their use for solar power plants may require slight modification. To determine the cost and performance data for this group, manufacturer surveys and JPL-commissioned studies have been conducted. The subsystems in this category include energy transport and the balance-of-plant components; i.e., controls, land and site preparation, substations, shipping fees, spare parts, temporary facilities, operations crew, building maintenance, and the fees of A&E and construction management firms.

The mature subsystems are those that currently exist in prototype form, but which are considered for purposes of this study to have achieved an improved state of development. The assumption of mature technological development was applied to the concentrators, receivers, energy conversion systems, and storage systems wherever performance limitations or high costs of present technologies significantly impair economic feasibility. The principal differences between the mature and the present technologies are the assumptions that the mature group incorporates component refinements, design faults are eliminated, and production levels of 25,000 units annually are achieved by 1990. The cost and performance of these subsystems were determined by using published studies. Whenever possible, manufacturer review and confirmation were obtained regarding the data derived from these studies.

The advanced subsystems currently exist only in feasibility studies. The realization of these subsystems would require that the results of successful research and development activities be integrated into complete subsystem designs. The cost and performance estimates for this group were based on projected developments in materials, engineering designs, and manufacturing techniques. The subsystems in this category include thin-film, inflatable, and plastic-surfaced concentrators, inflatable troughs, and advanced Stirling and Brayton engines.

The cost and performance parameters established were reviewed for technical validity and internal consistency. These values then served as the basis for the calculation of $\overline{BBEC}$.

C. DESCRIPTION OF SOLAR ENERGY SIMULATION COMPUTER CODE (SES II)

The characteristic variation of $\overline{BBEC}$ with capacity factor for each of the nine generic systems was determined by means of a computer simulation model (Reference 3), which utilized the results of the subsystem cost and performance analysis as inputs. The simulation model, known as the Solar Energy Simulation code (SES II), consists of three major programs: the FIELD program calculates collector field thermal energy output for specific insolation and meteorological conditions; the POWER program determines the electrical power production of the power conversion subsystem under specified conditions for selected concentrator areas and storage capacities; and the ECONOMICS program calculates energy costs for specific plant configurations. The model transmits data from the performance code to the economics code and selects the minimum cost plant configurations.

The complete simulation of a solar power plant is accomplished by consecutive application of the three main programs, which are linked to operate as one. Even though each one can be executed independently, the second and third programs (POWER and ECONOMICS) require inputs that ordinarily are transferred from the first and second programs, respectively. Thus, POWER requires input from FIELD, and ECONOMICS requires data from POWER. Figure 3-1 illustrates the operation of the SES II model.

In the FIELD program solar insolation data are acted upon by the performance characteristics of the collector. Input energy is reduced when encountering each of the subsystems by optical and thermal energy losses until it is delivered to either the power conversion or the thermal storage units. Thus, the FIELD program begins with solar insolation and ends with the thermal energy delivered by the thermal energy transport system to either the power conversion or thermal storage units.

Most of the FIELD program output is used as input to the POWER program. Time, solar insolation, ambient temperature, net energy collected, and efficiency of the collector are transferred from FIELD to POWER.

The POWER program calculates the total electrical power that is generated during a one-year time period. The program also records energy into and out of storage and energy wasted. These factors are evaluated for selected values of concentrator area and storage time. The appropriate mode of plant operation

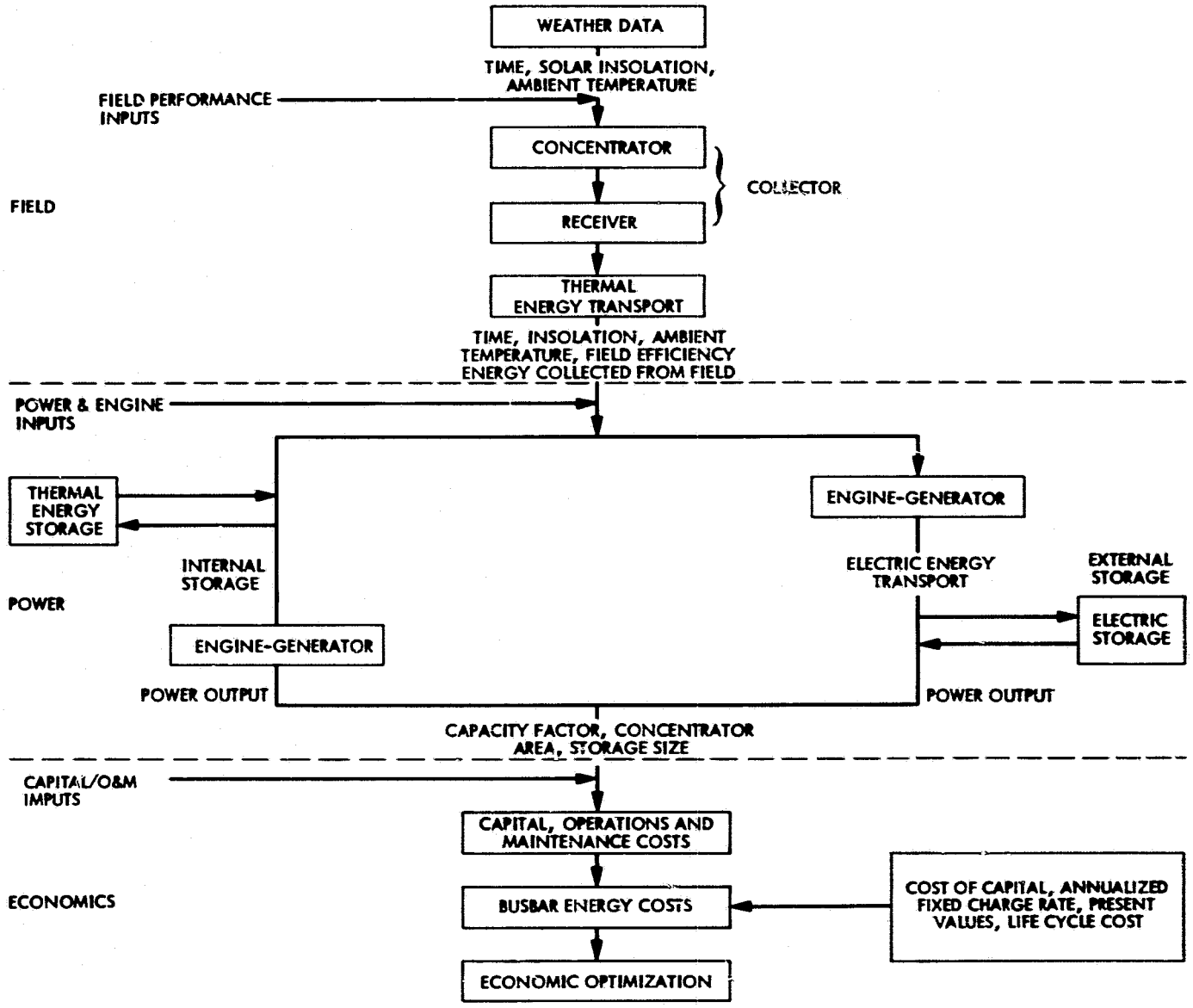

Figure 3-1. Simplified Flowchart Depicting the Operation of the SES II Computer Program

for hourly time increments is determined by the heat avail- able from the collector and the quantity of energy that is in storage. Both thermal and electrical storage systems can be addressed in POWER.

The ECONOMICS program determines capital and replacement/overhaul costs as well as operating and maintenance (O&M) costs for the power plant configurations being studied. It also calculates life-cycle cost and $\overline{\text{BBEC}}$. Once the costs have been calculated, this program optimizes each plant configuration by varying concentrator area and storage time, so that a minimum $\overline{\text{BBEC}}$ is obtained for varying capacity factors. A plot of capacity factor versus $\overline{\text{BBEC}}$ for all configurations is created, along with the minimum cost curve that joins the points of minimum $\overline{\text{BBEC}}$ for increasing values of capacity factor (see Figure 3-2).

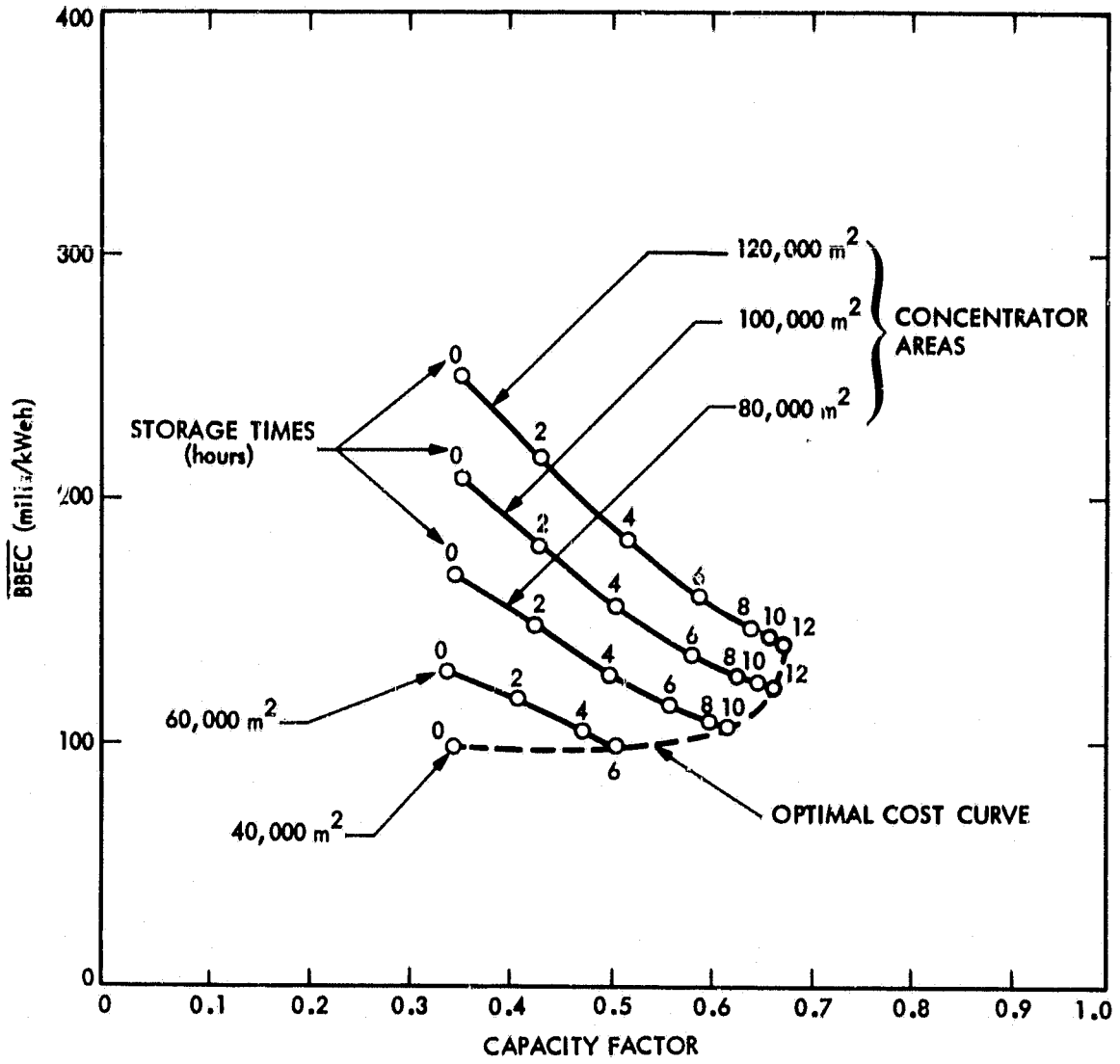

Figure 3-2. Example of Energy Cost Sensitivity to Capacity Factor Provided by the SES II Program

The algorithm within the ECONOMICS program, which calculates life-cycle cost and BBEC, was developed jointly by JPL and EPRI (Electric Power Research Institute) (Reference 5). It provides a standard technique for the calculation of consistent ranking of alternative energy system designs in terms of their cost-effectiveness for producing energy.

The costs addressed by this algorithm are those incurred as a direct result of purchasing, installing, and operating the energy system being studied. These costs are aggregated over the system lifetime and converted to a yearly basis. They are then divided by the expected yearly energy output of the specific system. The result is the BBEC for the system. If the system produces its predicted output, and if that output is sold at a price equal to its BBEC, the resultant revenues will recover exactly the full cost of the system during its lifetime, including a return on the investment of stockholders and creditors.

Levelized busbar energy cost is a single cost which represents an average of a distribution of varying charges. It is typical of the growing distribution of actual busbar energy costs because it represents a uniform distribution which, over the same time interval, has the same present value. Thus, the levelized charge represents an overcharge in early years and an undercharge in later years.

SECTION IV

SUBSYSTEM PRICE AND PERFORMANCE

This section presents the price and performance data of the various power plant subsystems as well as the associated rationale. As discussed in Section III, a major part of this effort was devoted to classifying the individual subsystems into three categories of development: present, mature, and advanced. Once the subsystem prices and performance were determined and reviewed, they were used as inputs to the SES II computer model so that overall generic plants could be equitably compared. The results of the simulation analysis are presented in Section V - Power Plant Cost and Performance Results. The individual subsystems to be discussed are collectors, energy transport, energy conversion, storage, and balance of plant.

A. COLLECTORS

To calculate collector price, a detailed evaluation of existing designs was performed for all collectors used in the study. The results of this effort showed that some designs have received more development and optimization than others. It was also deduced that all systems could benefit from the transfer of technology among the various concepts. Therefore, this transfer was assumed to take place in order to determine consistent production level costs for all systems. For example, Figure 4-1 shows that a heliostat concept may be readily adaptable to a dish system.

The basic collector components (reflective surface, receiver, receiver support, and foundation) were identified and compared with a baseline point-focusing central receiver system (Reference 22). In performing this analysis, studies conducted by manufacturing firms were reviewed. Some of these firms were E-Systems, Inc. (who evaluated the FMDF and PFCR collectors), Scientific-Atlanta, Inc. (LFDR-TR, LFDR-TC), and McDonnell Douglas Astronautics Company (PFCR, PFDR, LFDR-TC, and heliostat versus heliodish) (References 22, 23, 24, 25, 26).

Predicted collector operating characteristics and installed prices are given in Table 4-1. The two-axis concentrator systems (PFDR and PFCR) have the highest concentrator prices because of the utilization of more parts than either the line-focusing or non-tracking systems. The concentrator price includes the reflector, elevation tracking, and azimuth devices per unit concentrator area. The FMDF is also a two-axis system, but its concentrator does not move. Its receiver does the tracking and, therefore, it has low concentrator and high receiver prices. The receiver prices of the LFDR-TC and LFDR-TR systems are exceptionally low because most of the receivers are included in the price of the piping networks. The systems with the highest receiver support structure prices are those that use towers or movable struts. The low-cost receiver systems, such as PFDR and LFDR-TC, have fixed struts. The highest foundation prices are associated with stowable dishes and concentrators with large areas exposed to the wind.

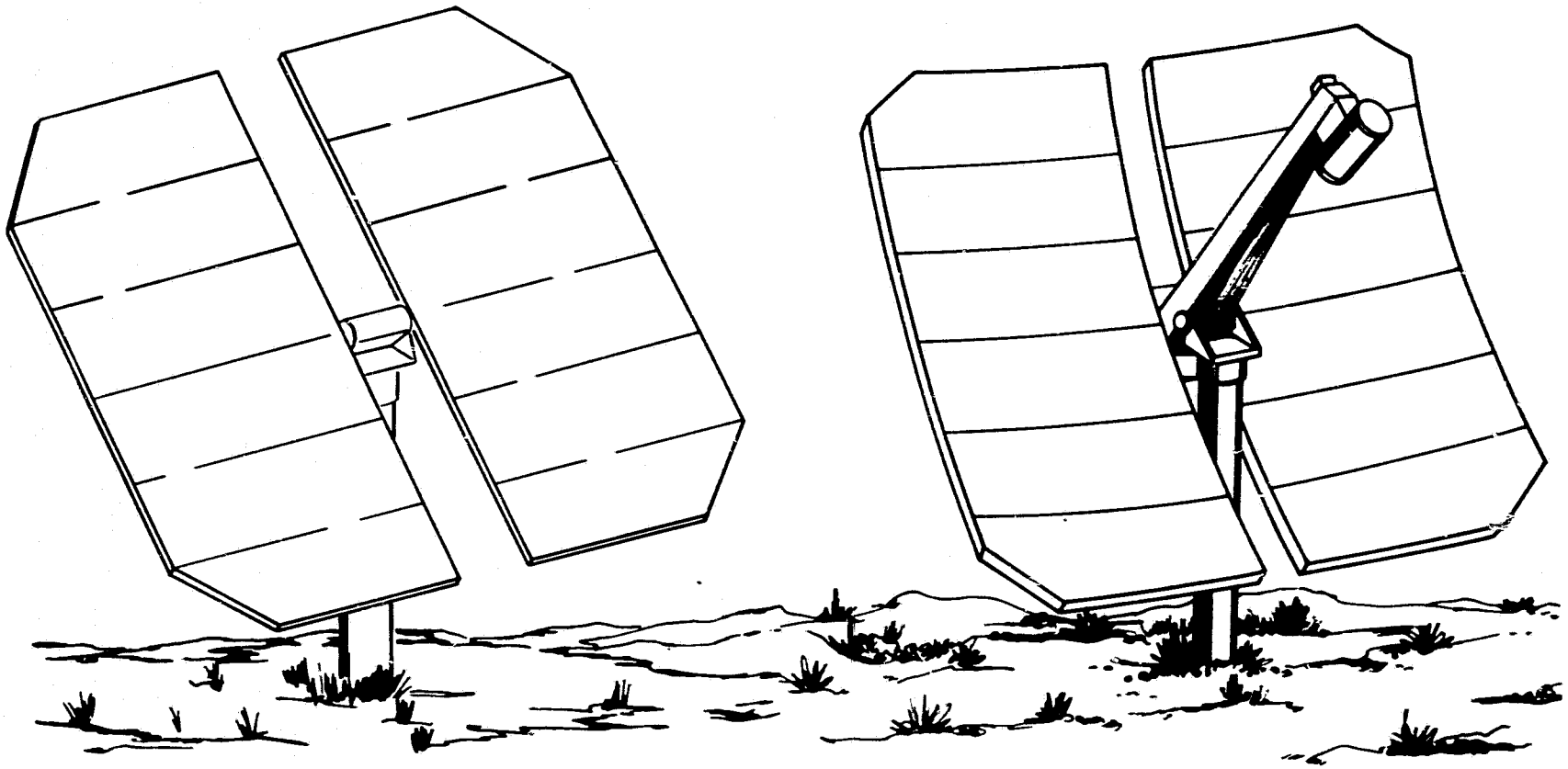

Figure 4-1. Adaptability of Heliostat Technology to Dish Systems

Table 4-1. Concentrator and Receiver Parameters

System	PFCR	PFDR/R	PFDR/S	PFDR/B	FMDF	LFCR	LFDR-TC	LFDR-TR	LCNT
				Operational Characteristics					
Type of Concentrator	Spherical	Parabolic	Parabolic	Parabolic	Spherical	Spherical	Moving Radial	Fixed Radial	Fixed Radial
Area of Each Concentrator Module (m^2)	49	92	92	92	2922	56	122	186	13
Receiver Operating Pressure (psig)	1500	1500	2000	0	1500	1500	50	50	50
				INSTALLED PRICES[a]					
Elevation and Tracking Device Price	15	15	15	15	0	15	15	0	0
Reflector Panel Price	34	43	43	43	34	34	34	30	30
Azimuth Device Price	10	10	10	10	0	0	0	0	0
Foundation Price[b]	16	18	18	18	12	16	10	8	8
Receiver Price	15	15	10	10	15	15	4	4	13
Receiver Support Structure Price	25	7	7	7	54	25	7	25	16
Total Price	115	108	103	103	115	105	70	67	67

[a]All prices are given in terms of $\$/m^2$ of concentrator area, 1978 dollars.
[b]Foundation prices are based on 30 mph design-point wind loading perpendicular to the concentrator or 90 mph in a stowed position, whichever produces the greatest load.

The values in Table 4-1 are based on production levels of 25,000 units annually as specified in the study's ground rule assumptions (Section I.C). Figure 4-2 shows how the installed concentrator price of the PFDR systems can vary with production level, while Figure 4-3 shows the PFDR/B and PFDR/S installed receiver price as a function of production level. These curves resulted from studies conducted by Sanders Associates, Acurex Corporation, General Electric Company, and Boeing Engineering and Construction Company (References 27, 28, 29, 30), and were used for sensitivity analyses with respect to production levels. These studies also determined collector maintenance costs by assessing failure rates and associated maintenance. An annual maintenance cost of 2.1% of initial concentrator price was established for all collectors. Therefore, the less complex collectors with a smaller number of components and lower initial prices also have lower maintenance costs.

1. Collector Optics

Several computer algorithms, which characterize the optics of each collector field, were used in order to determine field performance. The purpose of these models is to combine field performance with insolation in order to determine annual overall collector performance. The primary source of data for each system was:

System	Source
LCNT	University of Chicago, Argonne National Laboratory (References 6, 7)
LFDR-TC	Sandia National Laboratories (References 8, 9)
LFDR-TR	General Atomic Company (References 10, 11, 12)
LFCR	FMC Corporation (References 15, 16, 17 18)
FMDF	Texas Tech University, E-Systems, Inc. (References 19, 20, 21)
PFCR	McDonnell Douglas Astronautics Company, Sandia National Laboratories (References 13, 31)
PFDR/R,B,S	JPL, Ford Aerospace and Communications Corp. (Reference 32)

The collector performance data were used in conjunction with an insolation data tape for Barstow, California, in order to determine the quantity of energy that could be collected. Figures 4-4 and 4-5 illustrate overall collector field efficiencies for the summer solstice and the winter solstice. The efficiencies shown include losses resulting from blocking, shadowing, reflectance, angle of incidence, absorptance, radiation, convection, and conduction from the receiver.

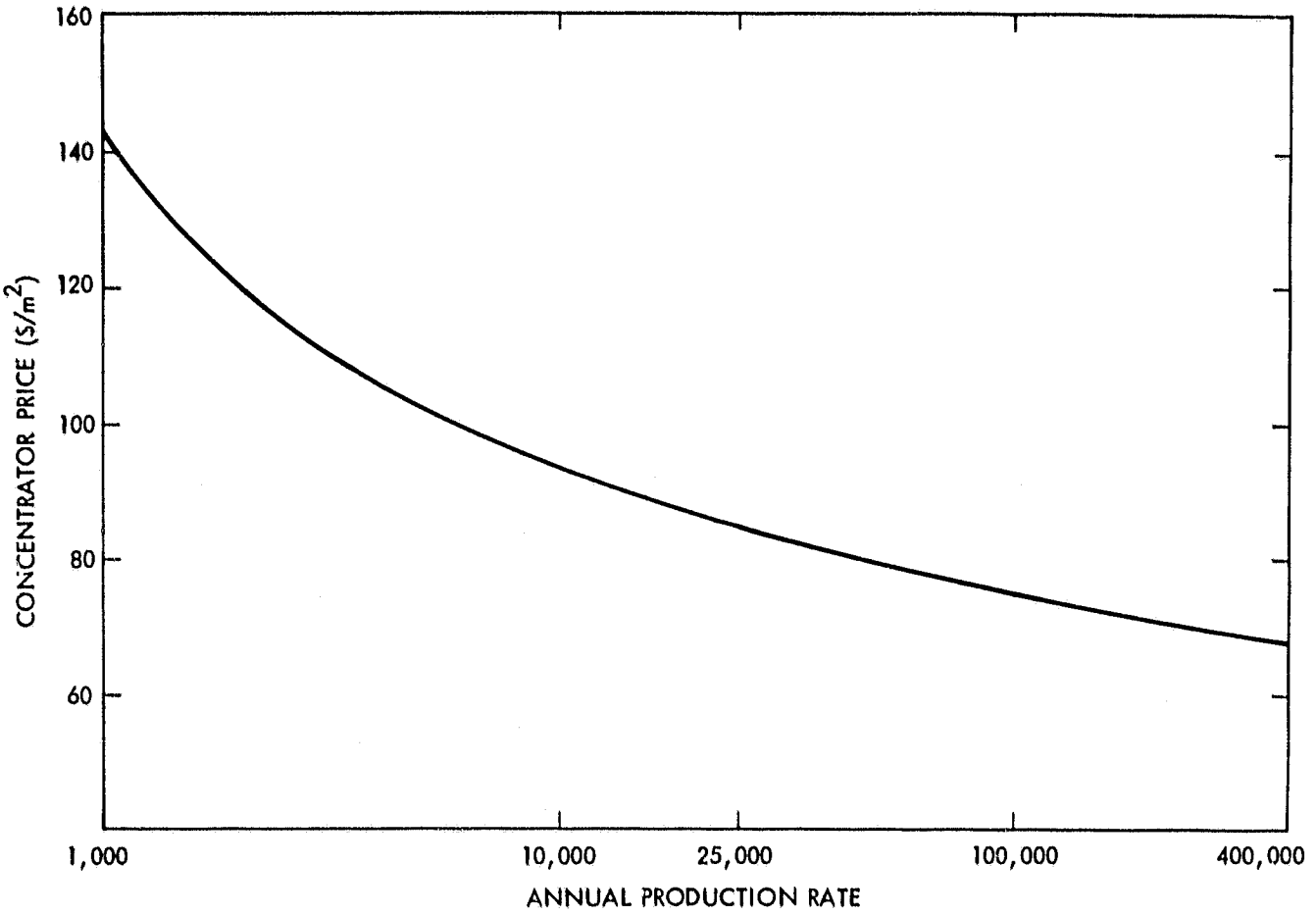

Figure 4-2. Concentrator Price as a Function of Annual Production Rate for PFDR Systems (1978 Dollars)

The PFDR systems have the highest efficiencies because they maintain alignment between the sun, concentrator, and receiver from sunrise to sunset throughout the year. The efficiency of the LCNT abruptly drops to zero 3-1/2 hours from solar noon because at that time the sun is beyond this system's acceptance angle. Unlike any other system, the LFDR-TC efficiency peaks four hours from solar noon. The focal plane of the line-focusing concentrator has a north-south orientation and forms an angle with the sun, which results in smaller cosine losses and a lower incidence angle late in the day and early in the morning. The deviation shown for the FMDF system in Figure 4-4, which occurs three hours from solar noon, is due to the utilization of two different operating temperatures needed in order to maximize performance.

B. ENERGY TRANSPORT

Three types of energy transport were used by the generic plants evaluated in this study: electric, thermal, and optical.

The PFDR/R, LFDR-TC, LFDR-TR, LCNT, FMDF, and LFCR systems use thermal transport. Energy is delivered from the collector to the power conversion

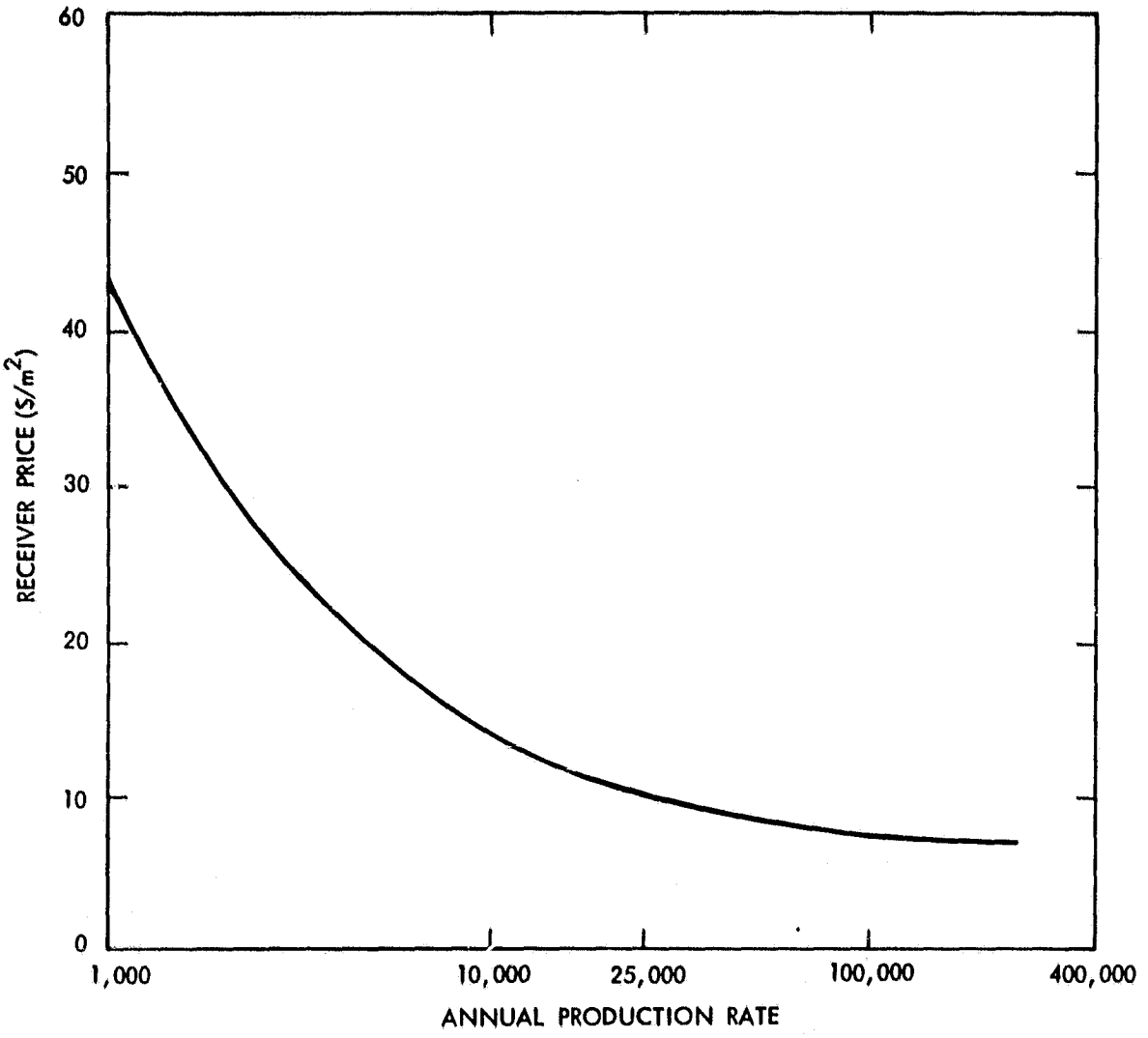

Figure 4-3. PFDR/S and PFDR/B Receiver Price as a Function of Annual Production Rate (1978 Dollars)

unit by use of a hot transport fluid. In addition, the PFCR and LFCR systems use small amounts of thermal transport even though the majority of their primary transport is optical.

The thermal transport subsystems assumed for this study are a result of the combined efforts of architectural and engineering (A&E) firms, manufacturers, and JPL (References 33, 34, 35). A mature design was used, employing insulated flexible metal hoses to connect the collectors to main header pipes. The utilization of the insulated flexible metal hose eliminates the need for omega (thermal expansion) loops, pipe supports, field welding, field installation of insulation, and also reduces the installation time of the thermal transport subsystem. Therefore, although the initial price of the flexible metal hose is greater than that for a conventional piping system, the installed price is significantly less because of labor cost reductions. Flexible hose technology and optimized grid layouts are currently undergoing

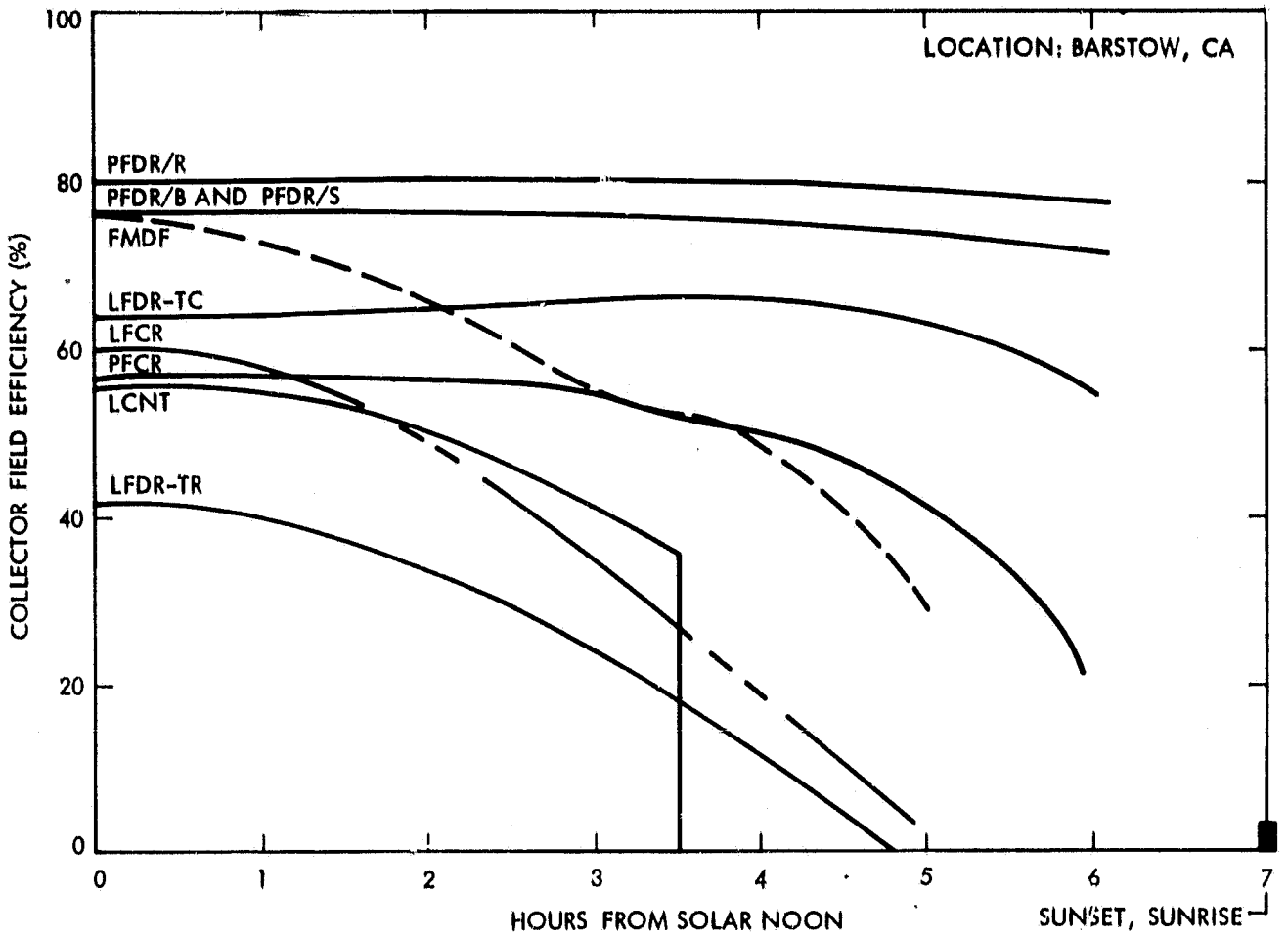

Figure 4-4. Collector Field Efficiency as a Function of Time at Summer Solstice (transport losses are not included)

further study. Additionally, JPL studies (Reference 36) indicate that the use of labor-saving and cost-reducing techniques such as automated factory procedures and semi-automated field assembly of pipe networks, can yield low costs comparable to those of the flexible pipe approach.

The performance characteristics of the various thermal transport systems were calculated with a computer code developed by JPL (Reference 37). This program uses data on the transport fluid, physical properties of the transport subsystem, insulation, and a plant cost estimate to calculate various energy transport system configurations for given collector networks. The program calculates the optimal transport and insulation configurations by trading off the amount of energy lost against the prices of the transport grid and the solar power plant. This is based on the assumption that if 10% of the heat collected is lost in the transport system, then the solar plant must be 10% larger to compensate for this loss. The final transport grid and operations and maintenance (O&M) costs were obtained by using data from an A&E firm

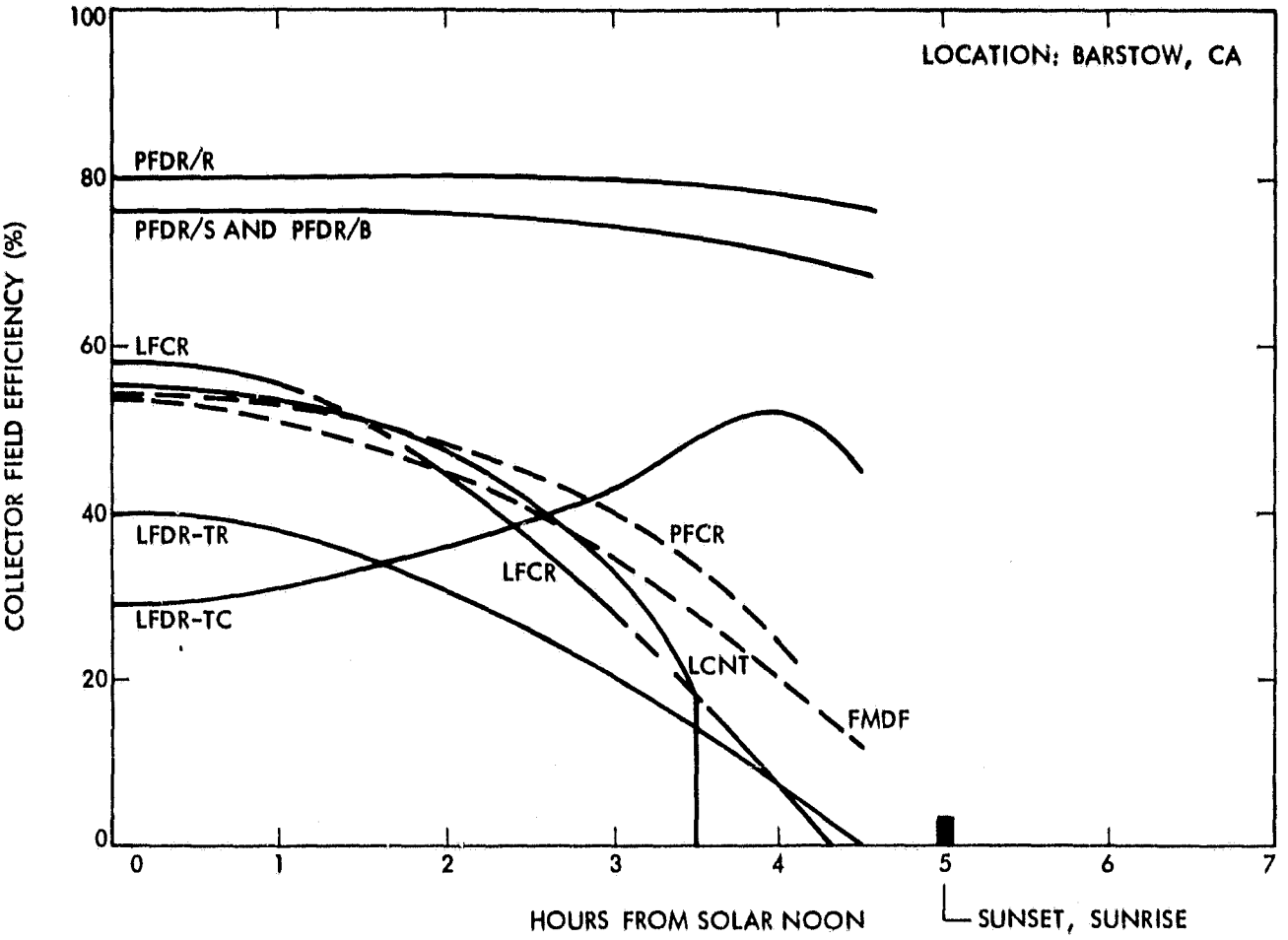

Figure 4-5. Collector Field Efficiency as a Function of Time at Winter Solstice (transport losses are not included)

and from estimates of flexible hose manufacturers. The collectors were assumed to be arranged so that the quantity of required pipes and valves would be minimized.

The PFDR/B and PFDR/S systems generate electricity at their focal point and, therefore, utilize electrical transport. This type of transport consists of power processing equipment between the generator and the substation field busbar. It includes remote control contactors, circuit breakers, engine auxiliaries, dish controls, and cable. The efficiency of this subsystem was estimated to be 95%. The electrical transport prices for the dispersed power generation systems were developed by a JPL contractor (Reference 38). The results of the thermal and electrical transport analysis are shown in Table 4-2. The elimination of trenching through the use of above-ground armored cables and the use of DC electrical cables to transmit control signals are two examples of possible further developments that are currently under investigation.

Table 4-2. Thermal and Electrical Transport Subsystem Parameters

Generic Plant Type	Pumping Loss (%)	Heat Loss (kWt/m^2)[a]	Electrical Loss (%)[b]	Thermal Transport Price ($/$m^2$)[a]	Installed Electrical Transport Price ($/$m^2$)[a]
PFDR/R	0.3	0.048	-	30.23	-
LFDR-TC	1.8	0.051	-	49.22	-
LFDR-TR	1.8	0.051	-	28.00	-
LCNT	3.5	0.084	-	42.95	-
FMDF	0.003	0.093	-	8.29	-
LFCR	0.004	0.023	-	0.15	-
PFCR	-	-	-	0.19	-
PFDR/B,S	-	-	5.0	-	13.24

[a]Values are given in terms of concentrator area, prices in 1978 dollars.
[b]Includes line, substation, and miscellaneous parasitic losses.

As mentioned earlier, the PFCR and LFCR systems use optical transport. Since optical transport involves the reflection of light from the concentrator to the receiver, only a minimal physical transport subsystem from the elevated receiver to the ground is needed. Therefore, a small additional transport price was included to the engine/generator price.

C. ENERGY CONVERSION

In an attempt to optimize the collector-engine combinations, the large variation in collector systems necessitated the consideration of several thermodynamic cycles. These included steam-Rankine, organic-Rankine, Stirling, and Brayton cycles. The engine design and price parameters are summarized in Table 4-3.

1. Rankine Cycle (Steam)

The steam-Rankine cycle studied was a typical axial-turbine/generator assembly, which has evolved to a point of almost maximum efficiency. It has also been well documented and, therefore, represents a present technology.

Table 4-3. Engine Design and Price Parameters[a] for 1-, 5-, and 10-MWe Systems

Engine Type	Steam Rankine	Organic Rankine	Organic Rankine	Organic Rankine	Stirling	Brayton
Solar Plant	FMDF LFCR PFCR PFDR/R	LFDR-TC	LFDR-TR	LCNT	PFDR/S	PFDR/B
Inlet Temperature (°C)	510	370	300	285	815	815
Design Ambient Temperature (°C)	50	50	50	50	50	50
Engine Life (yr)	30	30	30	30	30	30
Generator Efficiency (%)	95	95	95	95	94	89
Engine Size (kWe) - 1 MWe plant	1,000	1,000	1,000	1,000	25	23
- 5 MWe plant	5,000	5,000	5,000	5,000	25	23
- 10 MWe plant	10,000	10,000	10,000	10,000	25	23
Engine Efficiency (%) - 1 MWe plant	34	26	23	22	42	35
- 5 MWe plant	35	27.5	25	24	42	35
- 10 MWe plant	36.5	28.5	26	25	42	35
Engine/Generator Price ($ x 10^3/eng) - 1 MWe plant	300	425	425	425	5.12	3.16
- 5 MWe plant	1,500	2,125	2,125	2,125	5.12	3.16
- 10 MWe plant	3,000	4,250	4,250	4,250	5.12	3.16

[a]1978 dollars.

Note, however, that the sophisticated features of large steam-Rankine units, such as feedwater heating and multi-stage turbines, are generally not available in sizes smaller than 10 MWe. However, since there is no technical barrier that prevents this level of sophistication from being incorporated in smaller engines, it was assumed that a mature engine unit incorporating these features could be utilized in the 1-, 5-, and 10-MWe plants evaluated in this study. Therefore, this unit was used for the PFDR/R, PFCR, LFCR, and FMDF systems. Price and performance were established by evaluating manufacturer surveys (Reference 39). Based on data generated by Sandia National Laboratories, engine efficiencies were derived for various temperatures and plant sizes (References 40 to 48). These are shown in Figure 4-6. The engine operating and price parameters used for this engine are given in Table 4-3. The part-load characteristics are shown in Figure 4-7. Operations and maintenance (O&M) data for the steam Rankine were also obtained by JPL from manufacturer surveys and are given in Table 4-4 (Reference 49).

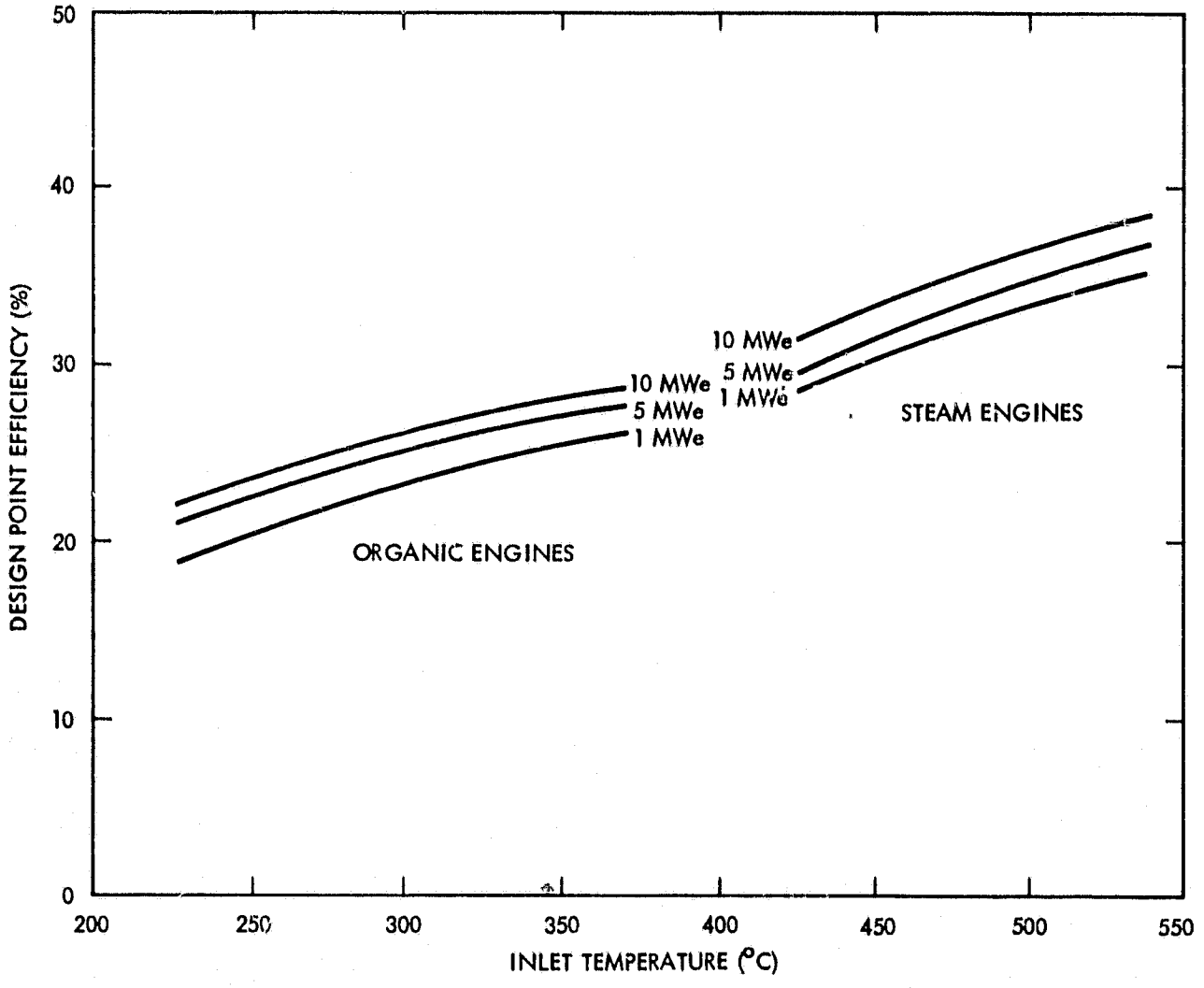

Figure 4-6. Steam and Organic Rankine Engine Efficiencies

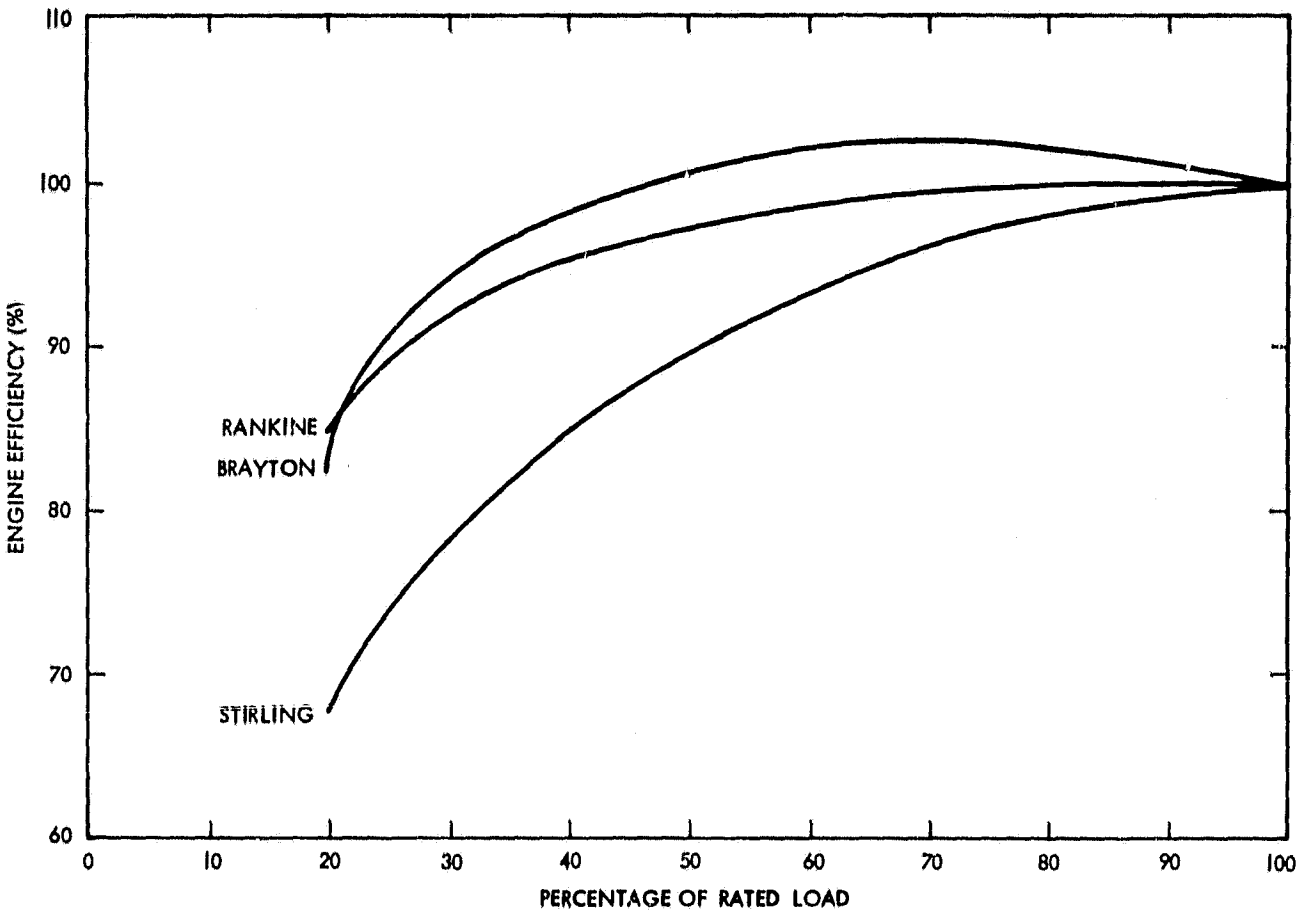

Figure 4-7. Engine Part-Load Efficiencies

2. Rankine Cycle (Organic)

Organic-Rankine engines operate on the same thermodynamic cycle as steam-Rankine engines. The main difference is the working fluid, which for the organic cycle can include toluene, flourinol, or several fluids in the Freon family. Toluene was selected for this study because the other fluids have lower maximum operating temperatures. Figure 4-6 shows the engine efficiency as a function of plant size and temperature. The part-load characteristics of the organic-Rankine cycle were assumed to be the same as those for the steam-Rankine cycle shown in Figure 4-7. The systems that use the organic-Rankine cycle are the LFDR-TC, LFDR-TR, and LCNT. The operating conditions and prices are given in Table 4-3 (References 39 to 48). O&M cost (see Table 4-4) was derived from a General Electric study, which investigated organic-Rankine engines as pipeline bottoming cycles (Reference 49).

When the organic-Rankine cycle is used, the machinery price is higher than that of the steam cycle because the organic cycle requires an additional boiler (vapor generator) in order to exchange heat between the thermal transport fluid and the working fluid of the engine. This additional price covers the organic-fluid boiler and all associated controls and piping.

Table 4-4. Engine Maintenance Costs for 5-MWe Plant Size (1978 Dollars)

Engine Type and Size (kWe/engine)	Steam Rankine 5,000[a]	Organic Rankine 5,000[a]	Stirling 25	Brayton 23
Annual Maintenance	Inspection and service of condenser, feed pump, lube system, pipes, valves, water purification system -- $8,500/yr	Inspection of boiler, condenser, feed pump, lube system, pipes, valves, fire control subsystem -- $9,350/yr	Quarterly inspection and service of helium, oil, and external auxiliary equipment -- $50/yr	Change of heat exchanger screen and inspection of engine -- $50/yr
Periodic Maintenance	Engine overhaul at 40% of original cost every 35,000 h -- $600,000/engine	Engine overhaul at 40% of original cost every 35,000 h -- $850,000/engine	Replace piston rings, seals, and coolant every 7,500 h period (except when engine is overhauled) -- $135/engine Engine overhaul at 40% of original cost every 15,000 h -- $1,658/engine	Replace starter and heat exchanger fan motor every 15,000 h -- $250/engine; No engine rebuild necessary

[a]Maintenance costs for 1,000 and 10,000 kWe engines are proportional to the values given on this table.

3. Stirling Cycle

The Stirling engine assumed for this study was the P-40 model, which is being developed by United Stirling-Sweden (USS) (Reference 50). There were two primary reasons for selecting this engine. First, it has a peak efficiency at about 25 kWe, which closely matches the capability of the 11-m concentrator dish under investigation by JPL. Second, the P-40 engine and the closely related P-75 have received more development than any other Stirling engine (Reference 50). Other less-developed Stirling options include engines that have free pistons and/or ceramic components that are capable of higher temperatures, as well as kinematic engines from other manufacturers. However, these less developed systems currently lack sufficient data to be incorporated into this study.

Since the P-40 engine assumed for this study operates at constant inlet and outlet temperatures and constant speed, there is no need to show the effect of operating temperature on engine efficiency in a figure. As the solar flux changes, the pressure of the helium working fluid is changed, thus regulating the amount of power delivered by the engine. Pressure regulation is achieved by an engine-mounted compressor, tank, and servo valve arrangement. Because of the small size (about 25 kWe) of the P-40 engine, different plant sizes do not affect engine efficiency since identical engines can be added as necessary.

The performance characteristics were obtained from USS and are shown in Table 4-3 (Reference 50). The part-load characteristics are shown in Figure 4-7 (Reference 38). The mass-production cost of the Stirling engine resulted from a cooperative study conducted by JPL and USS. Market price estimates of the Stirling engine are not currently available because it is not yet commercially mass-produced. In order to obtain an estimate of the future market price for such items, a methodology known as the Interim Price Estimation Guidelines (IPEG) was created by JPL (Reference 51). It utilizes the cost of purchasing manufacturing equipment, production levels, the plant size needed to produce equipment, labor cost, material cost, supply cost, operating energy expense, indirect expense, and overhead expense to calculate a manufacturer price. IPEG was exercised for both the Stirling and Brayton engines based on the economic assumptions given in Section I. These results are shown in Table 4-3 and are presented as a function of annual production level in Figure 4-8. Alternator price data were obtained from industrial alternator suppliers (Reference 52) and are presented as a function of volume in Figure 4-9. Maintenance costs for the Stirling engine were derived from information supplied by USS, Ford Aerospace and Communications Corporation, and JPL (see Table 4-4 and References 38, 50).

4. Brayton Cycle

Open-cycle, closed-cycle, supra-atmospheric, and sub-atmospheric Brayton engines were among the several configurations evaluated. For several reasons the sub-atmospheric engine, which was developed by Garrett AiResearch Manufacturing Company for the Gas Research Institute and DOE for space-conditioning applications, was chosen for this study (Reference 53). First, the sub-atmospheric engine operates with a non-pressurized receiver, while the supra-atmospheric engine requires a pressurized receiver. Since a pressure

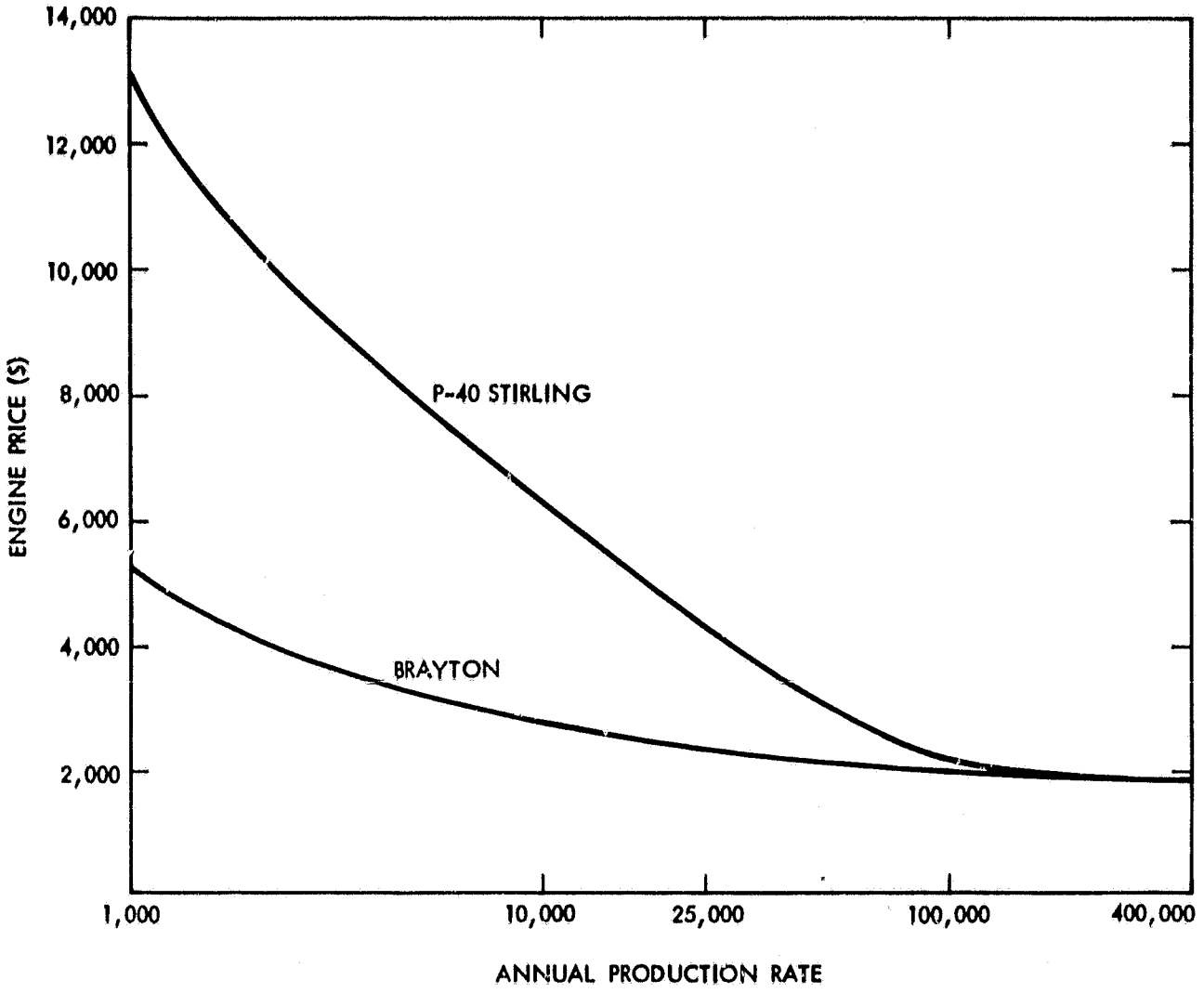

Figure 4-8. Stirling and Brayton Engine Prices versus Annual Production Rate (1978 Dollars)

drop through the receiver adversely affects overall engine efficiency, and since the pressure drop through the non-pressurized receiver was significantly lower, the sub-atmospheric engine in combination with the non-pressurized receiver was determined to be a more cost-effective choice. Second, a study conducted for JPL by Sanders Associates indicated that non-pressurized receiver designs cost about 50% less than a pressurized design (Reference 27). Other factors, which also contributed to this decision, were lower maintenance and possible market synergism between heat pump and solar uses. JPL is also investigating other advanced-Brayton engines such as engines with ceramic components, closed-cycle engines, automotive gas turbines, and engines that operate with working fluids other than air.

The selected Brayton cycle does not contain various components usually associated with large, industrial gas turbines. Fuel, fuel lines, filters,

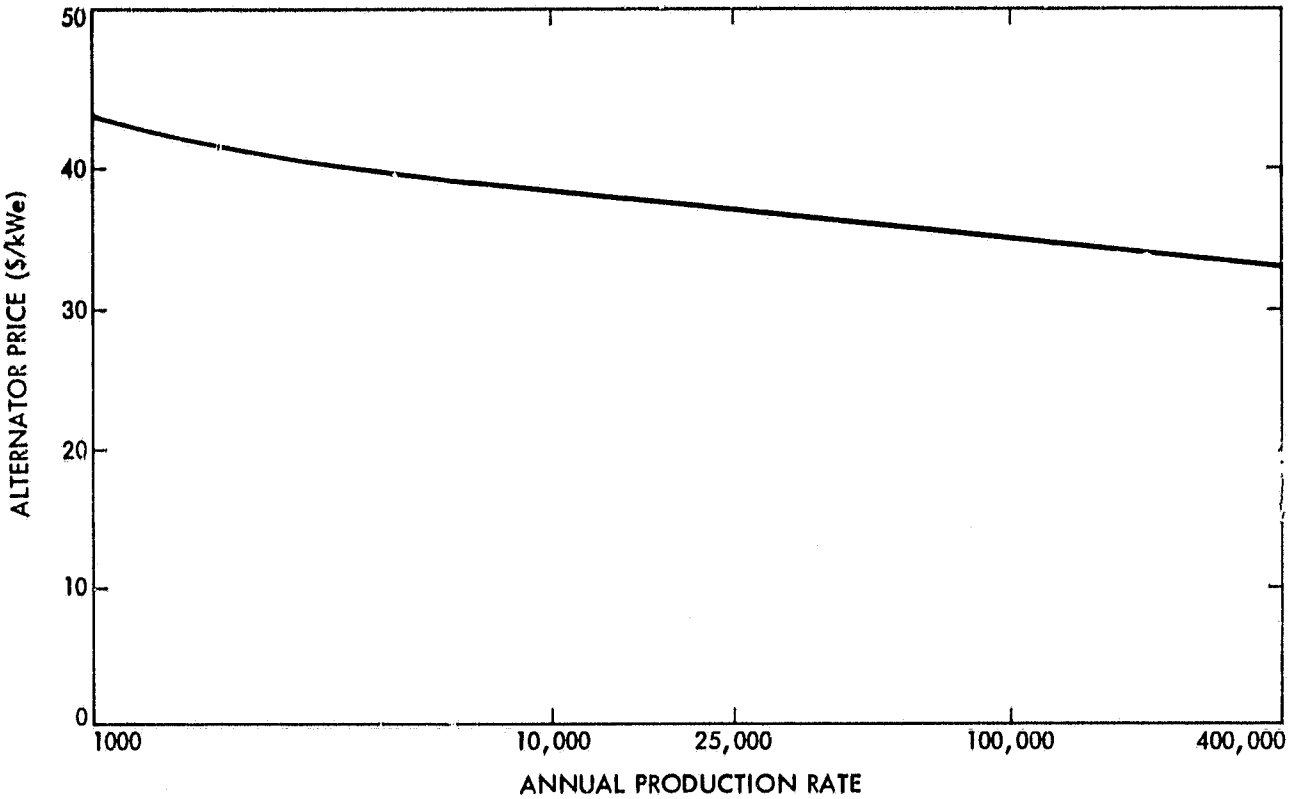

Figure 4-9. Stirling Alternator Price as a Function of Annual Production Rate (1978 Dollars)

pumps, governors, combustion cans, ignition system, and associated maintenance are not necessary for a solar engine. Furthermore, the solar design uses gas bearings that eliminate the need for an oil lubrication system. The use of these bearings is consistent with their implementation by the aircraft industry. Therefore, the costs and maintenance of the Brayton cycle were reduced from those of large, industrial gas turbines.

The final major difference between the solar Brayton and existing industrial turbines relates to the time between major engine overhauls. The type of fuel burned can have a significant impact on this interval. For instance, engines that have large time increments between overhauls (70,000 to 80,000 hours) burn clean fuels, such as natural gas. This fuel minimizes the occurrence of warping, liquid slugs, blade erosion, and corrosion. Since the solar Brayton burns heated gas (currently air) and operates most of the time at part-load and constant turbine inlet temperature, it therefore has low cyclic stress levels. It was assumed that the time between major engine overhauls would be greater than the life of the solar plant.

The price and performance characteristics of this engine were developed by a method similar to that used for the Stirling engine. These data are shown in Table 4-3 and Figure 4-7. The alternator price is the same as that for the

Stirling engine (see Figure 4-9). As was the case with the Stirling engine, there was only one design-point operating temperature for the Brayton, and the plant size did not affect engine efficiency. JPL, in conjunction with Garrett AiResearch Corporation, determined the engine mass-production cost (Reference 54). As discussed earlier, the Brayton engine price was estimated by applying the IPEG methodology. The O&M cost for the solar-Brayton engine (see Table 4-4) was developed with information from manufacturers, such as General Electric Company and Garrett AiResearch Corporation, and was appropriately adjusted (References 55, 56, 57, 58).

5. Advanced Engine Concepts

JPL, in conjunction with LeRC, is also currently investigating advanced (early 1990s) engine designs, which can achieve higher efficiencies or lower levels of maintenance than mature technologies through component improvements and/or higher temperature operation. These investigations include the development of an advanced low-maintenance Stirling engine as well as adaptation of an advanced automotive gas-turbine (Brayton) engine for high-temperature solar use. Table 4-5 lists the price and performance goals for these engines as described in the advanced solar engine plan of JPL and LeRC (Reference 59).

If these advanced engines become commercially available, the plants that use them should obtain favorable performance relative to the plants that do not use them. Even though the data exist in terms of goals, an attempt was made to survey the potential improvement that could be achieved by implementing these engines. The results of this analysis are shown in Section V.D - Sensitivity Analysis.

Table 4-5. Advanced Engine Price and Performance Goals (1978 Dollars)

Engine	Brayton	Stirling
Nominal Engine Size (kWe)	30	30
Inlet Temperature (°C)	1100	815
Engine/Generator Efficiency (%)	40	40
Engine/Generator Price ($/engine)	5400	5400
Annual Maintenance ($/kWeh)	0.001	0.001

D. STORAGE

When storage is implemented, the distributed engine systems (PFDR/B and PFDR/S) use electrical storage, while the central engine systems (all others) use thermal storage. Even though electrical storage is less efficient and more costly than thermal storage, electrical storage was assumed for the distributed engine systems because of the various piping complexities of thermal storage. Also, thermal storage is generally too heavy to be feasible for focal-point mounting. Therefore, its use is associated with the transport of heat from the focal point to the ground.

Many types of electrical storage systems are presently under development. Because of cost trade-offs, system efficiencies, and expected lifetimes, redox storage was chosen instead of battery storage. The redox storage subsystem chosen was based on designs of LeRC and associated DOE cost goals (Reference 60). Lead-acid battery storage was also examined in a sensitivity analysis (see Section V.D).

Based on the temperature range of operation, the thermal storage mediums assumed were Hitec, Syltherm 800, and Caloria HT43. Table 4-6 shows the various plants and the storage subsystems that were examined. The pricing of the thermal-energy storage subsystems was achieved by reviewing a survey conducted by General Electric Co.-Tempo Division (Reference 61). Additionally, the prices of the storage tank systems, storage materials, and installation were based on a McDonnell Douglas Astronautics Company report (Reference 22).

In addition to storage tanks, the thermal and redox energy storage systems also consist of piping and miscellaneous related equipment. A previous study conducted for JPL stated that the pipe-grid maintenance costs would amount to approximately 1.7% of the pipe system capital cost (Reference 33). Because of the additional presence of pumps and controls, this factor was raised to 1.9% for all the thermal and redox storage systems. This 1.9% figure was also used for the lead-acid battery storage systems, which do not have tanks, piping, or pumps. However, it was assumed that the lead-acid battery's fans, ducting, and controls would have the same price.

It was found that Hitec, Syltherm, and the redox medium, as used in this study, would be stable for a long period and that no replacement would be necessary, while Caloria would require 9% of its fluid to be replaced annually (Reference 62). This was accounted for in the maintenance cost.

E. BALANCE OF PLANT

The balance-of-plant system includes those items which were not covered previously. These include controls and cables, land cost, site preparation, temporary facilities, substations, control buildings, fees, shipping costs, and spare parts.

Table 4-6. Storage System Parameters (1978 Dollars)

	PFDR/B	PFDR/S	PFDR/R	PFCR	FMDF	LFCR	LFDR-TC	LFDR-TR	LCNT
Storage System[a]	Redox (Pb-Acid)	Redox	Hitec	Hitec	Hitec	Hitec	Sylltherm-Hitec	Caloria	Caloria
Storage Efficiency (%)	71 (72)	71	85	85	85	85	85	95	95
Storage not Retrieved (%)	10 (20)	10	10	10	10	10	10	10	10
Storage Equipment Price ($/kW)[b]	160 (65)	160	48	48	48	48	43	16.2	16.2
Storage Size Price ($/kWh)[b]	9.75 (50)	9.75	5.4	5.4	5.4	5.4	7.35	5.6	5.6
Storage Life (yr)	30 (6)	30	30	30	30	30	30	30	30

[a]The values associated with lead-acid batteries, which were used for senstivity analysis, are shown in parentheses beneath the redox values.
[b]Units are in kWe for the PFDR/B and PFDR/S and kWt for all other systems.

1. Controls

The control subsystem includes those devices necessary to regulate the total system, such as input-output devices, interconnecting cables, and microprocessors. This involves two main components. A supervisory system monitors the various microprocessors throughout the collector field, while the microprocessors control the various collectors, engines, and valves. The price data originated from work conducted by JPL contractors and from microprocessor manufacturers (References 38, 63, 64, 65, 66).

Since the most complex control subsystems were required by the dish-mounted engine plants (PFDR/B, PFDR/S), they were analyzed first and then the prices were related to all other systems as applicable. Two-axis tracking systems without dish-mounted engines (PFDR/R, PFCR) were assumed to use less powerful microprocessors and smaller input-output devices. Also, because of large concentrator areas, one-axis tracking system controls were assumed to be more cost efficient than two-axis tracking system controls. Fixed-concentrator systems were assumed to have limited controls. Table 4-7 presents the control prices assumed.

Table 4-7. Balance-of-Plant Prices -- Controls/Cables and Site Preparation (1978 Dollars)

	Controls/Cables ($/m^2)[a]	Site Preparation ($/acre)[b]
PFDR/B	15.0	14,200
PFDR/S	15.0	14,200
PFDR/R	8.6	14,200
PFCR	8.6	14,200
FMDF	0	24,700
LFCR	3.9	17,800
LFDR-TC	3.9	17,800
LFDR-TR	3.9	17,800
LCNT	0	24,700

[a] $/m^2 of concentrator area
[b] $/acre of land area

The O&M factor for the control subsystem for all plants was assumed to be 1.9% of the installed subsystem price. This value was based on a study of thermal transport and the assumption that the control system would require more equipment, but less labor.

2. Land and Site Preparation

The cost of land was one of the basic study assumptions ($5,000 per acre). The cost of site preparation was based on the experience of the Shenandoah Solar Total Energy - Large Scale Experiment Project and a study by the Burns and McDonnell Company (References 14, 67). In deriving this cost, items such as long access roads, major ground shaving, and tree removal were omitted in order to reflect site preparation prices associated with a production level plant in favorable locations. One-axis tracking and non-tracking systems require flat sites along the axis of rotation, while two-axis tracking systems are not as sensitive to terrain irregularities. Therefore, grading prices were adjusted accordingly (see Table 4-7).

3. Substation

The substation consists primarily of switchboards, transformers, and disconnect switching along with various other components such as gravel, lightning arrestors, and meters. Its physical makeup and price were estimated by JPL (Reference 68). The price estimates of three substations rated at 1, 5, and 10 MWe are shown in Table 4-8.

4. Miscellaneous

The miscellaneous balance-of-plant prices are those associated with control buildings, fees, shipping costs, spare parts, temporary facilities, operations crew, and building and ground maintenance costs. All these prices are presented in Table 4-8.

Buildings that may be required for the power conversion machinery or storage are included in the hardware prices for the appropriate subsystems. Also, outside storage buildings for spare parts would be utilized whenever possible.

There are two engineering and construction fees that are associated with the plant: an architectural and engineering (A&E) fee, and a construction management fee. Primarily, the A&E firm designs the plant, develops the construction drawings, prepares and obtains the necessary reports and permits, coordinates the logistics, purchases the component parts, and assists in the startup of the plant. This A&E fee is typically 10% of the installed capital cost. Generally, this percentage will decrease for larger jobs and will increase for smaller jobs. However, 10% was used for all plants in this

Table 4-8. Balance-of-Plant Prices -- Substation and Miscellaneous (1978 Dollars)

A&E Fees ($)	10% of Installed Capital Cost
Construction Management Fees ($)	10% of Installed Capital Cost
Shipping Fees ($)	1.5% of Equipment Price
Spare Parts ($)	5% of Equipment Price

	Plant Size		
	1 MWe	5 MWe	10 MWe
Temporary Facilities	$120,000	$120,000	$120,000
Substation	$ 69,000	$345,000	$690,000
Control Building	$ 64,000	$ 64,000	$ 64,000
Operations Crew (all except LCNT)	$ 4,000/yr	$ 8,000/yr	$ 8,000/yr
Operations Crew (LCNT)	$ 9,600/yr	$ 19,200/yr	$ 19,200/yr
Building and Ground Maintenance	$ 10,400/yr	$ 20,800/yr	$ 20,800/yr

study. Once the background work from the A&E firm is complete, a construction management firm takes delivery of the material, assembles it, and provides the necessary manpower, skills, and equipment. The construction management fee of this firm is typically 10% of the installed capital cost.

a. Shipping Costs. One hidden cost for all equipment is incurred for shipping the equipment from the manufacturer's plant to the site where it will be utilized. Research was conducted with the aid of Sandia National Laboratories and indicated that shipping costs are generally 1.5% of the equipment price.

b. Spare Parts. In a commercial plant, a quantity of spare parts must be on hand in order to maintain the plant with minimum loss of energy production. A generally accepted rule of 5% of the equipment price was used to obtain the spare parts price.

c. Temporary Facilities. During the construction phase, temporary facilities will be required to house records and plans, construction office, and some sensitive construction equipment. Items that fall into this category include:

(1) Contractor's office
(2) Architect's office
(3) Electric and water services
(4) Heating and cooling services
(5) Janitorial services
(6) Lavatories
(7) Signs
(8) Tool sheds
(9) Security
(10) Fences, walks, barricades
(11) First-aid equipment
(12) Dust and noise controls
(13) Communication equipment

The estimated price for these items was $120,000.

d. Operations Crew Cost. It was assumed that the solar power plants will be remotely monitored from a single dispatcher site. This arrangement is similar to currently utilized methods of controlling substations from a central site.

It was assumed for 5- and 10-MWe plants that one dispatcher could monitor and control five plants (10 plants for 1 MWe). Therefore, the yearly cost of a dispatcher, which was assumed to be $40,000 per year, was $8,000 per plant ($4,000 per 1-MWe plant).

These values were used for all systems except for the LCNT, which requires monthly collector adjustments. For 5- and 10-MWe plants, it was assumed that two men, each adjusting one collector every two minutes, would require 80 hours per workmonth to adjust the field. The rate for this type of skill was calculated at $10 per hour or $19,200 annually. This value was reduced by 50% for 1-MWe plants.

e. Building Maintenance Costs. Housekeeping costs will be incurred for all plants. Building maintenance services, such as janitorial, maintenance, and grounds keeping, will be required along with supplies, such as paints and fencing materials. This was estimated by assuming the cost of one man, full time, at $10 per hour. The resulting cost of $20,800 annually was assumed to cover all of the above services and supplies for all plants.

SECTION V

POWER PLANT COST[1] AND PERFORMANCE RESULTS

A. INTRODUCTION

This section presents the results of the cost and performance analysis for the various generic power plants as determined by the SES II computer program. The first results given are the total subsystem costs and annual average efficiencies for each plant. These results are followed by the BBEC results of the simulation analysis. Also presented is a total plant cost breakdown of capital, insurance, taxes, and O&M. The results of a sensitivity analysis are also provided. This analysis evaluates the impact of changes in the input assumptions having the greatest projected uncertainties.

B. SUBSYSTEM COST AND PERFORMANCE RESULTS

The component and subsystem cost and performance values determined in Section IV were used as inputs to the SES II model in order to calculate overall system performance and energy costs. The average hourly efficiencies of the collector, power conversion unit, and overall power plant as analyzed by SES II are given in Table 5-1. These results are for 5-MWe power plants with no storage. In accordance with Section IV, the point-focusing systems that utilize cavity receivers have the highest collector efficiencies (74% for the PFDR/S and PFDR/B). The PFDR/R is slightly lower (72%) because of thermal transport losses.

The average annual power conversion efficiencies include losses incurred by the engine, alternator, and electrical transport subsystems. The effects of part-load engine efficiency, plant dispatching methodology, and ambient temperature are included in the average annual efficiency.

The Stirling engine system, PFDR/S, which has the highest design-point engine efficiency, also has the highest annual average power conversion efficiency (36%). The power conversion efficiency is also high (26 to 29%) for the Brayton and steam-Rankine systems (PFDR/B, PFCR, PFDR/R, FMDF, and LFCR).

The overall average plant efficiency is defined as the annual energy delivered to the busbar divided by the quantity of energy received by the concentrator. Therefore, the overall plant efficiency is the product of the collector and power conversion efficiencies. The PFDR/S, which has the highest collector and power conversion efficiencies, also has the best overall plant efficiency (26%). The other point-focusing systems (PFDR/B, PFDR/R, and PFDR) also have high plant efficiencies, which range from 17 to 21%.

---

[1] In this section, cost refers to the market price paid by the utility.

Table 5-1. Annual Average Plant Efficiencies for 5-MWe Plants With No Storage (%)

Location: Barstow, CA

System	Collector[a]	Power Conversion	Overall Plant
PFDR/S	74	36	26
PFDR/B	74	28	21
PFDR/R	72	29	21
PFCR	59	29	17
FMDF	43	27	12
LFDR-TC	43	23	10
LFCR	36	26	9
LFDR-TR	28	21	6
LCNT	26	21	5

[a]Includes thermal transport losses where applicable.

The subsystem total capital cost (plant construction cost) for each generic plant at the 5-MWe size, as well as the optimal (lowest energy cost) no-storage concentrator area, are presented in Table 5-2. The balance-of-plant costs include such items as spare parts, construction management fees, A&E fees, temporary facilities, land, shipping, site preparation, installation, checkout, and substations. The values on Table 5-2 do not include the effects of inflation, annual O&M costs, or engine overhaul costs.

The optimal no-storage concentrator area is determined by the overall plant efficiency and dispatching strategy. The dispatching strategies assumed were equivalent for all systems. Each plant delivers power equal to or less than its rating whenever insolation is available. Therefore, plants with higher efficiencies require smaller concentrator areas to produce equivalent quantities of energy. Since the concentrator is a major cost driver, the point-focusing systems have the lowest subsystem total costs. The lowest cost system, PFDR/S ($5.26 M), is also the system that has the highest efficiency.

C. PERFORMANCE RESULTS

Figure 5-1 presents the results of the performance and $\overline{\text{BBEC}}$ analysis for all power plants at the 5-MWe size. The costs shown at the varying capacity factors represent the optimal, least expensive configurations of concentrator areas and storage capacities for each generic plant. $\overline{\text{BBEC}}$ values are expressed in 1978 dollars. The dashed line on the left side of each curve represents configurations that have no storage. An abrupt change in the slope of the curves occurs once storage is added. This happens because there is only one optimal no-storage case for each system (at the lowest point on the dashed curve) and once the $\overline{\text{BBEC}}$ curve slope begins to increase rapidly, the addition of storage mitigates the rise.

The two-axis tracking systems have the lowest $\overline{\text{BBEC}}$s. The point-focusing systems vary from 89 mills/kWeh at a capacity factor of 0.31 to 130 mills/kWeh

Table 5-2. Capital Costs for 5-MWe Power Plants With No Storage[a] ($ x 10^6; 1978 Dollars)

Location: Barstow, CA

	PFDR/S	PFDR/B	PFDR/R	PFCR	FMDF	LFCR	LFDR-TC	LFDR-TR	LCNT
Area (m^2)	18,000	23,000	24,000	27,000	31,500	35,000	45,000	56,000	55,000
Concentrator	1.22	1.56	1.61	1.59	0.95	2.03	2.21	1.68	1.65
Receiver	0.30	0.38	0.52	1.08	2.17	1.66	0.46	1.61	1.60
Power Conversion	1.09	0.94	1.50	1.50	1.50	1.50	2.13	2.13	2.13
Transport	0.24	0.30	0.73	0.01	0.26	0.01	2.21	1.57	2.36
Balance-of-Plant Cost	2.41	2.80	2.83	3.07	2.84	3.94	3.51	3.93	3.96
Total Cost	5.26	5.98	7.19	7.25	7.72	9.14	10.52	10.92	11.70

[a]Replacement costs are not included.

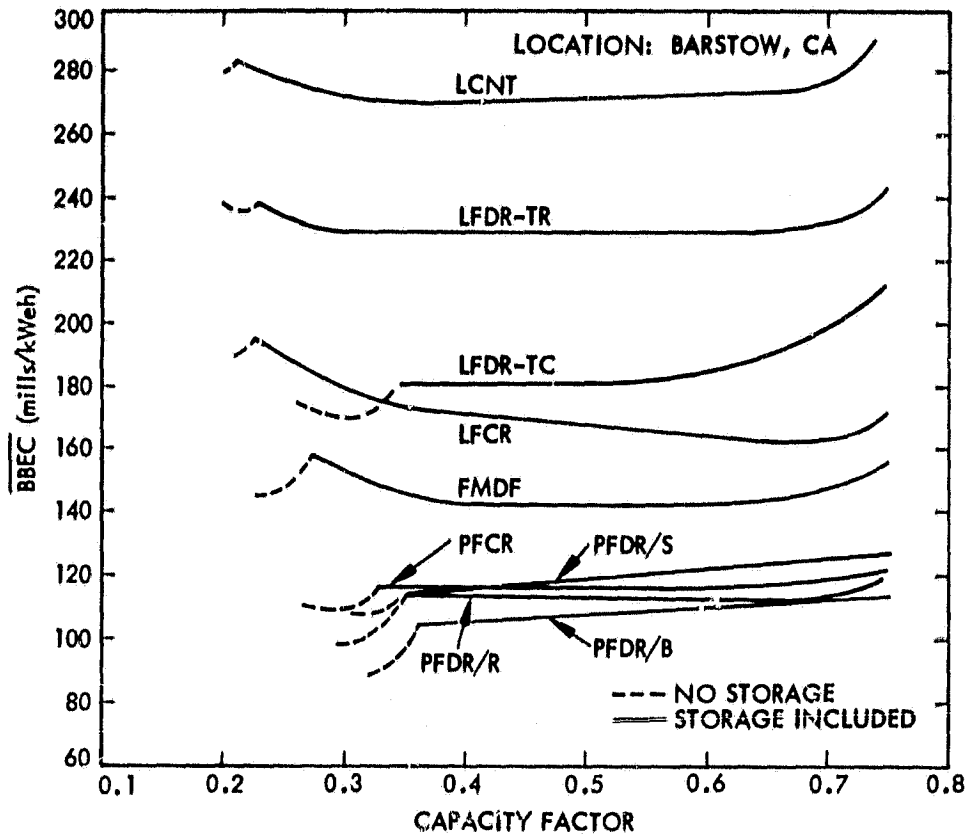

Figure 5-1. Energy Cost as a Function of Capacity Factor for 5-MWe Power Plants (1978 Dollars)

at a 0.75 capacity factor. Meanwhile, the single-axis tracking or non-tracking systems vary from 163 mills/kWeh at a 0.68 capacity factor for the LFCR system to 289 mills/kWeh at a capacity factor of 0.75 for the LCNT system. The distributed engine PFDR/B is the best overall performer at 89 mills/kWeh with no storage at the 0.31 capacity factor, 106 mills/kWeh at the 0.4 capacity factor, and 114 mills/kWeh at the 0.70 capacity factor. The second best performer with no storage is the distributed engine PFDR/S at 98 mills/kWeh. The second best performer with storage and the overall best central engine system is the PFDR/R (114 mills/kWeh at 0.40 and 0.70 capacity factors).

One result of particular note is that of the PFDR/S system. Even though the capital cost for this system was the lowest (see Table 5-1) and its system efficiency was the highest (see Table 5-2), the PFDR/S still drops to second, third, or fourth place (depending on capacity factor) in terms of $\overline{\text{BBEC}}$. This is primarily the result of the Stirling engine's higher overhaul costs relative to the other systems.

It does not appear that the addition of storage significantly impacts the relative cost and performance ranking, although it should be noted that the slopes of the cost curves for the electrical storage systems (PFDR/S and

PFDR/B) increase slightly when compared with those systems that utilize high-temperature thermal storage. This is due to the higher cost and lower efficiency of electrical storage. Also, thermal storage allows the engines to operate at design-point ratings for longer periods of time. Therefore, the better performing systems (PFDR/B and PFDR/S), which utilize electrical storage, do not have as much of a cost advantage at higher capacity factors.

The LFDR-TC system also has a positive increasing slope, even though it employs thermal storage, because its storage medium is Caloria, which is relatively expensive. The LCNT, LFDR-TR, and LFCR systems have curves with negative initial slopes. This is due to the fact that as capacity factor increases, the engines are used more effectively while engine price becomes a lower portion of total life-cycle costs. Furthermore, the addition of relatively inexpensive storage to achieve higher capacity factors does not outweigh this impact. The three curves of the LCNT, LFDR-TR, and LFCR systems reach a minimum energy cost when the continued addition of storage no longer results in large performance improvements. (All $\overline{\text{BBEC}}$ values begin to increase rapidly when storage time extends beyond 16 hours, since on most days a sunrise would occur before all storage was utilized. Therefore, the cost of excess capacity is incurred, while the extra generation capability cannot often be utilized.)

The lowest-cost, no-storage case for each system in Figure 5-1 is displayed in bar-chart form in Figure 5-2. This case is important for two primary reasons. First, the application of solar power to a utility network, where all of the energy produced would be supplied to a grid, may reduce the need for storage. Second, because of the nature of energy load demand, most peaking- and intermediate-load power plants operate at annual capacity factors of 0.50 or less (Reference 69). The capacity factors at no storage vary between 0.20 and 0.32. Therefore, storage may not play an important role if plants are operated at relatively low capacity factors. The no-storage $\overline{\text{BBEC}}$ varies from 89 to 145 mills/kWeh for the two-axis tracking plants. The no-storage $\overline{\text{BBEC}}$ of the one-axis tracking and non-tracking systems are higher and vary from 171 to 275 mills/kWeh.

Figure 5-2 also shows the cost distribution for the various plants. The capital charges (which include the concentrator, the receiver, the power conversion unit, energy transport, balance of plant, and engine overhaul costs) account for 43 to 46% of the total $\overline{\text{BBEC}}$ that would be charged to consumers. The remainder consists of income taxes and insurance (40 to 44%) and O&M (10 to 17%). These percentages are based on the assumption that $\overline{\text{BBEC}}$ has the same component breakdown as the present value of life-cycle cost. It was also assumed that the capital charges are adjusted for the tax effects of depreciation.

As can be seen in Figure 5-2, the engine overhaul cost component of the PFDR/S system (10 mills/kWeh), as opposed to the low overhaul cost of the PFDR/B system (2 mills/kWeh), moves the PFDR/S system up to the second lowest cost position. This difference is accentuated by the fact that income taxes and insurance cost are proportional to capital costs plus overhaul. The PFDR/B system also has low power conversion costs, which improve its standing relative to the other systems.

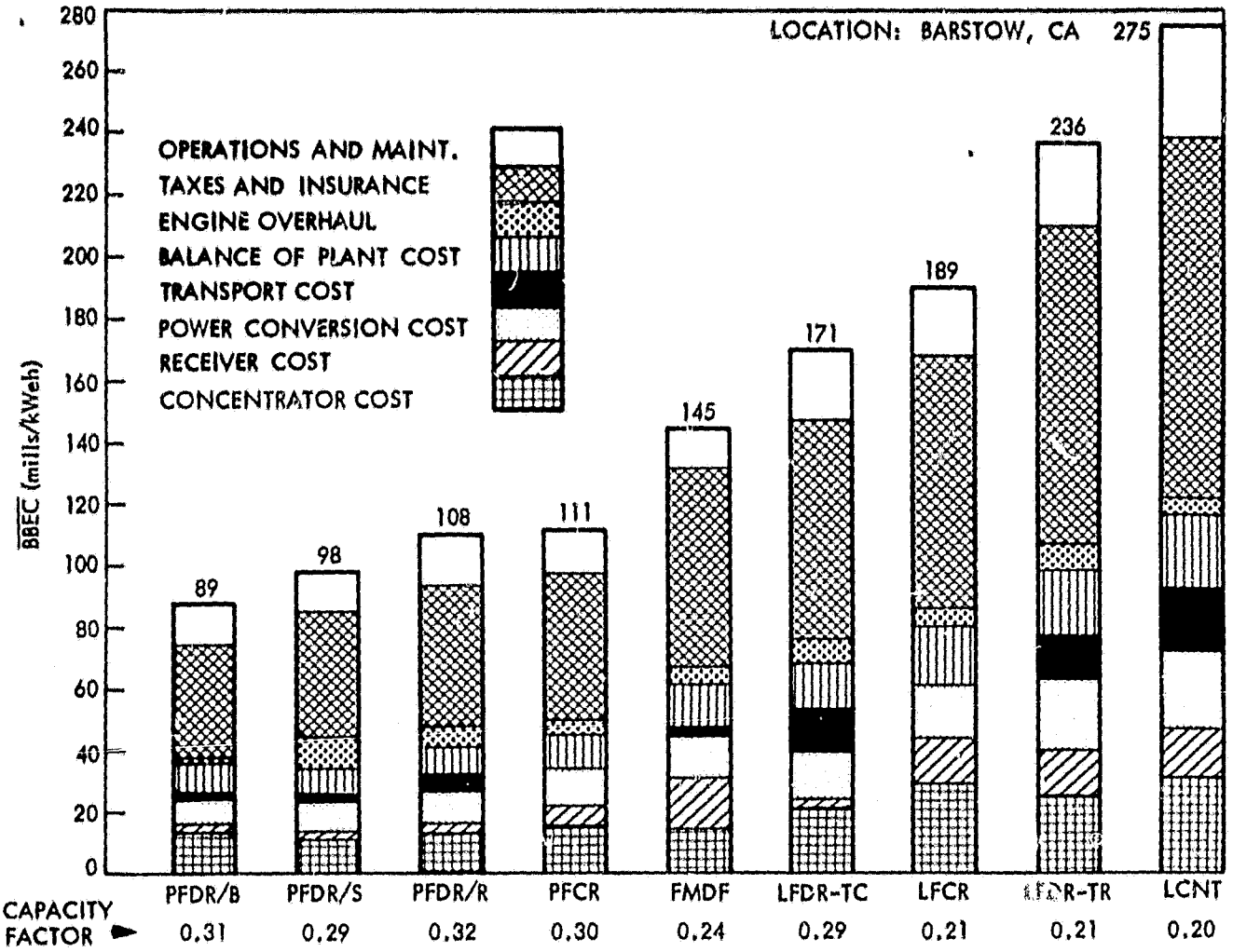

Figure 5-2. Cost Distribution for Optimal No-Storage 5-MWe Power Plants (1978 Dollars)

The LFCR, LFDR-TR, and LCNT systems have the highest collector costs, since their inefficient collector fields require large concentrator areas. These large areas also cause a high balance-of-plant component for these systems. The FMDF system has a higher receiver cost component than any other system because of its expensive support structure. The LCNT, LFDR-TC, and LFDR-TR systems have expensive energy transport systems. This is more evident with the LCNT system, which appears to be competitive with the LFCR and LFDR-TR when only the concentrator, receiver, and power conversion units are considered. However, the LCNT's very large piping system drives the transport cost to 24 mills/kWeh. Furthermore, it must be remembered that income taxes and insurance cost are directly proportional to total capital cost. This factor accentuates any capital cost differential between the systems. Finally, the costs of the different plants shown on Figure 5-2 represent varying capacity factors. This is due to the differing performance and physical characteristics of the various plants. However, higher no-storage capacity factors (about 0.30) were generally associated with lower energy costs. Costs based on equivalent capacity factors can be achieved by the introduction of storage (See Figure 5-1).

Figure 5-3 shows the energy cost curves for the better performing systems with storage at a plant size of 1 MWe. It can be seen that $\overline{BBEC}$ has increased when compared with the 5-MWe case. There are two reasons for this: (1) fixed-cost items such as the operations crew, building and ground maintenance, and temporary facilities make up a higher proportion of total costs, while the energy generated is lower than that for the 5-MWe case; and (2) the systems requiring large central Rankine engines (FMDF, PFCR, and PFDR/R) use smaller, less-efficient engines to generate 1 MWe. On the other hand, the distributed engine systems (PFDR/B and PFDR/S) use fewer engines of the same size and efficiency for generating 1 MWe. Therefore, the distributed systems are slightly more favorable in the 1-MWe case when compared with the central engine systems. The PFDR/B is the lowest-cost system at 1 MWe (114 mills/kWeh at the 0.4 capacity factor, and 118 mills/kWeh at the 0.7 capacity factor).

The energy cost curves for the lowest cost central and distributed power generation plants (PFDR/R and PFDR/B) are shown in Figure 5-4 at the 10-MWe size. At this size the $\overline{BBEC}$s of the two systems are very close. The PFDR/R system now has the lowest $\overline{BBEC}$ at capacity factors between 0.5 and 0.7 (108 to 112 mills/kWeh). The PFDR/B is still the lowest cost system at the 0.4 capacity factor (104 mills/kWeh).

When going from 1 to 5 MWe, the $\overline{BBEC}$ of the PFDR/R system decreases by 7 to 9%; whereas, in moving from 5 to 10 MWe, the improvement varies between 2 and 5% (see Figure 5-5a). With respect to the PFDR/B system, the two decreases

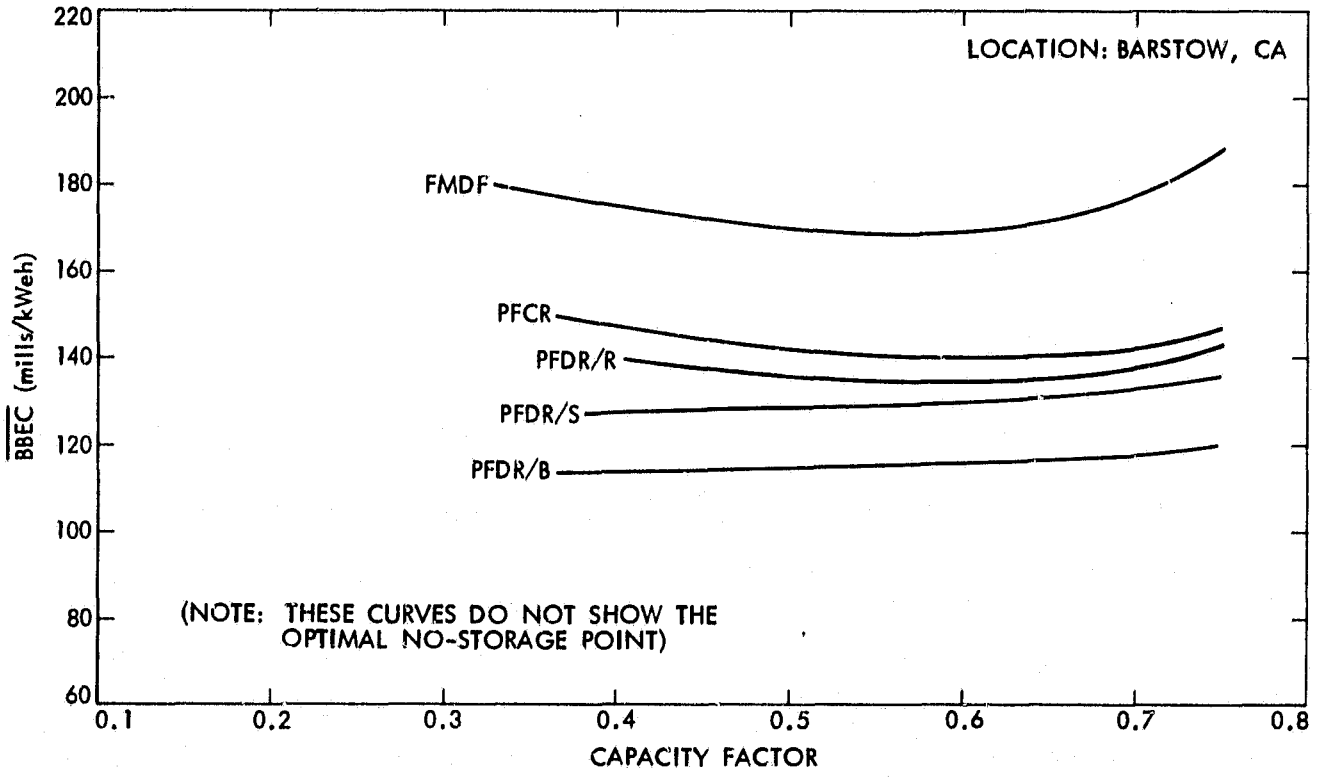

Figure 5-3. Energy Cost as a Function of Capacity Factor for Selected 1-MWe Power Plants (1978 Dollars)

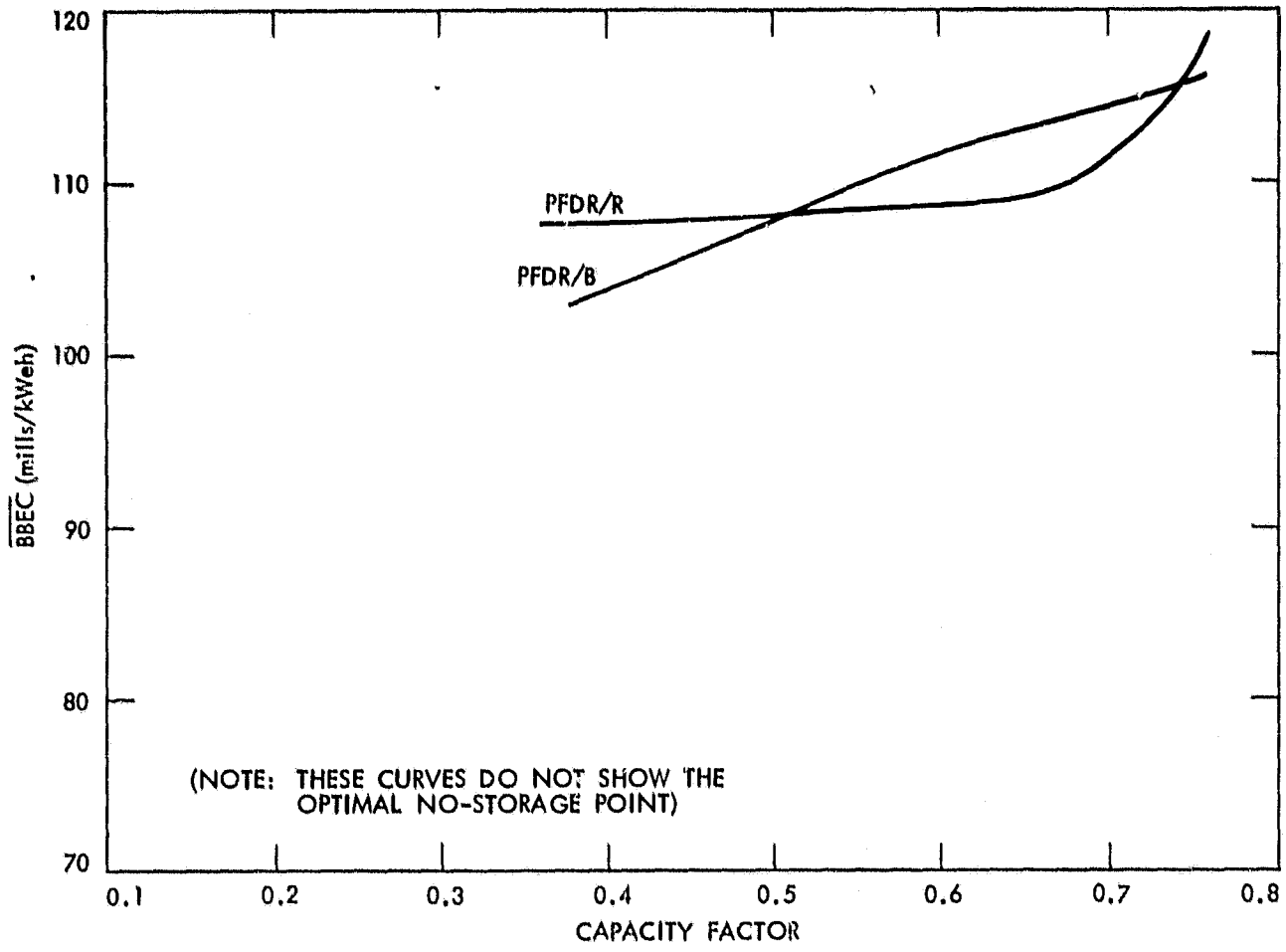

Figure 5-4. Energy Cost as a Function of Capacity Factor for Selected 10-MWe Power Plants (1978 Dollars)

are 3 to 7% and 0 to 2% (see Figure 5-5b). The main reason for the improvement in BBEC as size increases from 5 to 10 MWe is that the plant-generated output increases while some costs remain fixed or level off. However, the incremental improvements in energy cost are not as great as when the plant size increases from 1 to 5 MWe because the larger concentrator area now necessitated by the 10-MWe size has several associated costs that begin to outweigh the effects of the fixed costs. Also, the larger plants have a longer construction period, which tends to increase BBEC because of inflation impacts. The leveling off of improvement in BBEC as power generation size increases has a more marked impact on distributed engine systems than on central generation plants. The reason for this is the converse of the engine efficiency change described earlier for the 1-MWe case where decreased plant size adversely impacts central engine plants as compared to distributed engine plants. As plant size increases, the central generation plants use larger, more efficient engines while the distributed systems use more engines of the same size and efficiency as in the 1- and 5-MWe scenarios.

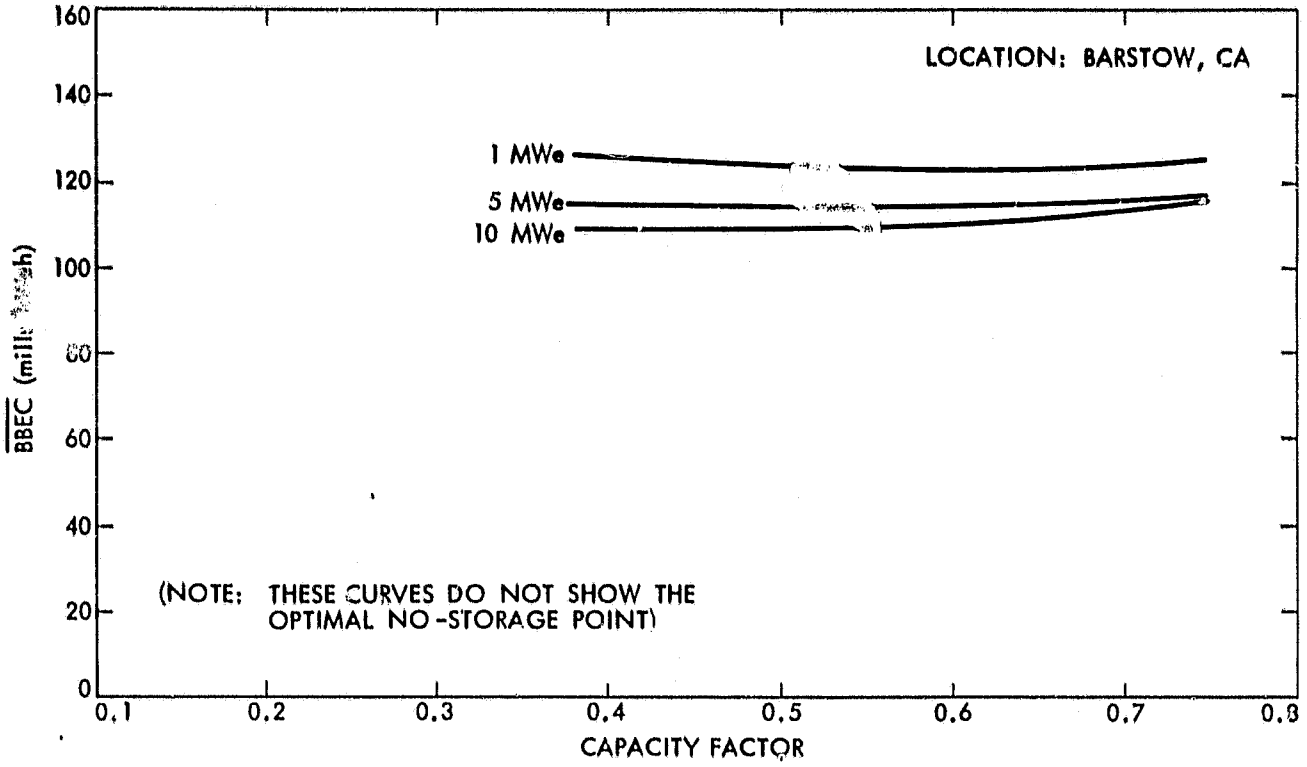

(a) Point-Focusing Distributed Receiver/Central Rankine Engine (PFDR/R)

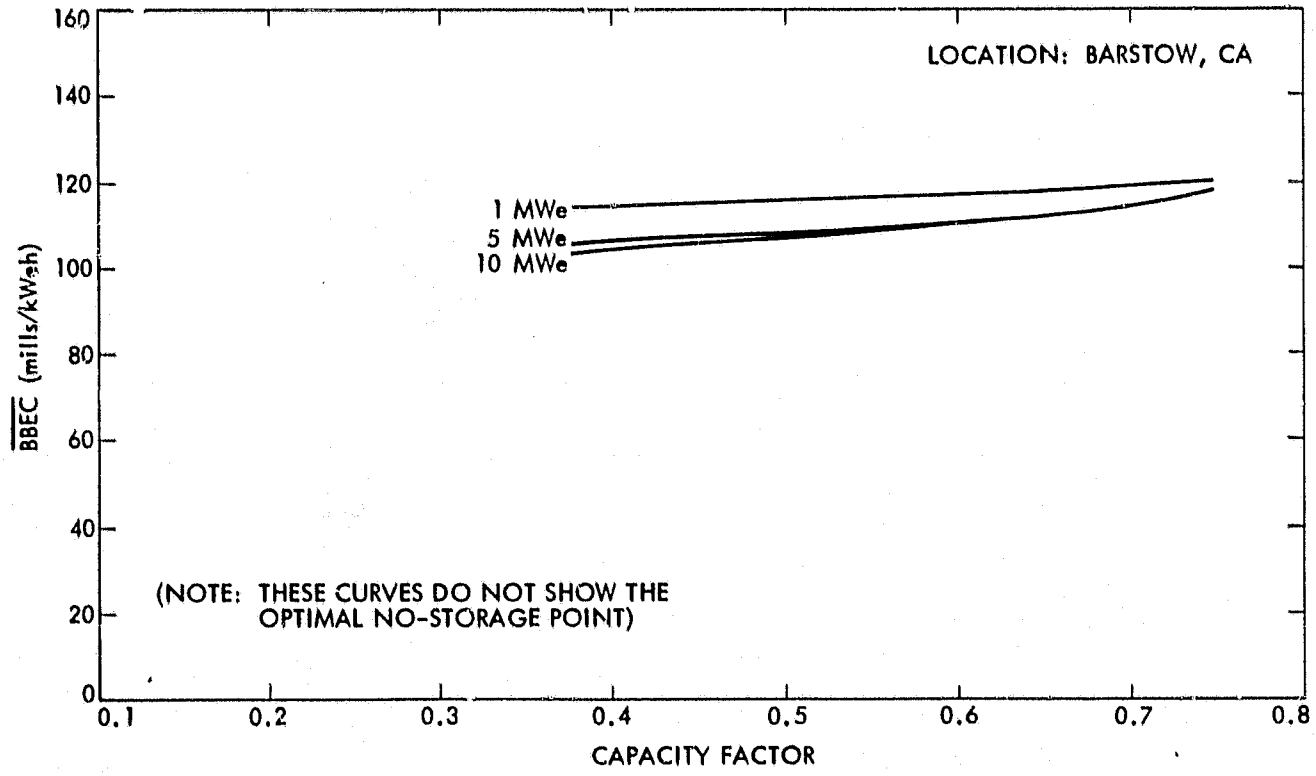

(b) Point-Focusing Distributed Receiver/Distributed Brayton Engine (PFDR/B)

Figure 5-5. Effects of Power Plant Size on Energy Costs (1978 Dollars)

D. SENSITIVITY ANALYSIS

As indicated earlier in Section IV, at the present early stage in solar thermal power technology development, uncertainty exists regarding projected costs and performance of the various subsystems. This study was based on the best information available in conjunction with assumptions made for each plant relative to potential cost and performance improvements. However, some baseline input values have a higher degree of uncertainty than others. For example, with respect to engines, increased research and development could result in lower costs and higher efficiencies. On the other hand, projected cost and efficiency improvements, which are speculative, may not materialize. Therefore, major assumptions that may have a potentially high variance from the baseline input values were tested for their impacts on plant performance and energy costs.

The following sensitivity analyses include changes in engine efficiencies, increased engine overhaul intervals, advanced engine designs, various component production levels, lower transport costs, electrical storage batteries, and varying financial assumptions. All sensitivities are based on a plant size of 5 MWe. Evaluation of the sensitivity results makes it possible to determine which changes have the greatest impact on costs and performance.

1. Engine Efficiencies

The engine efficiencies for the baseline generic systems evaluated in the study represent a mature state of development. To ascertain the impact on energy generation costs for efficiencies different from the baseline scenario, a sensitivity analysis was performed. Stirling, Brayton, and Rankine engines, which have developed to a production state but have not achieved the expected mature baseline efficiencies, were analyzed for three of the lower cost systems (PFDR/S, PFDR/B, and PFDR/R). Table 5-3 shows the design-point engine efficiencies for the baseline (mature) and lower efficiency (present) scenarios. The present efficiencies for the Stirling and Brayton engines were based on communications with USS and Garrett AiResearch of California (References 70, 71). It was assumed that all other engine performance and cost data were the same for the present as in the mature baseline cases. Figure 5-6 presents the results of this analysis at various capacity factors for both the

Table 5-3. Design-Point Engine Efficiencies for Mature and Present Scenarios

Engine	System	Present Scenario Engine Efficiency (%)	Mature Baseline Scenario Engine Efficiency (%)
Stirling	PFDR/S	38	42
Brayton	PFDR/B	32	35
Steam Rankine	PFDR/R	32	35

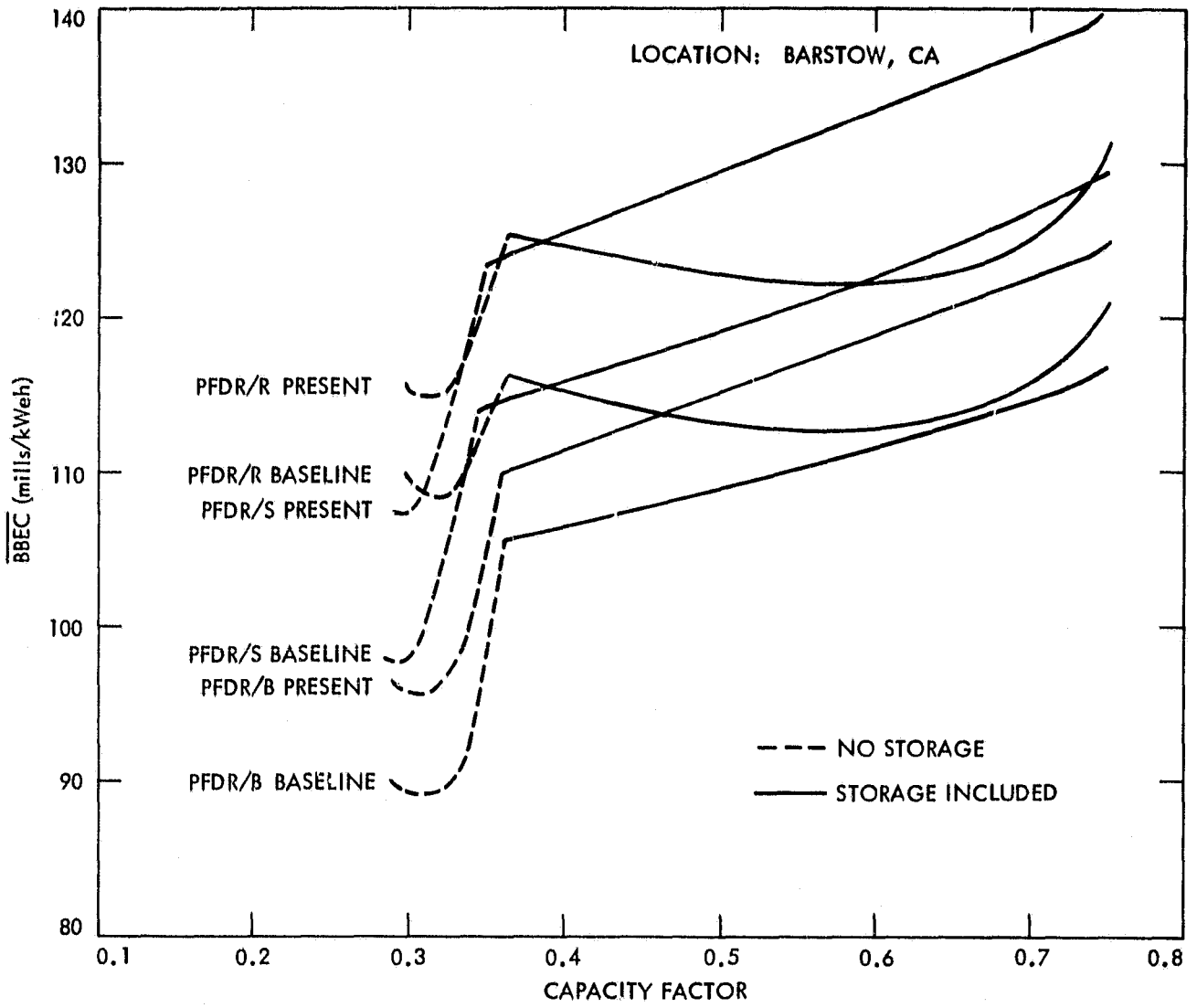

Figure 5-6. Sensitivity of Energy Cost to Engine Efficiency Changes -- Present versus Baseline Designs (1978 Dollars)

present and mature systems. For each percentage-point decrease in engine efficiency, there is approximately a 2 to 3 mills/kWeh increase in $\overline{\text{BBEC}}$. The total increases in $\overline{\text{BBEC}}$ as a result of failing to obtain the desired, mature efficiences is about 7 to 10%. These systems would, therefore, still be competitive with the other concepts even if the mature engine efficiences are not reached. Note that the present PFDR/B system has a lower $\overline{\text{BBEC}}$ than the mature PFDR/S system.

An increase in engine efficiency by operating at temperatures above those projected for the baseline case would most likely produce a smaller magnitude improvement in $\overline{\text{BBEC}}$ than 2 to 3 mills/kWeh per percentage point. This would be due to higher temperature operation of the receiver, which would reduce

collector efficiency. An advanced engine design, which includes a higher efficiency than the mature case, as well as several other changes, is discussed later in Section V.D.3.

2. Engine Overhauls

Since engine overhauls were a major cost driver for the PFDR/S mature baseline scenario (see Figure 5-2), it was decided to examine the effects of an improved overhaul scenario separately while retaining the remainder of the baseline assumptions. The time between major overhauls for the Stirling engine was increased from 15,000 to 50,000 hours. This is the level of improvement that may be attainable from an advanced Stirling design. The PFDR/R system was also added to this analysis. Its average time between overhauls was also extended from 35,000 to 50,000 hours. There is no engine overhaul sensitivity for the Brayton engine since the mature baseline case requires no major overhauls. The resulting energy costs for the low overhaul systems were then compared with the mature baseline PFDR/S and PFDR/R systems (see Figure 5-7). It can be seen that the PFDR/S cost improves considerably while the PFDR/R cost shows only a slight gain when compared with their respective mature baseline cases (13% improvement for the PFDR/S versus 3% for the PFDR/R). The low overhaul PFDR/S system costs slightly less than the mature baseline PFDR/B system at most capacity factors. At high capacity factors (greater than 0.52), the low overhaul PFDR/R system is also less costly than the PFDR/B system because of comparatively lower thermal storage costs, as opposed to higher electrical storage costs of the baseline PFDR/B system.

3. Advanced Designs

As discussed in Section IV.C.5, advanced (early 1990s) Brayton and Stirling engines are currently under investigation by JPL in conjunction with LeRC. These designs can achieve higher efficiencies and/or lower levels of maintenance than the baseline technologies through component improvements and/or higher temperature operation. Therefore, these advanced designs enhance those sensitivities discussed earlier since they incorporate both engine efficiency and overhaul changes. For the case of the advanced PFDR/B, the design-point engine efficiency is projected to increase from 35 to 42.5% as a result of utilizing a high-temperature receiver and engine (1100°C at the engine inlet). Although this power conversion unit is projected to cost more than the baseline case ($180/kWe versus $137/kWe), its maintenance cost was reduced by using self-cleaning filters and an integral starter/generator unit.

With respect to the advanced PFDR/S system, this engine will be redesigned to include advanced components so that maintenance reductions can be incorporated. Engine/generator cost is $180/kWe in the advanced scenario versus $205/kWe in the baseline case. The maintenance cost is reduced to the same level as that of the advanced PFDR/B system. The performance and inlet temperatures for the advanced PFDR/S engine are the same as in the baseline scenario.

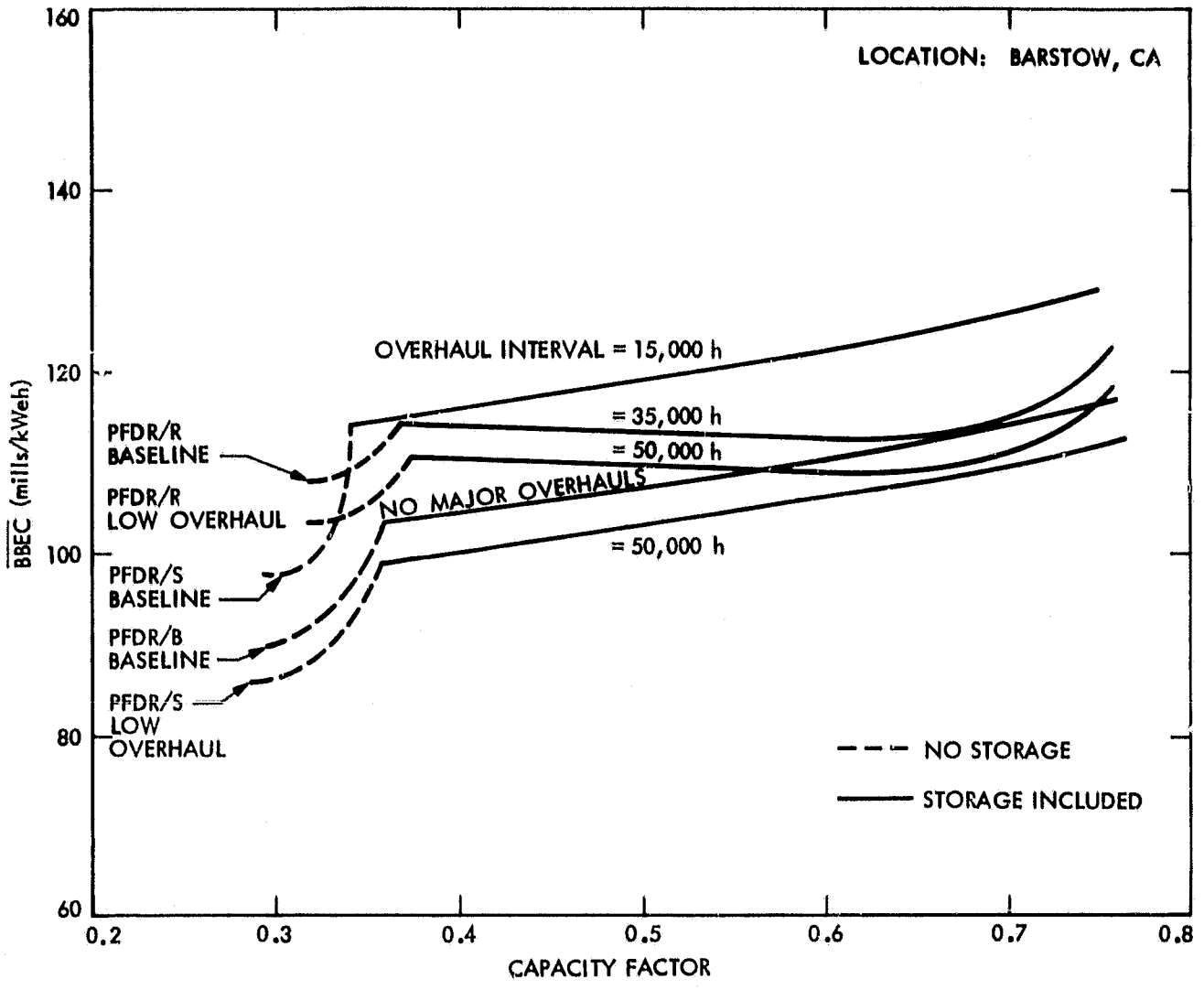

Figure 5-7. Sensitivity of Energy Cost to Engine Overhaul Improvements (1978 Dollars)

The results of the advanced design analysis are shown in Figure 5-8. The advanced PFDR/B engine now has a $\overline{BBEC}$ that varies between 82 and 109 mills/kWeh, while the advanced PFDR/S engine varies from 76 to 101 mills/kWeh. The $\overline{BBEC}$ of the PFDR/B system has improved by 6 to 8%, while the PFDR/S system has improved by 20 to 22% when compared with the mature baseline systems. With respect to the PFDR/S system, the $\overline{BBEC}$ was lowered in the earlier overhaul sensitivity case by 13% only because of reductions in major overhaul costs (see Figure 5-7). Therefore, eliminating all overhauls, greatly reducing regular maintenance, and slightly raising engine cost add another 7 to 9% to the cost reduction.

Figure 5-9 compares the no-storage case of the two advanced systems with their baseline counterparts. The cost distributions for both advanced systems are fairly similar to the mature baseline cases. The major differences from

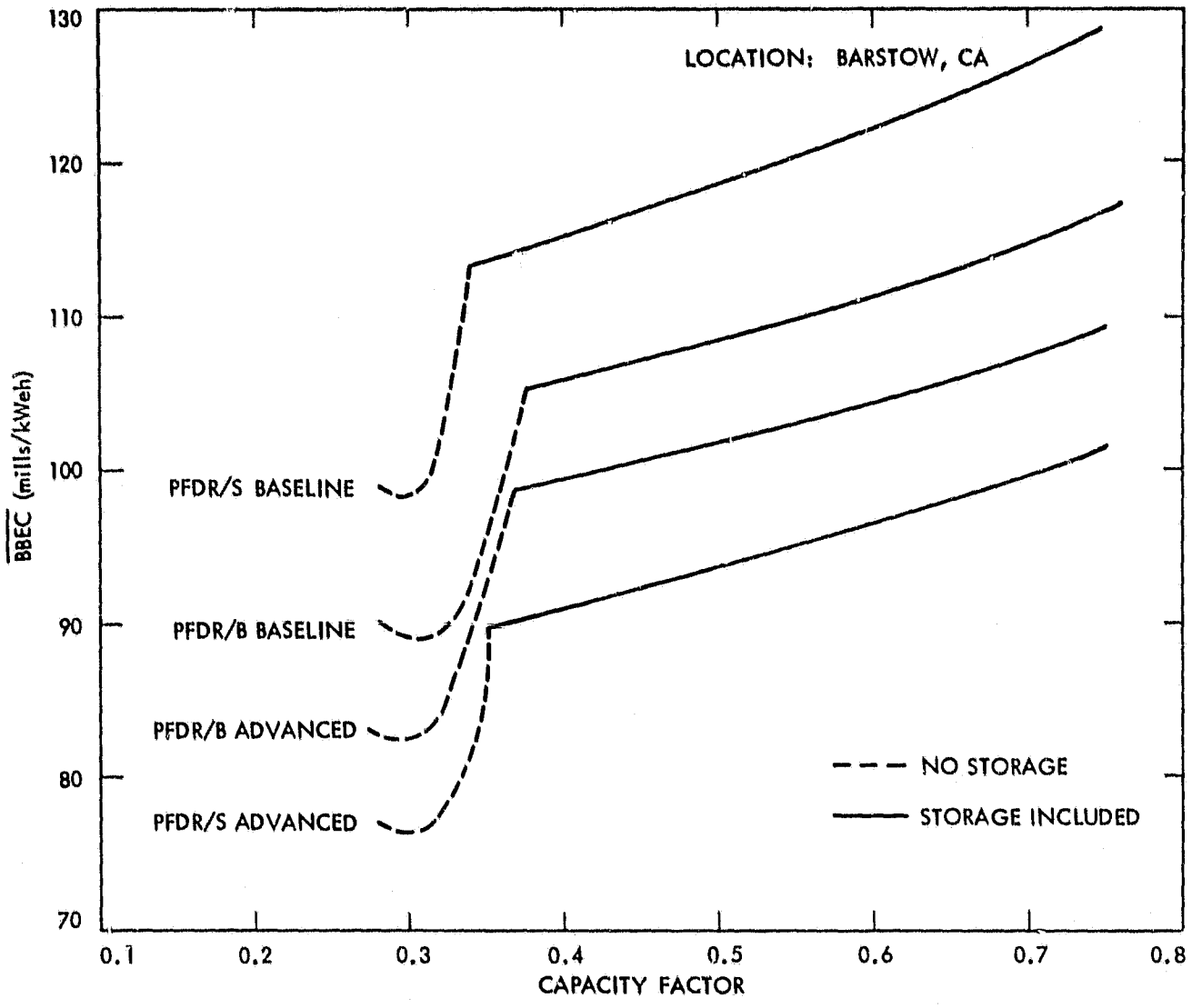

Figure 5-8. Sensitivity of Energy Cost to Engine Efficiency Changes--Advanced Engine Designs (1978 Dollars)

the mature baseline scenarios are the elimination of the engine overhaul component from the Stirling engine and the lowering of O&M and overhaul costs in the case of the Brayton system. Since income taxes and insurance cost are functions of total capital cost and overhauls are treated as a capital cost item, reductions in overhauls result in associated cost reductions in income taxes and insurance. This sensitivity analysis shows that a low-cost solar thermal electrical energy system can be obtained by following one of two routes: either the Brayton engine can be improved to operate at a higher efficiency, higher temperature, and lower maintenance levels; or the Stirling engine can be developed to the point where its engine overhaul and maintenance components are greatly reduced or eliminated.

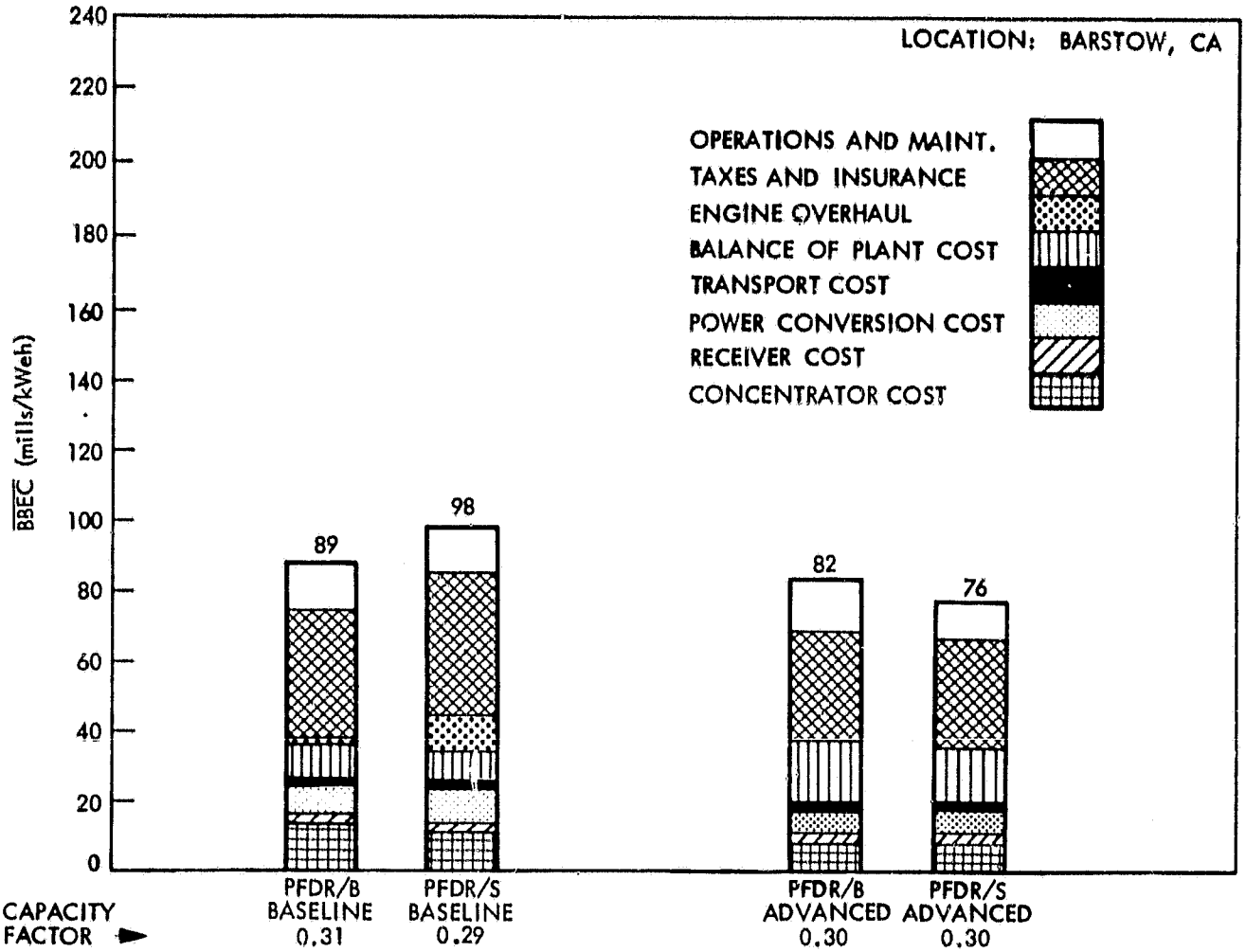

Figure 5-9. Cost Distribution for Optimal No-Storage 5-MWe Power Plants -- Baseline and Advanced PFDR/B and PFDR/S Systems (1978 Dollars)

4. Production Levels

The previous results were based upon production levels of 25,000 units annually. From among those systems found to have the greatest potential for providing low-cost energy, the no-storage case for the baseline PFDR/B and PFDR/S designs were evaluated for other production levels to determine the impact of economies of scale on energy costs. At different production levels, the concentrator, receiver, and engine/generator costs will vary as shown in Figures 4-2, 4-3, 4-8, and 4-9. Figure 5-10 shows the resultant $\overline{\text{BBEC}}$ for production levels varying from 1,000 units annually, which is akin to large farm machinery production levels, up to an automotive-type production level of 400,000 units annually. It appears that the PFDR/S system becomes competitive with the PFDR/B system at approximately the 50,000 level and, in fact, costs slightly less at the highest production levels. The PFDR/B system ranges from a high of 138 mills/kWeh at 1,000 units annually to a low of 78 mills/kWeh at 400,000 units. (The PFDR/S system reaches 76 mills/kWeh at 400,000 units.) Thus, it is apparent that very high annual production rates can bring about the

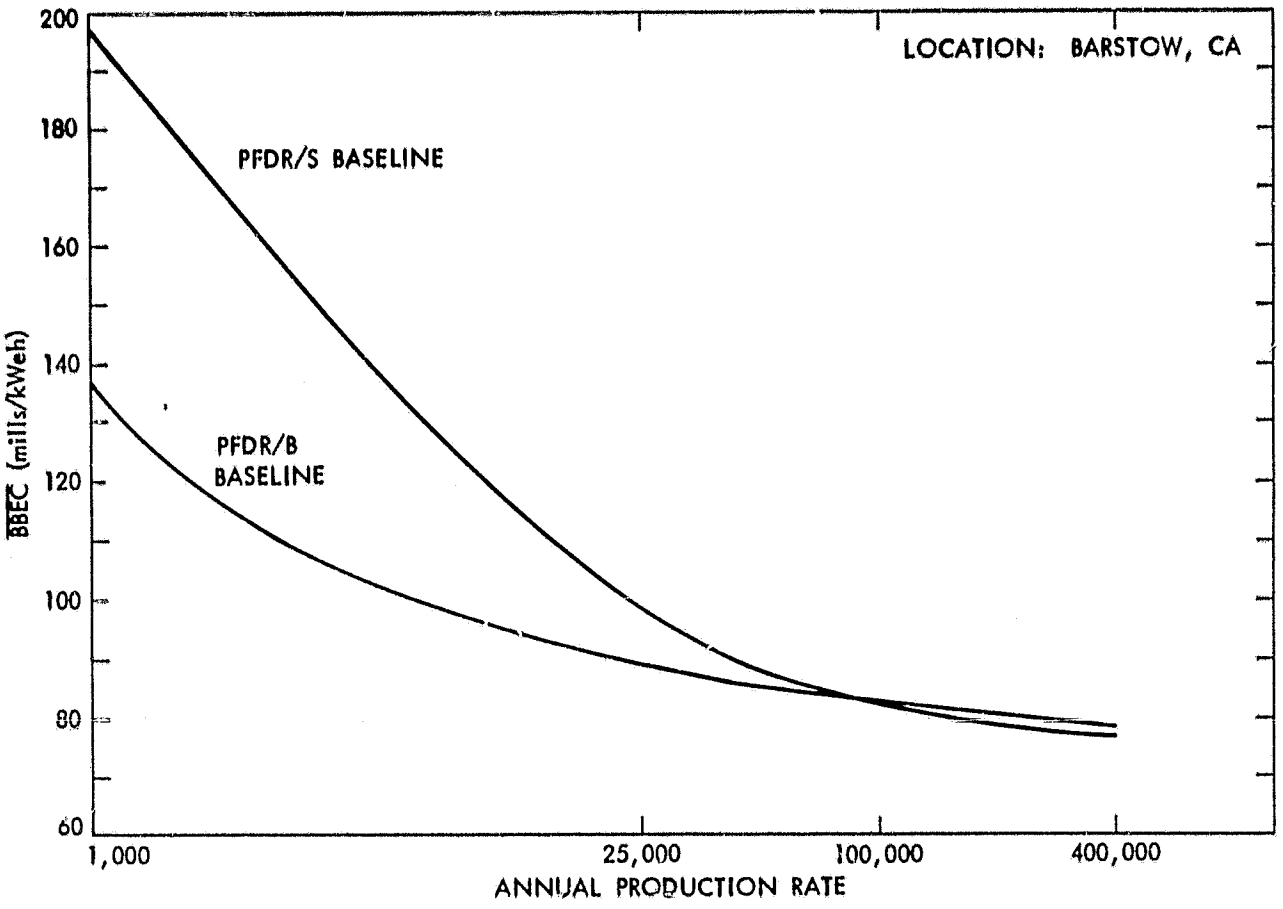

Figure 5-10. Sensitivity of PFDR/B and PFDR/S Energy Costs With No Storage to Production Level (1978 Dollars)

same improvement in $\overline{\text{BBEC}}$ as the implementation of advanced engine designs. Table 5-4 summarizes the sensitivity of the energy cost for the baseline PFDR/S and PFDR/B systems to changes in their major component costs. It appears that a decrease in $\overline{\text{BBEC}}$ is more closely dependent upon reductions in concentrator costs than upon reductions in the other components. Additionally, differences between the two systems seem to be directly dependent on engine/generator costs.

5. Transport Cost

Thermal transport cost is another item that has the potential for better than projected cost reductions. Based on current investigations, it is estimated that transport costs could be reduced by as much as one-third as a result of further optimization activities and advanced fabrication techniques. The best performing system which utilized thermal transport was the PFDR/R. Its transport cost was reduced from $\$30/m^2$ to $\$20/m^2$, and then compared with the baseline PFDR/B (see Figure 5-11). It appears that the transport cost

Table 5-4. Major Component Costs and $\overline{BBEC}$ for Varying Production Levels (1978 Dollars)

Location: Barstow, CA

Annual Production Rate	Concentrator Cost ($/m^2) Baseline PFDR/S and PFDR/B	Receiver Cost ($/m^2) Baseline PFDR/S and PFDR/B	Engine/Generator Cost ($/engine) Baseline PFDR/S	Engine/Generator Cost ($/engine) Baseline PFDR/B	$\overline{BBEC}$ (mills/kWeh) Baseline PFDR/S	$\overline{BBEC}$ (mills/kWeh) Baseline PFDR/B
1,000	143	44	13,990	6,153	196	136
25,000	85	10	5,120	3,321	98	89
100,000	75	7	3,004	2,861	81	81
400,000	68	7	2,666	2,616	76	78

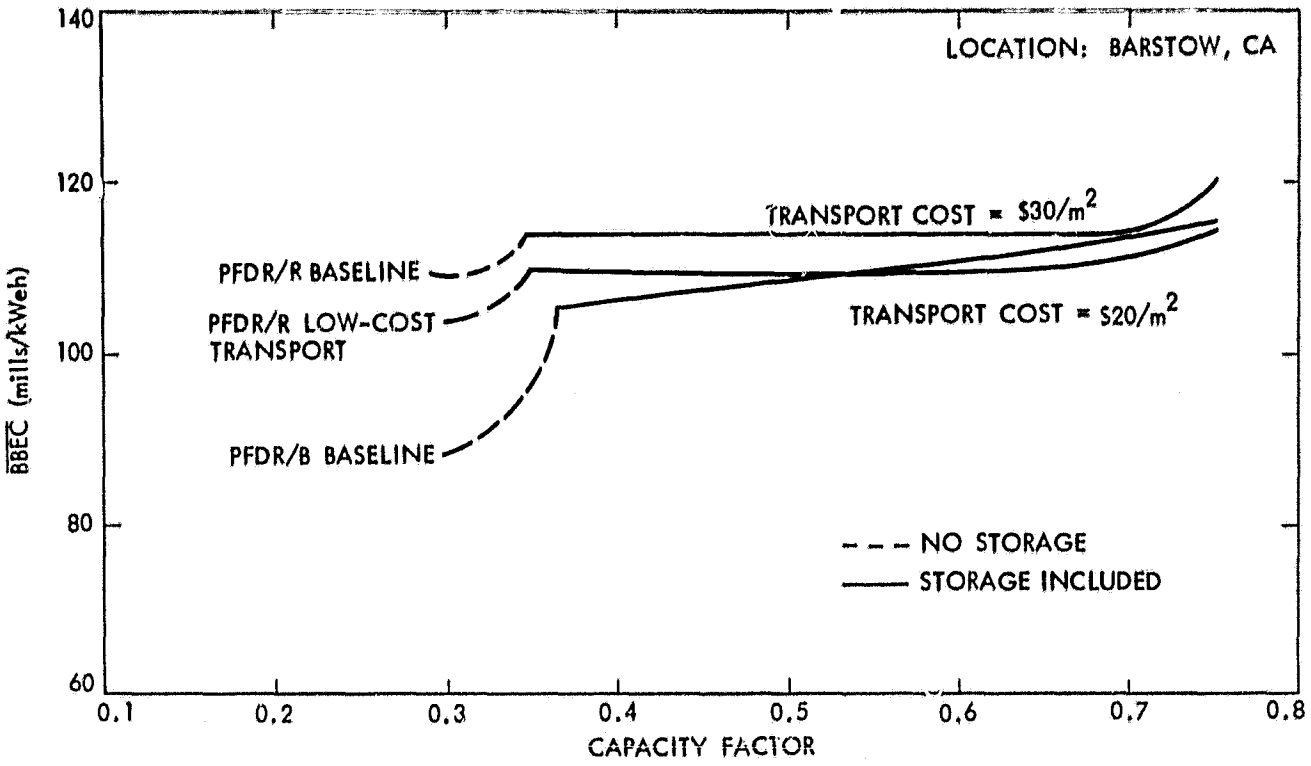

Figure 5-11. Energy Cost as a Function of Capacity Factor for Different Thermal Transport Costs (1978 Dollars)

improvement does not significantly impact overall energy costs (there is a small 4% improvement). Once again, as in the previous engine overhaul sensitivity, the low transport PFDR/R system has a lower cost than the PFDR/B system at high capacity factors because of comparatively lower thermal storage costs.

6. Electrical Storage Cost

The last physical component tested in the sensitivity analysis was electrical storage cost. The high cost and low efficiency of electrical storage compared with thermal storage was previously shown to be a significant cost driver for the PFDR/B and PFDR/S systems at high capacity factors. It was also stated that it would be infeasible for these systems to use thermal storage because of transport complexities. However, if the baseline scenario redox electric storage system is not developed by 1990, it may be necessary to utilize one of several generic electrical storage batteries. Lead-acid batteries were chosen as the sensitivity alternative. Performance of other types of electrical storage batteries would probably fall somewhere between redox and lead-acid batteries. As indicated in Section IV, the major differences between redox systems and batteries were that batteries have a shorter lifetime (about 6 years versus 30 years for redox) and higher storage-size cost. The behavior of both types are shown for the baseline PFDR/B system in Figure 5-12. It can be seen at low capacity factors (where the quantity of storage required is low) that lead-acid battery storage can achieve almost as

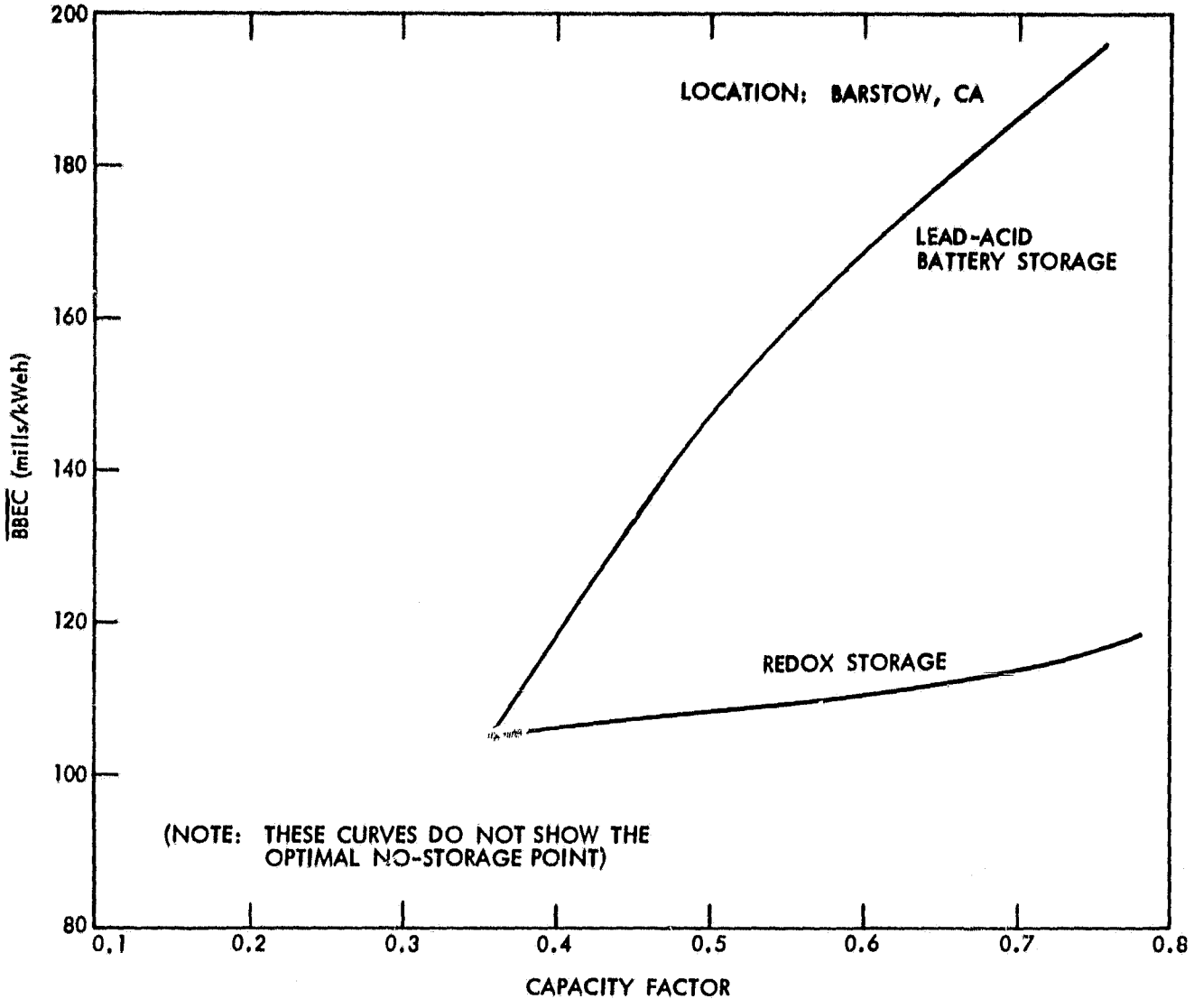

Figure 5-12. Energy Cost of PFDR/B as a Function of Capacity Factor for Lead-Acid Battery and Redox Storage Systems (1978 Dollars)

low energy costs because its required conditioning equipment is not as complex. However, as capacity factor and storage size increase the redox system achieves as much as a 20% lower energy cost because it has significantly lower capacity-related costs which more than compensate for higher conditioning equipment costs. Therefore, it does not seem that lead-acid battery storage systems can perform as well as the redox design at most capacity factors when storage is utilized.

7. Financial Parameters

There are also non-physical input parameters that affect energy cost and are also subject to uncertainty. These are the financial values

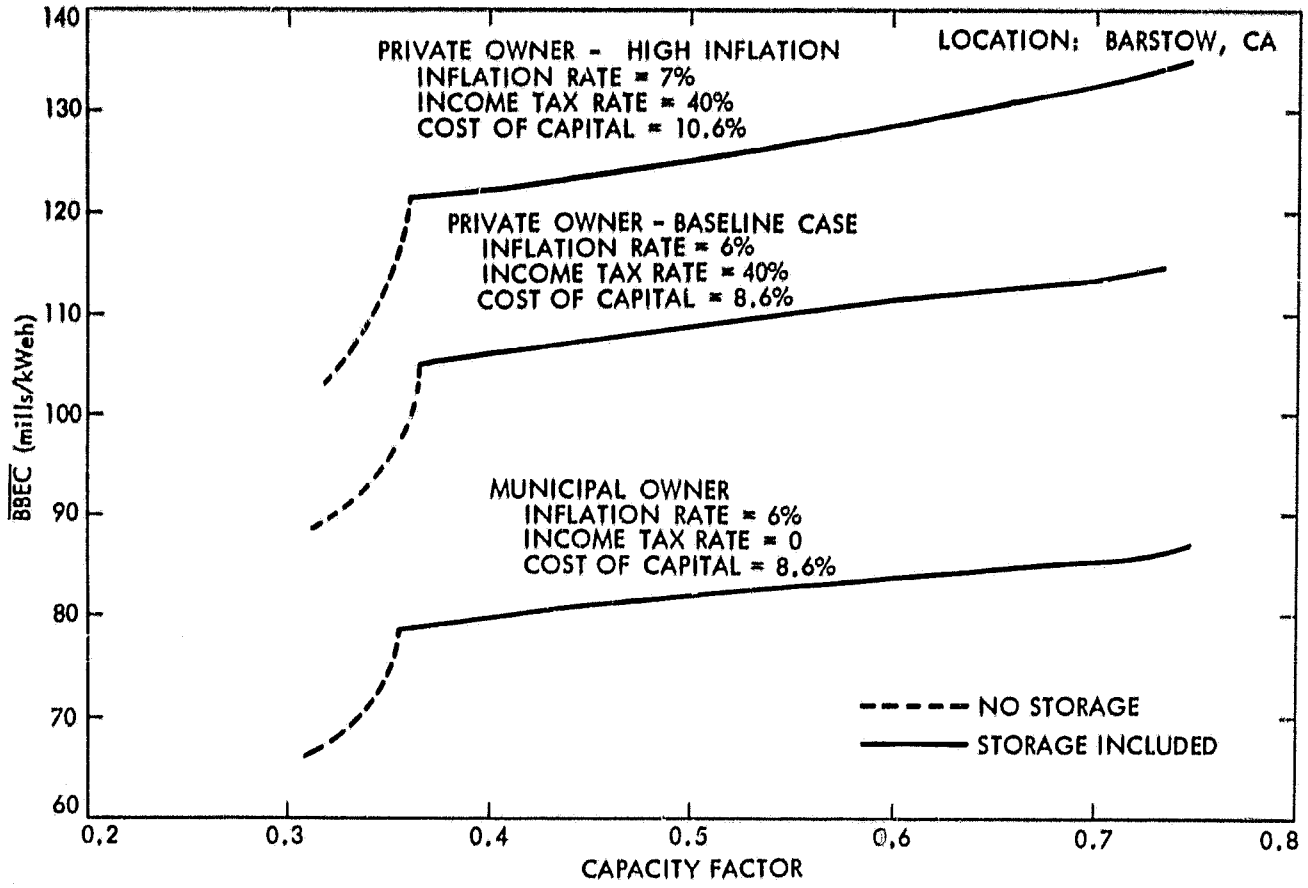

Figure 5-13. Impact of Various Financial Scenarios on the $\overline{\text{BBEC}}$ of PFDR/B System (1978 Dollars)

assumed. Therefore, another pertinent sensitivity effort involved varying the financial parameters that were used to develop $\overline{\text{BBEC}}$. The baseline assumptions were given in Section I.C. These parameters included a general inflation rate of 6% and a capital cost of 8.6% during the total lifetime of the plant. In view of the current state of the United States economy, an inflation rate of 7% annually was considered. Furthermore, in this higher inflation case, the cost of capital was changed to 10.6%. This was the current rate used by Southern California Edison. Figure 5-13 shows the impact of the higher rate on the baseline PFDR/B system. The $\overline{\text{BBEC}}$ for this case increases by about 18% (i.e., $\overline{\text{BBEC}}$ increases from 89 to 105 mills/kWeh with no storage). Both the baseline and the higher inflation scenarios are based on a private, investor-owned utility. However, public ownership is another option that may be of interest. In this scenario the major change from the baseline case is that no income taxes are paid. Energy costs decrease by 24% when compared with the baseline scenario (68 versus 89 mills/kWeh with no storage).

SECTION VI

CONCLUSIONS

The primary finding of the cost and performance analysis is that the point-focusing systems provide equivalent quantities of energy at lower costs than either the one-axis or non-tracking plants. The point-focusing systems had the highest collector and power conversion efficiencies. They also had the best overall plant efficiencies (17 to 26%). The most efficient system was the PFDR/S. Since the higher efficiency plants require smaller concentrator areas to produce equivalent quantities of energy, and since the concentrator is a major cost component, the point-focusing systems also have the lowest total subsystem costs. The lowest capital cost for any system was the PFDR/S ($5.26 M with no storage at 5 MWe).

It follows that the point-focusing systems achieved the lowest $\overline{\text{BBEC}}$ (89 to 130 mills/kWeh at 5 MWe). The PFDR/B system is the least expensive performer by a very small margin over the PFDR/R, PFDR/S, and PFCR systems, primarily because of low engine overhaul costs. Actually, the PFDR/R system is as low cost as the PFDR/B system at high capacity factors for the 5-MWe size because of its utilization of thermal storage rather than electrical storage.

For all power plants evaluated, less than 50% of the $\overline{\text{BBEC}}$ to be charged to consumers is made up of capital costs (43 to 46%). The remainder consists of O&M, income taxes, and insurance costs. At a size of 1 MWe, the energy costs for all plants are somewhat higher than those for the 5-MWe case. This occurs because fixed-cost items make up a higher proportion of total costs while power generated is lower. Also, the systems using large central-Rankine engines use smaller less-efficient units to generate 1 MWe than they do to generate 5 MWe. Meanwhile, the distributed engine systems (PFDR/B and PFDR/S), which utilize small concentrator-mounted power conversion units, use fewer engines of the same size and efficiency at 1 MWe as compared to the 5-MWe case. Therefore, these systems are slightly more favorable in the 1-MWe case when compared to central engine plants. At the 10-MWe size, energy costs for all plants are lower than in the 5-MWe case because of an increase in energy output while some costs remain fixed or level off. The incremental change between 5 and 10 MWe is not as great as between 1 and 5 MWe because larger concentrator areas begin to outweigh the effects of the fixed costs. In contrast to the 1-MWe case, at 10 MWe the central generating plants use larger, more efficient engines while distributed engine efficiencies remain the same as in the 1- and 5-MWe cases. Therefore, at 10 MWe the central generating systems (i.e., PFDR/R and PFCR) improve in the overall ranking to the point where the PFDR/R system is the lowest cost performer at capacity factors between 0.5 and 0.75.

It can be concluded from the sensitivity analyses that the absolute value of $\overline{\text{BBEC}}$ may be more sensitive to economic and financial factors than to those of a technological nature. Even so, it was also found that if emphasis is placed on improving engine efficiency, reducing engine overhauls, and/or increasing production rates, then the resulting $\overline{\text{BBEC}}$ has the greatest chance of being decreased from the baseline case.

REFERENCES

1. Thornton, J. P., et al., Comparative Ranking of 1-10 MWe Solar Thermal Electric Power Systems, Report TR-35-238, Solar Energy Research Institute, Golden, Colorado, September 1979.

2. Laity, W. W., et al., Assessment of Solar Options for Small Solar Power Systems Applications, Report PNL-4000, Battelle Pacific Northwest Laboratory/DOE, Richland, Washington, September 1979.

3. Rosenberg, L. S., Revere, W. A., and Selcuk, M. K., "The Application of Simulation Modeling to the Cost and Performance Ranking of Solar Thermal Power Plants," Solar Engineering - 1981, ASME Conference Proceedings, pp. 642-653, April 1981.

4. Yinger, R. J., The West Associates' Solar Resource Evaluation Project, Solar Energy Measurements During 1976, Southern California Edison, Rosemead, California, June 1977.

5. Doane, J. W., et al., The Cost of Energy from Utility-Owned Solar Electric Systems," Publication ERDA/JPL 1012-76/3, Jet Propulsion Laboratory, Pasadena, California, June 1976.

6. Selcuk, M. K., A Fixed Solar Collector Employing Reversible Vee Trough Reflectors and Vacuum Tube Receivers," Final Report, Publication DOE/JPL-1024-1, JPL Publication 77-78, Jet Propulsion Laboratory, Pasadena, California, December 1977.

7. O'Gallagher, J., Personal Communication, University of Chicago, June 12, 1979.

8. Thunborg, S., Personal Communication, Sandia National Laboratories, Albuquerque, New Mexico, December 1978.

9. Ratzel, A. C., "Thermal Parametric Studies for the Second Generation Ninety-Degree Parabolic Collector," Interoffice Memorandum RS 1262/1008, Sandia National Laboratories, Albuquerque, New Mexico, June 1978.

10. Russel, J. L., Jr., DePlomb, E. P., and Bansal, R. K., Principles of the Fixed Mirror Solar Concentrator, Report GA-A12902, General Atomic Company, San Diego, California, May 31, 1974.

11. Russel, J. L., Jr., Investigation of a Central Station Solar Power Plant, Report GA-A12759, General Atomic Company, San Diego, California, August 31, 1973.

12. Walker, W. E., Conceptual Design of a Demonstration Fixed Mirror Solar Concentrator, Report GA-13926, General Atomic Company, San Diego, California, July 1, 1976.

13. Hallett, R. W., and Gervais, R. L., Central Receiver Solar Thermal Power System, Final Technical Progress Report, Report SAN-1108-76-7, McDonnell Douglas Astronautics Company, Huntington Beach, California, May 1978.

14. Solar Total Energy-Large Scale Experiment at Shenandoah, Georgia, Document 78 SDS4234, General Electric Company - Space Division, Valley Forge, Pennsylvania, July 10, 1978.

15. Semiannual Review, Solar Thermal Electric Central Receiver Research Study, FMC Corporation, Santa Clara, California, December 1976.

16. Interim Report, Solar Thermal Electric Central Receiver Research Study, Document R-3617, FMC Corporation, Santa Clara, California, February 1977.

17. Monthly Technical Progress Report No. 10, Central Receiver Research Study, Document 3630, FMC Corporation, Santa Clara, California, March 1977.

18. Interim Report, Solar Thermal Electric Central Receiver Research Study, FMC Corporation, August 1977.

19. Crosbyton Solar Power Project, Phase 1, Interim Technical Report, Report CSP-TR-1, Texas Tech University, Lubbock, Texas, February 1977.

20. Crosbyton Solar Power Project, Review of Conceptual Design Details of 65-Foot FMDF Test Collector, Report ETC-103178-39, E-Systems Inc., Dallas, Texas, November 1, 1978.

21. Crosbyton Solar Power Project, Design Review of the 65-Foot FMDF Test Collector, Report ETC-112878-10, E-Systems Inc., Dallas, Texas, December 1, 1978.

22. Holl, R. J., Phase I of the First Small Power System Experiment (Engineering Experiment No. 1), Final Technical Report, Report MDC G7819, McDonnell Douglas Astronautics Company, Huntington Beach, California, March 1979.

23. Hesse, W. J., "Interim Report on Projected Prices for the FMDF System," Letter to G. Braun/DOE, E-Systems Inc., Dallas, Texas, November 1, 1978.

24. Design and Performance of a Fixed Faceted Mirror Concentrator, Final Report, Contract E-(40-1)-4970, Scientific-Atlanta Inc., Atlanta, Georgia, September 1977.

25. Eason, E., Comparable Cost Estimates for Heliostats, Parabolic Dishes, and Parabolic Troughs, Report 8326, Sandia National Laboratory, Livermore, California, 1979.

26. Easton, R., "Adaptation of Heliostat Design and Production Technology to Point-Focus Concentrators," viewgraph presentation made to JPL, McDonnell Douglas Astronautics Company, Huntington Beach, California, May 21, 1979.

27. Phase 1, Final Report for the Development of an Air Brayton Solar Receiver, JPL Contract 955120, Sanders Associates Inc., Nashua, New Hampshire, January 18, 1979.

28. Nelson, E., Low-Cost Point-Focus Solar Concentrator, Phase 1 - Final Report, Report 79-340, Acurex Corporation, Mountain View, California, March 1979.

29. Low Cost Point Focus Solar Concentrator Phase 2 - Preliminary Design, Final Study Report, JPL Contract 955210, General Electric Company - Advanced Energy Programs, Valley Forge, Pennsylvania, March 16, 1979.

30. Zimmerman, D., Low Cost Point Focus Solar Concentrator, Phase I, Final Report, JPL Contract 955209, Boeing Engineering & Construction - Advanced Solar Energy Systems Division, Seattle, Washington, March 1979.

31. Eiker, P., Personnal Communication, Sandia National Laboratories, Livermore, California, April 18, 1979.

32. Phase I, First Small Power System Experiment (Experiment System No. 1), Progress Reviews, JPL Contract 955115, Ford Aerospace & Communications Corporation, Newport Beach, California, May 1979.

33. Analysis of Steam Piping System and Costs to Serve a Solar Heat Generating Plant, Report W/035, JPL Contract 955041, Architects and Engineers Collaborative, Los Angeles, California, April 18, 1979.

34. Nettel, J., and Genshino, W., Personal Communication, Anacondia American Brass Company - Metal Hose Division, Waterbury, Connecticut, August 1979.

35. Anacondia 'BWF-21 Metal Hose Catalog, No. CR(5 ED), Anacondia American Brass Company - Metal Hose Division, Waterbury, Connecticut.

36. Biddle, J., Revere, W., and Fujita, T., "Low-Cost Thermal Transport Piping Networks for Solar Industrial Process Heat Applications," paper presented at the 5th Annual Solar IPH Conference in Houston, Texas, Jet Propulsion Laboratory, Pasadena, California, December 16-19, 1980.

37. Turner, B., "Economic Optimization of the Energy Transport Component of a Large Distributed Collector Solar Power Plant," IECEC Conference Paper 769216, 1976.

38. Phase I, First Small Power System Experiment - Final Report, Report 4-6529, Ford Aerospace & Communications Corporation, Newport Beach, California, May 5, 1979.

39. Revere, W., "Cost Survey of Power Conversion Equipment," Interoffice Memorandum 353-81-154, Jet Propulsion Laboratory, Pasadena, California, December 28, 1978.

40. Holl, R. J., and Dawson, R. P., Phase I of the First Small Power System Experiment (Engineering Experiment No. 1), Quarterly Technical Progress Report MDC G7553, McDonnell Douglas Astronautics Company, Huntington Beach, California, January 1979.

41. Abbin, J. P., Jr., Rankine Cycle Energy Conversion System Design Considerations for Low and Intermediate Temperature Sensible Heat Sources, Report SAND 76-0363, Sandia National Laboratories, Albuquerque, New Mexico, May 1977.

42. Barber, R. E., "Current Costs of Solar Powered Organic Rankine Cycle Engines," Solar Energy, Vol. 20, January 6, 1978.

43. Ichikawa, S., and Watanabe, M., "Organic Rankine Cycle Development and Its Application to Solar Energy Utilization," Heliotechnique and Development, pp. 739-752, published by Development Analysis Associates, Inc., Cambridge, Massachusetts, 1976.

44. Niggeman, R. E., et al., "Fluid Selection and Optimization of an Organic Rankine Cycle Waste Heat Power Conversion System," ASME Paper 78-WA-ENER-6, 1978.

45. Morgan, D. T., et al., "High Efficiency Diesel/Organic Cycle Combined Power Plant," ASME Paper 75-DPG-13, 1975.

46. Doyle, E., Personal Communication, Thermo Electron Corporation, Waltham, Massachusetts, March 1979.

47. Santucci, M. D., Personal Communication, Sundstrand Energy Systems, Rockford, Illinois, March 1979.

48. Toluene Engines, Commercial Literature, Sundstrand Energy Systems, Rockford, Illinois, March 1979.

49. Alpaugh, R. T., and Rossbach, R. J., Pipeline Bottoming Cycle Study, General Electric Company - Advanced Energy Programs, Cincinnati, Ohio, October 31, 1978.

50. Sjoestedt, L., "Efficiency and Power Levels for Solar Powered Stirling Engines," Telex Memorandum, United Stirling-Sweden, Malmo, Sweden, November 7, 1979.

51. Aster, R. W., and Chamberlain, R. G., Interim Price Estimation Guidelines: A Precursor and Adjunct to SAMIS III Version One, Internal Report 5101-33, Jet Propulsion Laboratory, Pasadena, California, September 10, 1977.

52. Krauthamer, S., "Solar Thermal Project/Alternator Study for Advanced Systems," Interoffice Memorandum 342-79-C-114, Jet Propulsion Laboratory, Pasadena, California, May 23, 1979.

53. "Application of the GRI/DOE Subatmospheric Brayton Engine to Solar Power Generation," Presentation S-28672-A, Garrett AiResearch Manufacturing Company of California, Torrance, California, November 9, 1978.

54. Fortgang, H., and Mayers, H., Cost and Price Estimations of Braytor and Stirling Engines and Selected Production Volume, Internal Report 5105-29, Jet Propulsion Laboratory, Pasadena, California, May 31, 1980.

55. Bescaby, F., Personal Communication, Garrett AiResearch Manufacturing Company of California, Torrance, California, November 16, 1979.

56. Broadbent, L. L., "A Review of Gas Turbines," (unpublished gas turbine lecture material), May 13, 1975.

57. Kaupang, B. M., Typical Generation Planning Inputs, General Electric Company - Electric Utility Systems Engineering Department, Schenectady, New York, August 15, 1978.

58. Mackay, R., Gas Turbines and Cogeneration, Report SPA-5919, Garrett AiResearch Corporation, Los Angeles, California, April 1979.

59. Jaffe, L. D., and Pham, H. Q., "Heat Engine Requirements for Advanced Solar Thermal Power Systems," SAE Conference Paper 810454, February 1981.

60. Thallen, L., Redox Flow Cell Development and Demonstration, A Technology Review, NASA Lewis Research Center, Cleveland, Ohio, November 1978.

61. Hausz, W., Berkowitz, B., and Hare, R., Conceptual Design of Thermal Energy Storage Systems for Near Term Electrical Utility Application, Report DOE/NASA/0012-78/1, General Electric Company - Tempo Division, Santa Barbara, California, October 1978.

62. V. P. Burolla, Prediction of Yearly Fluid Replenishment Rates for Hydrocarbon Fluids in Energy Storage Systems, Report SAND-79-8209, Sandia National Laboratories, Albuquerque, New Mexico, April 1979.

63. Hobson, D. L., Personal Communication, Ultra Electronics Inc., Peoria, Illinois, September 1979.

64. Hanlon, G., Personal Communication, Hawker Siddley Dynamics Engineering Ltd., Hertfordshire, England, September 1979.

65. Programmable Plant Control - Microprocessor Controller Type C4E87, User Catalog, Ultra Electronics Inc., Peoria, Illinois, 1979.

66. SEQUEL: Programmable Control System, User Catalog, Hawker Siddley Dynamics Engineering Ltd., Hatfield, England.

67. Steitz, P., Mayo, L. G., and Perkins, S. P., Jr., Assessment of the Potential of Solar Thermal Small Power Systems in Small Utilities, JPL Contract 954971, Burns & McDonnell Engineering Company, Kansas City, Missouri, November 1978.

68. Wester, G. W., "SPSA Project - Electrical Subsystem Conceptual Design and Preliminary Assessment," Interoffice Memorandum 342-358, Jet Propulsion Laboratory, Pasadena, California, February 2, 1979.

69. California Electricity Generation Methods Assessment Project, Report 1459.77.009EJ, TRW Inc., Redondo Beach, California, January 1977.

70. McDonnel, G., Personal Communication, Garrett AiResearch of California, Torrance, California, January 1978.

71. Revere, W. R., "Meeting between United Stirling-Sweden and Jet Propulsion Laboratory Representatives," Interoffice Memorandum 353-079-361, Jet Propulsion Laboratory, Pasadena, California, June 18, 1979.